AD-A149 776 ACTIVE DETECTION OF TUNNELS BY INDUCED SEISMIC SPECTRA 1/1
(U) ARMY ENGINEER WATERWAYS EXPERIMENT STATION
VICKSBURG MS GEOTECHNICAL LAB R F BALLARD ET AL.
UNCLASSIFIED SEP 84 WES/MP/GL-84-18 F/G 17/10 NL

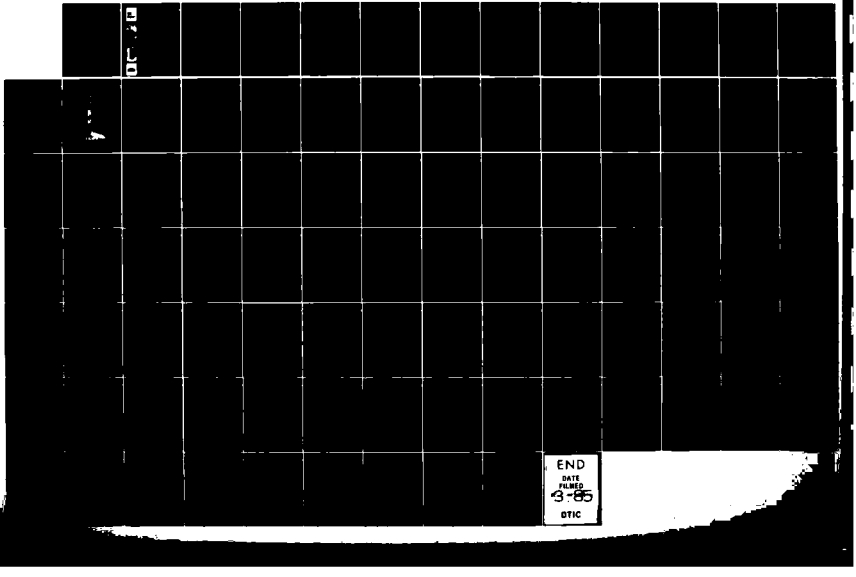

END
DATE FILMED
3-85
DTIC

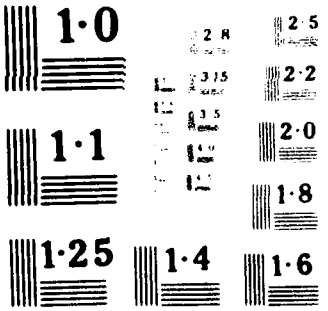
1·0
1·1
1·25
1·4
1·6
1·8
2·0
2·2
2·5

US Army Corps of Engineers

GEOTECHNICAL LABORATORY

ACTIVE DETECTION OF TUNNELS BY INDUCED SEISMIC SPECTRA

by

Robert F. Ballard, Jr., Thomas B. Kearfott
Richard D. Lewis, George E. Smith, Jr.

Geotechnical Laboratory

DEPARTMENT OF THE ARMY
Waterways Experiment Station, Corps of Engineers
P.O. Box 631
Vicksburg, Mississippi 39180-0631

September 1984
Final Report

DEPARTMENT OF THE ARMY
Belvoir Research and Development Center
Fort Belvoir, Virginia 22060

Destroy this report when no longer needed. Do not return it to the originator.

The findings in this report are not to be construed as an official Department of the Army position unless so designated by other authorized documents.

The contents of this report are not to be used for advertising, publication, or promotional purposes. Citation of trade names does not constitute an official endorsement or approval of the use of such commercial products.

Unclassified
SECURITY CLASSIFICATION OF THIS PAGE (When Data Entered)

REPORT DOCUMENTATION PAGE

READ INSTRUCTIONS BEFORE COMPLETING FORM

1 REPORT NUMBER: Miscellaneous Paper S-84-2

2 GOVT ACCESSION NO: AD-A149 776

3 RECIPIENT'S CATALOG NUMBER:

4 TITLE (and Subtitle): SEISMIC DETECTION OF TUNNELS BY INDUCED P-WAVE SPECTRA

5 TYPE OF REPORT & PERIOD COVERED: Final Report

6 PERFORMING ORG. REPORT NUMBER:

7 AUTHOR(s): Thomas B. Kean II; George E. Smith, Jr.

8 CONTRACT OR GRANT NUMBER(s):

9 PERFORMING ORGANIZATION NAME AND ADDRESS: U.S. Army Engineer Waterways Experiment Station, Geotechnical Laboratory, P.O. Box 631, Vicksburg, Mississippi 39180-0631

10 PROGRAM ELEMENT, PROJECT, TASK AREA & WORK UNIT NUMBERS:

11 CONTROLLING OFFICE NAME AND ADDRESS: Department of the Army, Belvoir Research and Development Center, Fort Belvoir, Virginia 22060

12 REPORT DATE: September 1984

13 NUMBER OF PAGES: 71

14 MONITORING AGENCY NAME & ADDRESS (if different from Controlling Office):

15 SECURITY CLASS (of this report): Unclassified

15a DECLASSIFICATION/DOWNGRADING SCHEDULE:

16 DISTRIBUTION STATEMENT (of this Report): Approved for public release; distribution unlimited

17 DISTRIBUTION STATEMENT (of the abstract entered in Block 20, if different from Report):

18 SUPPLEMENTARY NOTES: Available from National Technical Information Service, 5285 Port Royal Road, Springfield, Virginia 22161

19 KEY WORDS (Continue on reverse side if necessary and identify by block number):
Detection (LC)
Seismic waves (LC)
Seismology (LC)
Tunnel detection (LC)

20 ABSTRACT (Continue on reverse side if necessary and identify by block number):

A series of crosshole tests were conducted at the Colorado School of Mines Test Facility located near Idaho Springs, Colo. The primary objective of the study was to determine the modifications imposed on a seismic signal originating from a repeatable source caused by presence of a tunnel. The seismic source was a modified air gun, designed for generation of midfrequency range P-waves. In this study, 50- to 500-Hz frequencies were used. As tests were made in crosshole fashion at different elevations between the boreholes, alterations in the frequency spectrum were attributed either to material changes or (Continued)

DD FORM 1 JAN 73 1473 EDITION OF 1 NOV 65 IS OBSOLETE

Unclassified
SECURITY CLASSIFICATION OF THIS PAGE (When Data Entered)

PREFACE

The study reported herein was performed by personnel of the Geotechnical Laboratory (GL) and Instrumentation Services Division (ISD), US Army Engineer Waterways Experiment Station (WES), during the period 1 July 1982 through 1 July 1984. The investigation was sponsored by the Belvoir Research and Development Center (BRADC), formerly Mobility Equipment Research and Development Command (MERADCOM), Fort Belvoir, Virginia, under Project Order No. A2239. The MERADCOM Technical Monitor was Mr. A. H. Granahan.

The project was conducted under the general supervision of Dr. W. F. Marcuson III, Chief, GL, and under the direct supervision of Dr. A. G. Franklin, Chief, Earthquake Engineering and Geophysics Division, GL. The report was prepared by Messrs. R. F. Ballard, Jr., and T. B. Kean II, Dr. R. D. Lewis, all of GL, and Mr. G. E. Smith, Jr., ISD.

COL Tilford C. Creel, CE, was Commander and Director of WES during the preparation of this report. Mr. Fred R. Brown was Technical Director.

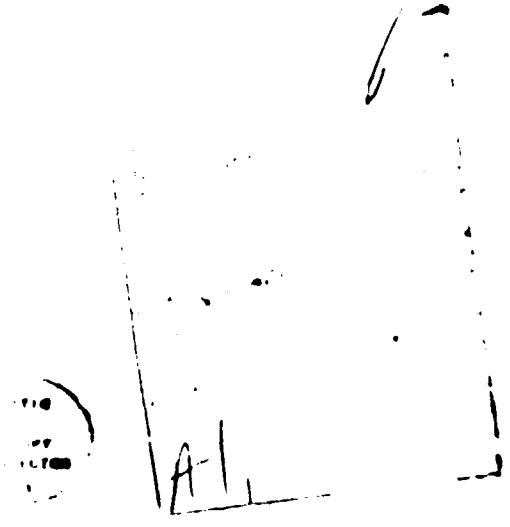

CONTENTS

CONVERSION FACTORS, U. S. CUSTOMARY TO METRIC (SI) UNITS OF MEASUREMENT

U. S. customary units of measurement used in this report can be converted to metric (SI) units as follows:

Multiply	By	To Obtain
feet	0.3048	metres
inches	2.54	centimetres
miles (U. S. statute)	1.609347	kilometres
pounds (force)	4.448222	newtons
pounds (force) per square inch	6.894757	kilopascals

ACTIVE DETECTION OF TUNNELS BY INDUCED SEISMIC SPECTRA

PART I: INTRODUCTION

Background

1. The problem of detecting and locating clandestine subterranean activities has been addressed for a number of years. Various geophysical methods thought to be applicable to the problem have been evaluated at a variety of sites and under a variety of geologic conditions as described by Ballard (1982). Many of these techniques have been applied from the ground surface as well as in boreholes.

2. To date, only those geophysical techniques used on the ground surface or subsurface geophysical methods which originate in boreholes have shown any promise in the detection of underground tunnels or cavities. Tunnel detection by remote sensing methods has proved to be relatively ineffective. The use of satellite photography, infrared imaging, etc., can be used to detect road work or surface spoil areas. However, deep-based tunneling activity has, thus far, eluded the state-of-the-art high-altitude remote sensing technology. Such methods as surface electrical resistivity, microgravity, ground-penetrating radar, crosshole seismic, and radar techniques have proven to be effective under the geological conditions which are conducive to each of the methods.

3. The thrust of this research effort has been directed toward the application of crosshole seismic techniques. Recent work at the U. S. Army Engineer Waterways Experiment Station (WES) has led to the development of a downhole vibrator system which can be accurately controlled over a frequency range between 50 to 500 Hz. The device has been successfully used in the determination of shear-wave velocities of rock and soils between the vibrator and receiver. In the course of investigating many sites throughout the United States, it has been observed that earth materials exhibit discrete frequency spectrum characteristics which can be attributed to many different factors, some of which would be the granular structure, density, moisture content, state of stress, etc. This observation leads to the suggestion that earth materials can be characterized by their wave propagation spectra in a manner analogous to optical spectrographic analysis procedures used

in other fields. Therefore, if an anomalous condition such as a tunnel should appear between boreholes in the geophysical seismic survey, its presence should have an effect on both the arrival time of the seismic signal and its frequency content. The degree of change of the total seismic signature in frequency content, amplitude, and arrival time is the primary factor which is addressed in this effort.

Objective

4. The broad objective of this project is to determine the modifications imposed on a seismic signal originating from a repeatable source caused by the presence of a tunnel. It has already been established by Price (1982) and others in previous studies that the time of arrival of the seismic wave train will be lengthened by the presence of an air-filled void (tunnel). This phenomenon results from the additional time the signal must take to travel around the cavity when traveling from the source to the receiver. These studies have prompted the following specific objectives: (a) identify the seismic wave types that are influenced by the presence of a tunnel, (b) determine whether or not receiver orientation (vertical or horizontal) would enhance the ability to detect a tunnel, (c) to determine if frequency change and amplitude loss can be directly associated with the presence of a tunnel.

Approach

5. WES has acquired two novel seismic sources which are intended for borehole use. An inhole vibratory source was developed primarily for the determination of vertically polarized in-situ shear-wave velocities. Recent experiments using this device have shown that it has potential in other applications as well. Accordingly, the microprocessor control network has been altered so that the vibrator is now capable of responding to programmed swept frequencies, discrete frequencies, and white noise random excitation. Observations using the random excitation input mode in conjuction with real-time fast Fourier spectral analysis, cross-correlation, and phase relations have shown that definite spectral signatures are characteristic of different soil and rock materials. Additionally, the spectral signature

can be drastically altered by the presence of an anomalous condition such as an air-filled void between two borings as theoretically demonstrated by Lytle and Portnoff (1984). With these present modifications, even more diagnostic tunnel signatures can be obtained. Typically, if tests are conducted between two borings at a number of different elevations and the spectral content recorded, the presence of a "seismic obstruction," such as a tunnel between the boreholes, will cause an alteration of the frequencies whose wave lengths are compatible with that of the tunnel's geometry. Not only will certain frequencies be absorbed or shifted to other frequencies by the presence of the void (tunnel) but the shear-wave velocity will also be affected (decreased). The second seismic source used at the Idaho Springs test site was an air gun which was designed for the generation of midfrequency range P-waves. In this study, 50 to 500 Hz were used. Since this source is essentially repeatable, as tests were made in crosshole fashion at different elevations between the boreholes, alterations in the frequency spectrum could be attributed either to material changes or the presence of anomalies in a manner similar to that observed using the vibratory shear-wave source.

6. Tests conducted within the boreholes were designed so that multiple receivers could be located in more than one boring at a time. In the vicinity of the tunnel, tests were conducted with receivers at varying angles and elevations from the source so that a two-dimensional geometry of the tunnel between the boreholes might be investigated by alterations in seismic signatures.

Scope of Report

7. Even though numerous attempts were made to transmit a random signal from the borehole vibratory source to receivers located in adjacent boreholes, the effort was unsuccessful due primarily to the relatively high concentration of vertical fracturing which was prevalent at the test site and the low force level (10 lb*) generated by the vibrator. As a consequence, this technique was abandoned and emphasis was placed upon use of the air gun. The primary emphasis of this report will be placed upon the presentation and discussion of data obtained by using the air gun as a seismic source for the crosshole tests. It will also include a brief description of the vibrator concept and its test because its application might prove successful at another site.

* A table of factors for converting U. S. customary units of measurements to metric (SI) units is given on page 3.

PART II: SITE DESCRIPTION AND TESTS CONDUCTED

Idaho Springs Site

8. The test site is located about 1/4-mile north of Idaho Springs, Colorado, at an altitude of approximately 8,000 feet. Mine workings and several tunnels are owned and operated by the Colorado School of Mines on an experimental basis. In the late 1800's, the workings were operated as a gold mine to exploit the Edgar vein and other less important veins. Rock in the vicinity of the tunnels consist mainly of intimately interlayered pegmatite, granite gneiss, amphibolite, biotite gneiss, and microcline gneiss. These rocks are complexly folded and cut by pigmatite dikes dipping steeply northwest. A more detailed geologic description is available from the U. S. Geological Survey (USGS) and the Colorado School of Mines (Amuedo and Ivey, 1984). The Belvoir Research and Development Center (BRADC), formerly the Mobility Equipment Research and Development Command (MERADCOM), entered into an agreement with the Colorado School of Mines to make use of the tunnels as a test site. Several borings were placed from a man-made plateau at an elevation approximately 160 feet above the centerline of one of the tunnels. The borings were used by several contractors prior to the construction of a new adit which advanced the tunnel between several of the borings. Tests were then repeated by a number of contractors prior to WES arrival on the site. Figure 1 shows a surface layout of the borings which were available from the working platform. Most of the borings were drilled to a depth of approximately 280 feet with a diameter of 6 to 7 inches. The borings were uncased except for PVC pipe which existed in the upper 8 to 10 feet of the borings. It had been noted by one contractor that fracturing prevented the borings from retaining water, which necessitated remedial action by grouting and redrilling some of the borings. This procedure was not totally successful, so bentonite was used in an attempt to seal the leaks and retain more water. This attempt was only partially successful, and water could only be retained for a short period of time before drawdown occurred. For WES purposes, it was necessary that water be present only in the air gun seismic source borehole when conducting the crosshole tests.

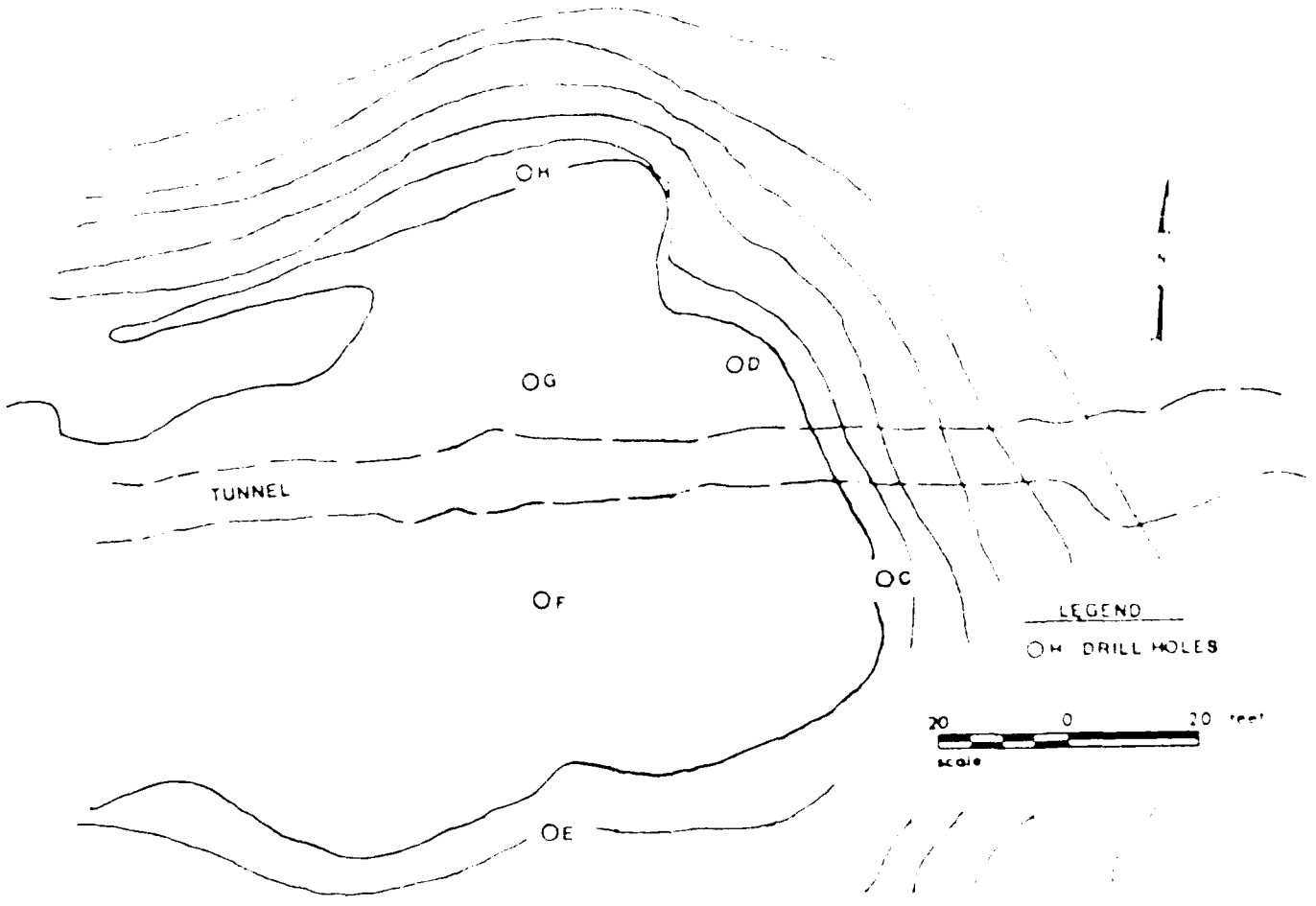
OH
OG
OD
TUNNEL
OF
OC
OE
LEGEND
OH DRILL HOLES
20 0 20 feet
scale

Vibratory Seismic Rationale

9. The WES borehole vibratory source, shown in Figure 2, was developed primarily for the production of high-quality, vertically polarized shear waves. The device is normally used for the determination of shear-wave velocity through materials existing between two or more boreholes. In practice, the vibrator is locked into position within a borehole by an inflated rubber bladder. One or more geophone receiver packages are locked into position in a similar manner in adjacent borings at the same elevation as the vibrator. The borehole vibrator, controlled by a power amplifier and sine wave oscillator, is then swept through a frequency range of approximately 50 to 500 Hz. The receivers are constantly monitored during the frequency sweep, and those frequencies which propagate well, as evidenced by high amplitudes, are noted. A tone burst generator is then used to transmit a burst of a given number of signal cycles, usually eight, of one of the chosen frequencies. A geophone incorporated within the vibrator body is used as the reference standard to compare the phase delay which is recorded by the receivers. That difference in travel time, when combined with the distance source and receiver, is used to determine the velocity of the shear-wave within the medium. Using this procedure at a number of different test sites throughout the continental United States, it has been observed by WES personnel that different sites exhibit markedly different preferences for frequencies which transmit well. In other words, the earth materials act as band-pass filters for specific frequencies. Also, when anomalous conditions occur, such as highly fractured rock or possibly air-filled voids, a noticeable decrease in received high-frequency signal content can be observed as noted by Curro (1983).

10. Since the vibrator is an electromechanical device whose performance can be controlled by electrical signal input, experiments were performed on the WES reservation to determine the uniformity of signal output if a white noise random input source were used as the controlling factor. White noise was chosen because it has the characteristic of equal amplitude content in all frequencies. Consequently, signal loss in any frequency band can be related to energy absorption within the medium. The amplitude spectrum of the borehole vibrator in the random excitation mode proved to be essentially uniform over a frequency range of 80 to 500 Hz. This plot is shown in Figure 3.

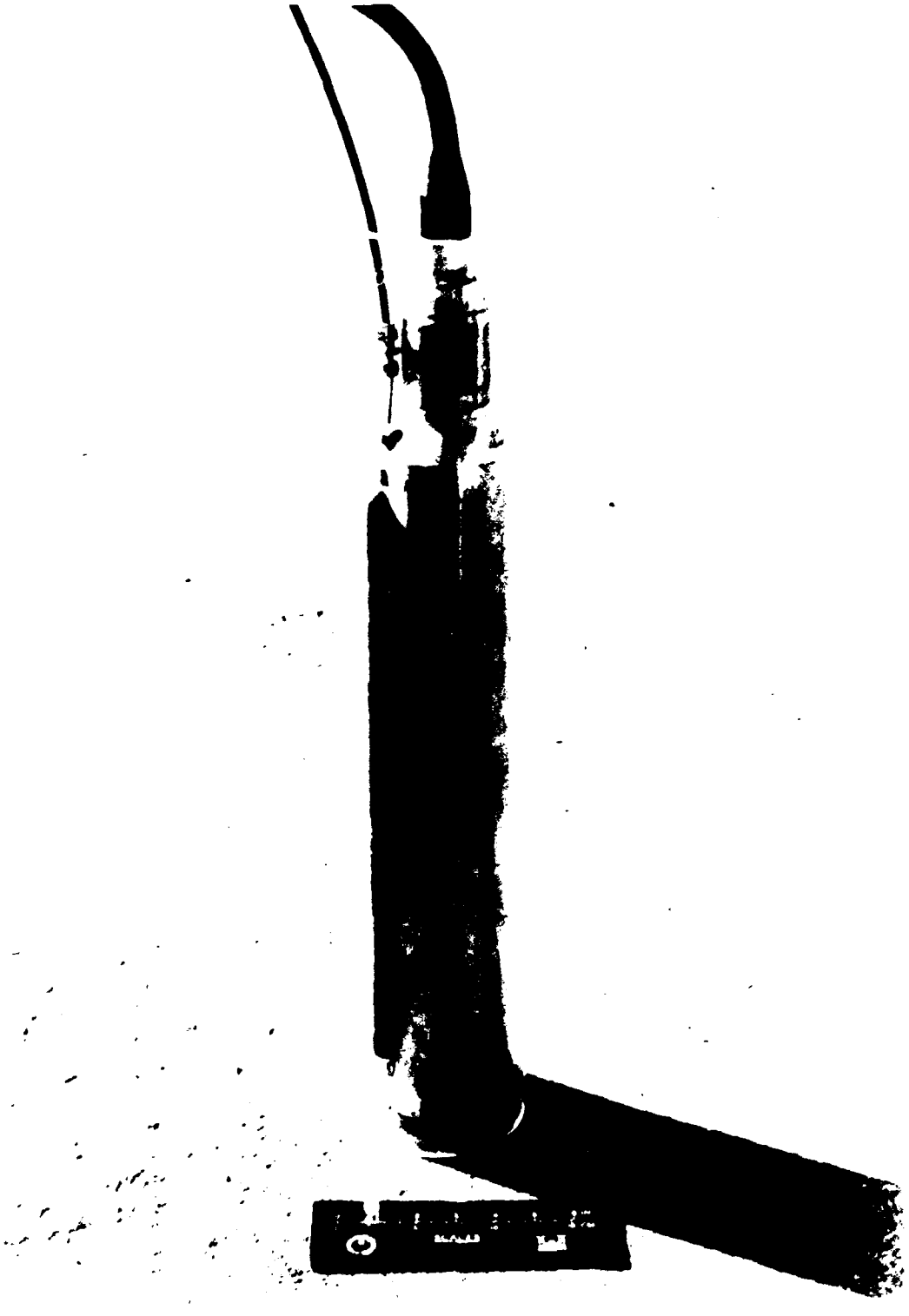

Figure 2. Waterways Experiment Station Borehole Vibrator

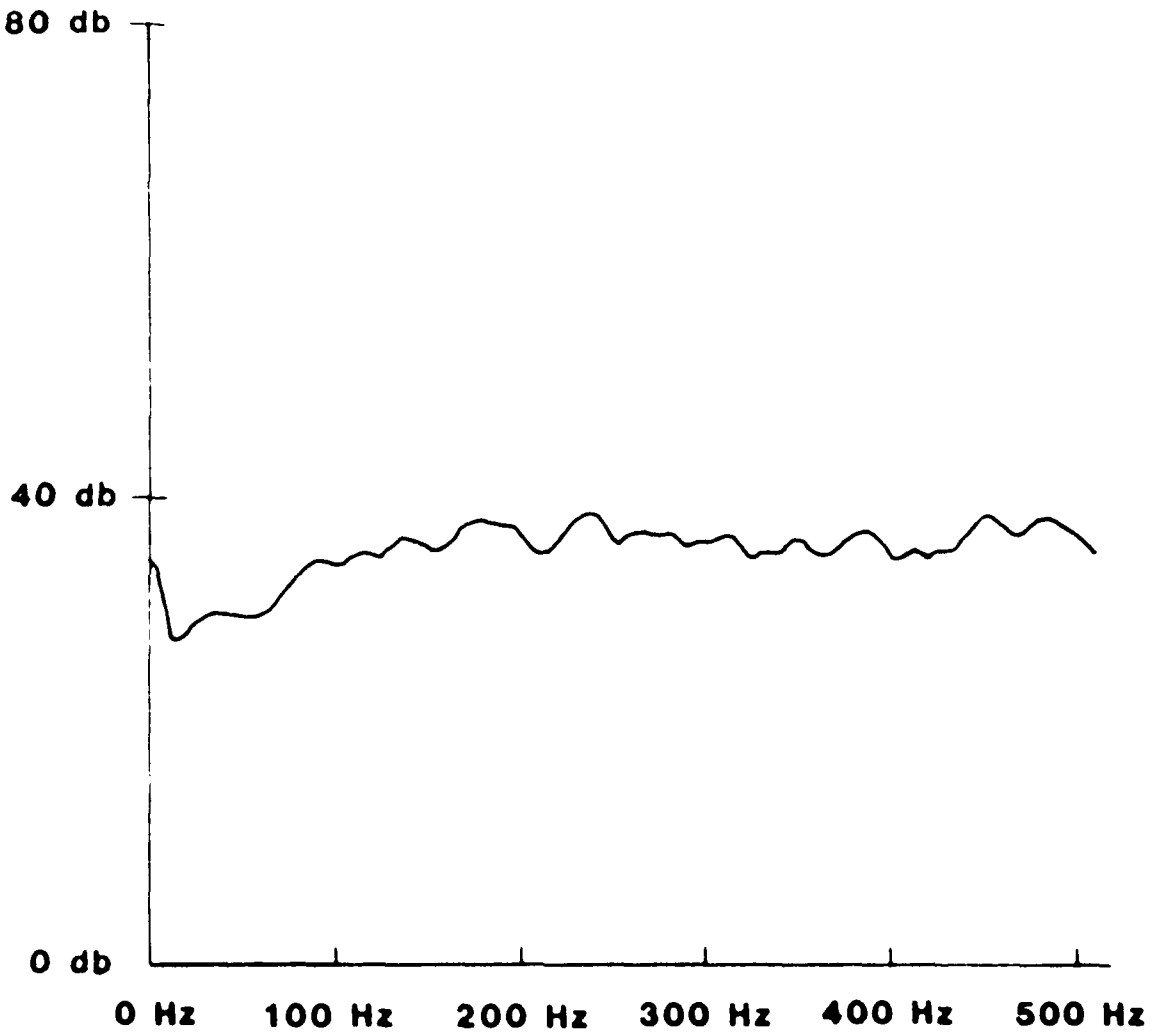

Figure 3. Amplitude spectrum of SES borehole vibrator monitor geophone driven by random noise band limited to 500 Hz

While this test was being conducted, a receiver was placed at the same depth (20 feet) in an adjacent borehole, approximately 50 feet laterally from the borehole vibratory source. The amplitude spectrum received at this geophone is shown in Figure 4. It can be seen from this figure that the peak frequency on this curve is approximately 225 Hz. This compares quite well with other observations using a swept sine-wave frequency; a frequency of 221 Hz exhibited less signal attenuation or loss than any other frequency.

11. As previously stated, tests of this type were attempted at the Idaho Springs, Colorado site, but the highly vertically fractured material caused such severe signal losses that no reliable data could be obtained. Several attempts were made using different borings and elevations within the borings before it was decided that further attempts should be abandoned. All of the crosshole data obtained at this site used an underwater air gun as the seismic source. These tests will be described in subsequent paragraphs.

Air Gun Seismic

12. The Bolt D500 air gun is a pneumatically chargeable, electrically fired device (presently under study for use as a multi-wave generating source). The air gun system consists of a high-pressure air or gas source connected to the gun through a high-pressure feeder hose and a battery-powered firing control box connected to the gun through a stress member reinforced co-axial cable. The air gun system is usually used in offshore seismic reflection surveys; therefore, in order to use it as a crosshole survey source, several modifications have been made. Because the system is normally mounted on a marine vessel equipped with high-pressure compressors, the first modification had to be the air pressure supply system. The system now uses 2,500 psi nitrogen bottles to supply the required gas pressure. This decision had two beneficial effects; it eliminated (a) the need for a large volume compressor with its attendant logistic problems, and (b) high background seismic noise problems caused by running of a compressor.

13. In addition to the gas modification, two additional modifications were made to the air gun; (a) a piezo crystal accelerometer was added to the firing system by the factory (this modification was needed to activate the recording seismograph), and (b) a hydrophone was suspended 5 inches below the gas exit orifice to sense a "zero time" for the pulse initiation.

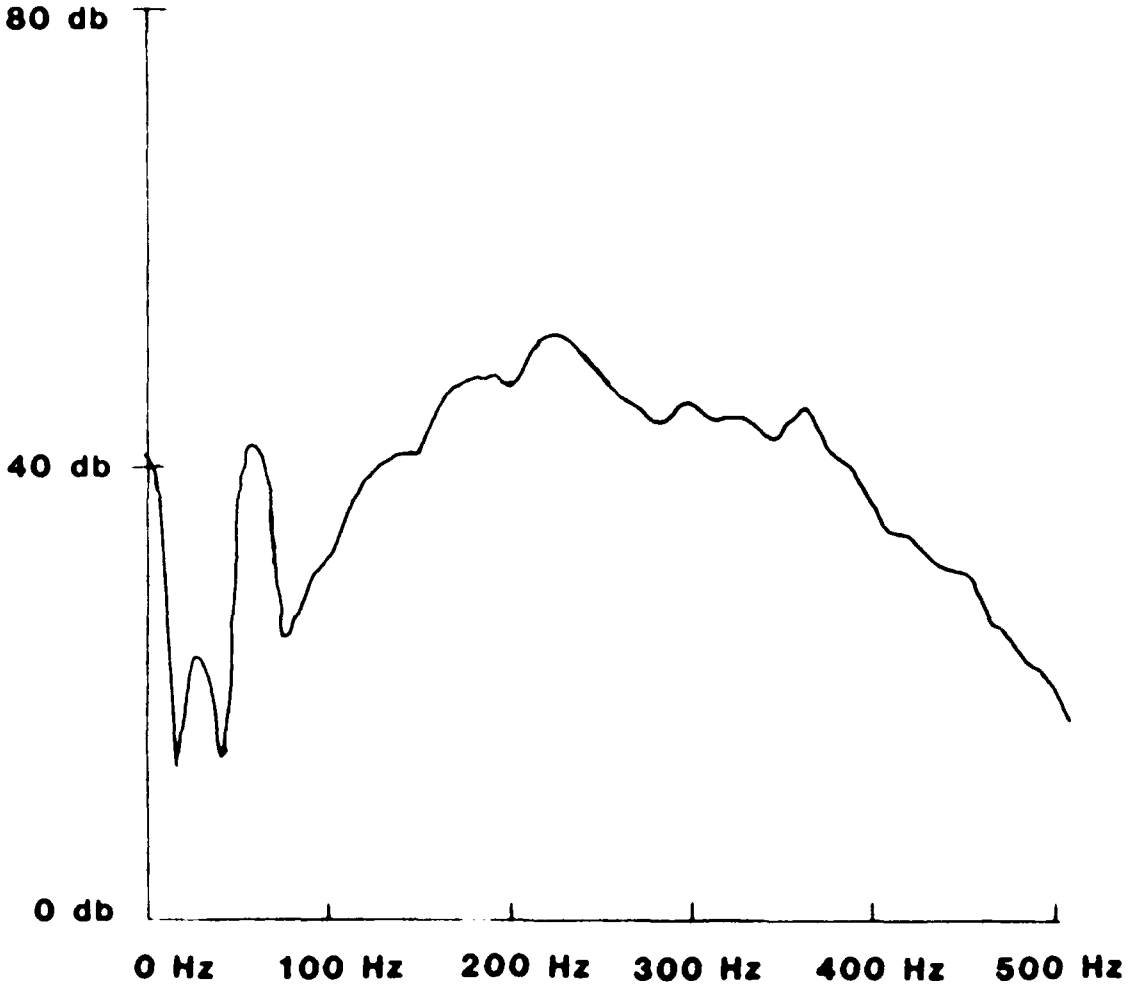

Figure 4. Amplitude spectrum of vertical receiver borehole geophone 50 ft from vibrator--both at 20 ft depth

14. The receiving units used in this experiment were two calibrated downhole triaxial geophone sets (Mark Products L-15-3DSWC). Each triaxial geophone set consisted of one vertical geophone and two horizontal geophones mounted at right angles to one another. These downhole geophones were handled by a stress member and connected to the different recording devices through an electrically shielded cable. To obtain the desired geophone-to-borehole sidewall coupling, the downhole geophones were equipped with high pressure inflatable bladders. In order to minimize extraneous ground noise and vibrations, these bladders were connected through their air lines to nitrogen bottles instead of the usual small-volume compressor generally used to supply air to the system.

15. In order to build some degree of redundancy into the program and provide on-site "quick look" capability, two data collecting systems were employed. One system was an SIE 49R 24-channel seismograph mated to a 7-channel analog tape recorder which was used to make analog recordings of the wave trains. These recordings were later returned to WES where they were digitized and processed by the Instrumentation Services Division. (This procedure is described more fully in the "Data Reduction" section of this report.) The second system was the EG&G Geometrics ES1210F digital 12-channel seismograph which was used to make permanent hard copies of the tests so that each test would have a uniform relationship. All tests in the crosshole series were conducted with amplifier gains pre-set at an optimum level and unaltered throughout the tests so that all data could be directly compared on a relative basis. To maintain this standardization and because the SIE recorder combination did not have enhancement capabilities, single shots of the air gun charged to 500 psi were used with both of the two seismic recording systems. The sequence used to record each event was one shot with the EG&G connected to the receivers and another single shot in rapid succession with SIE and tape recorder connected to receivers.

16. A variety of test geometries were employed so that various wave reactions to an anomalous condition could be studied. Tests were conducted by repositioning the source and receivers at various elevations in different holes. Figures 5 through 12 show plan (a) and profile (b) views for all test conditions reported herein. Tests were numbered consecutively. Each test number is followed by a letter designating the borehole in which the receiver was fixed. The scheme of the data acquisition program intentionally

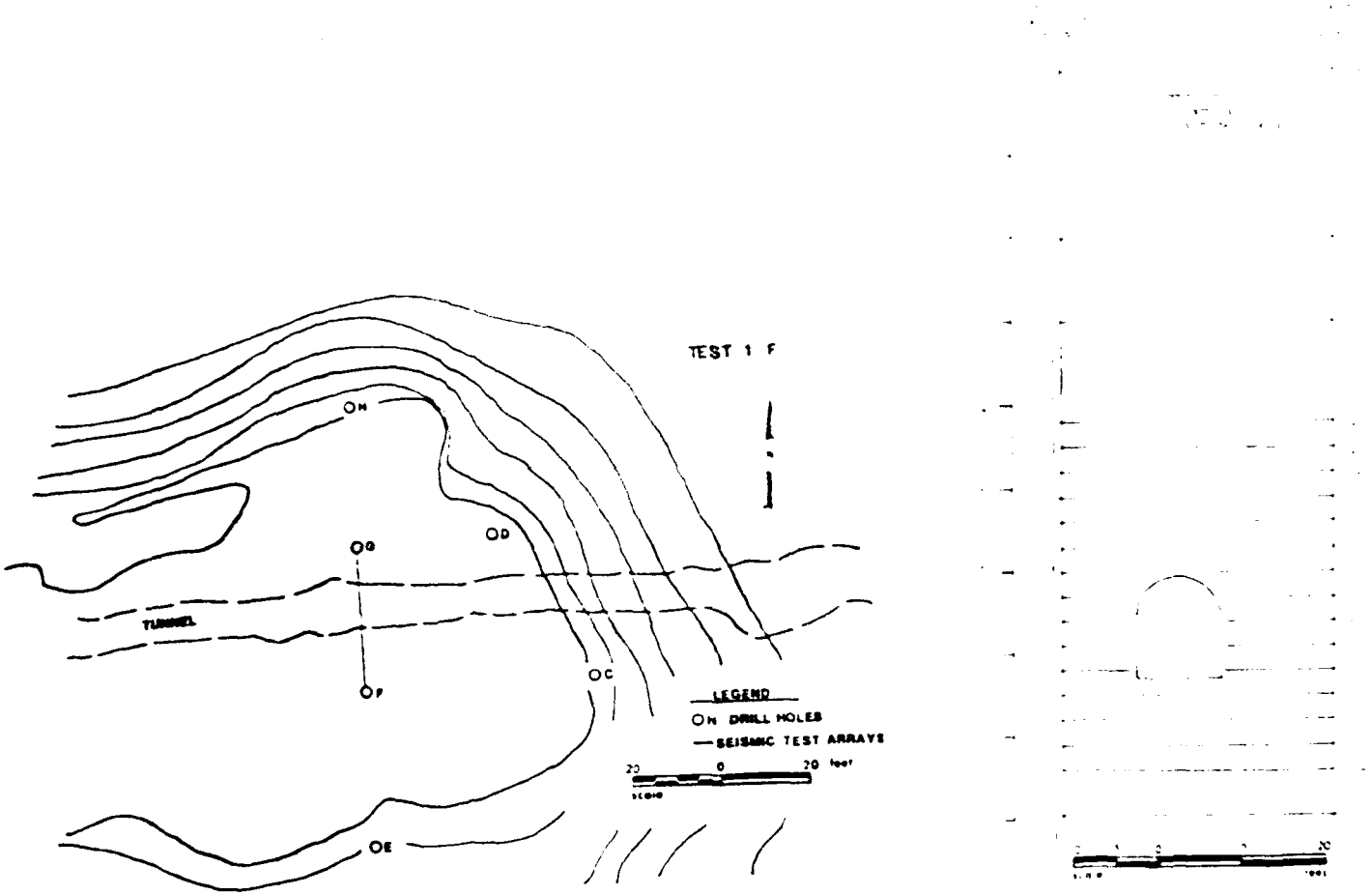

(a) Plan view

(b) Profile view

Figure 5. Test 1 F schematic

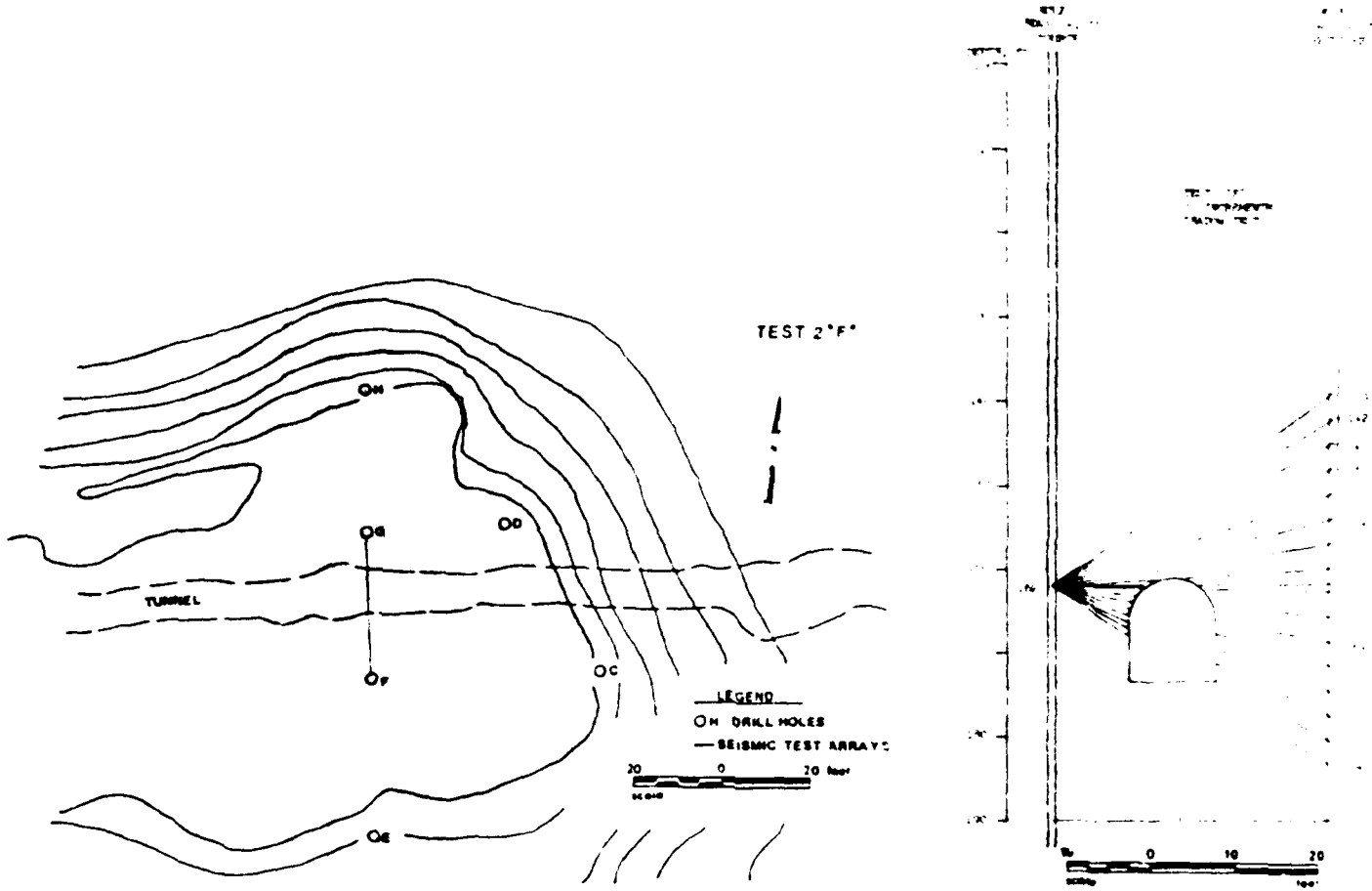

(a) Plan view

(b) Profile view

Figure 6. Test 2 F schematic

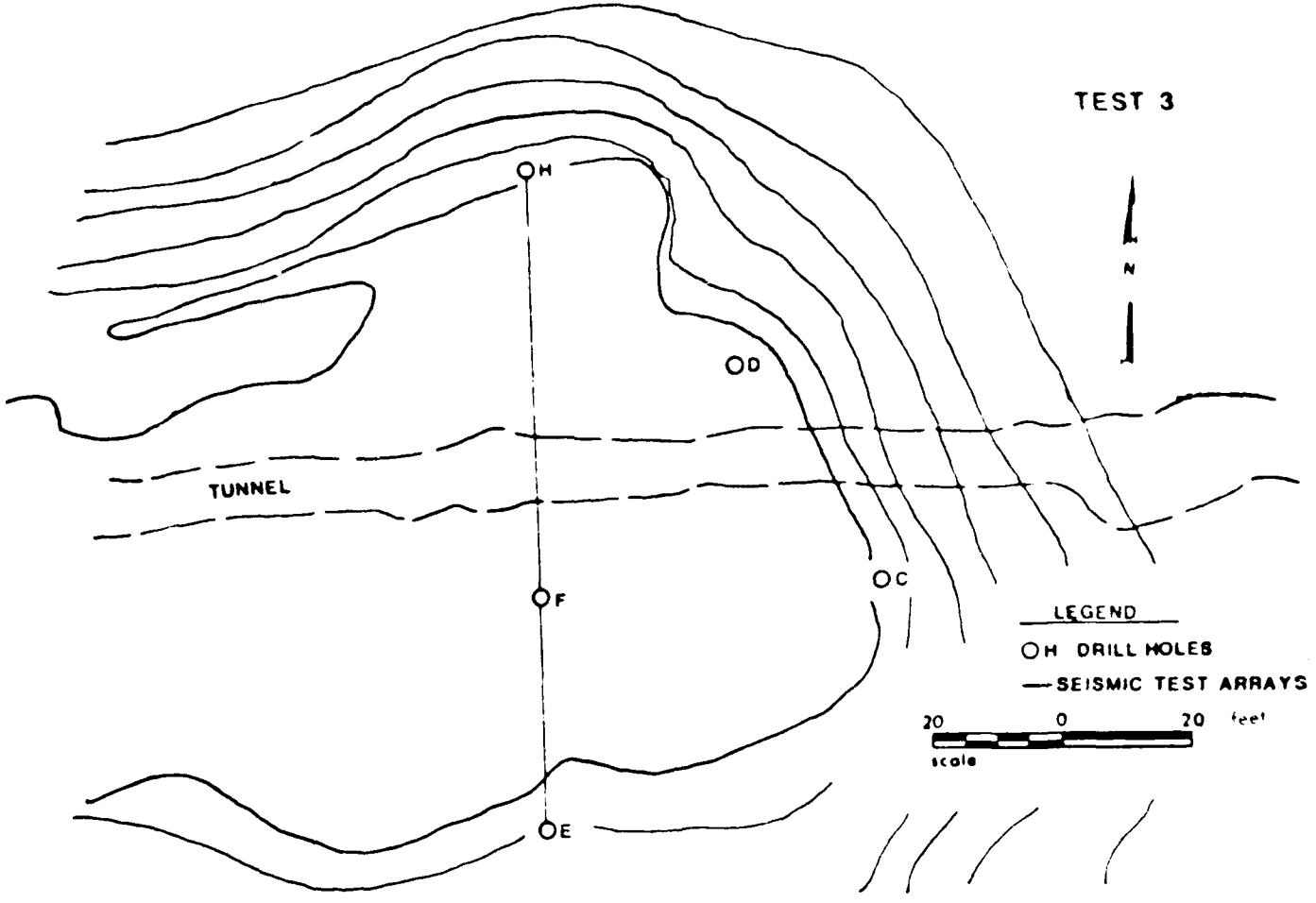

Figure 7.1. Test 3 F plan view

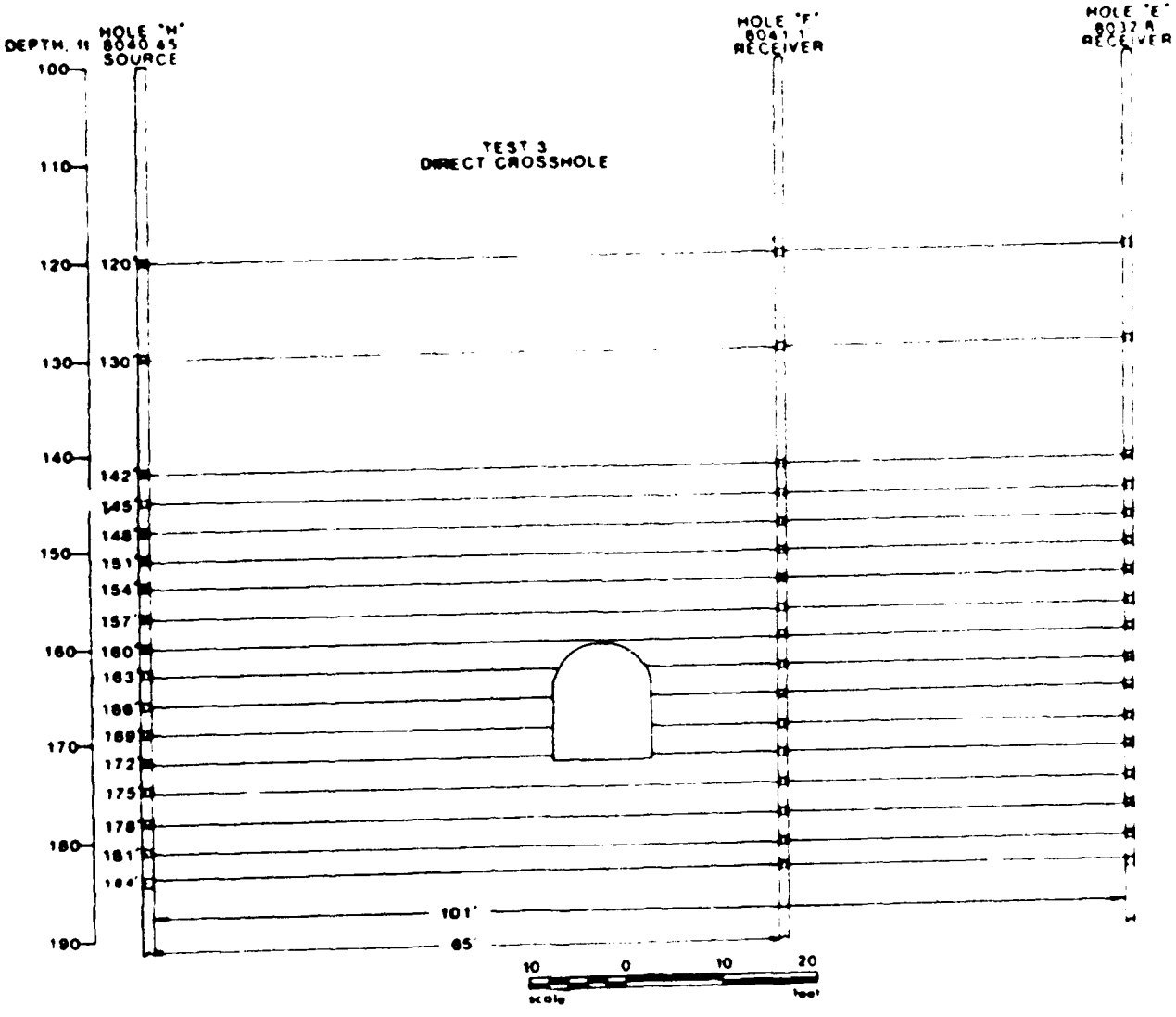

Figure 7b. Test 3 F profile view

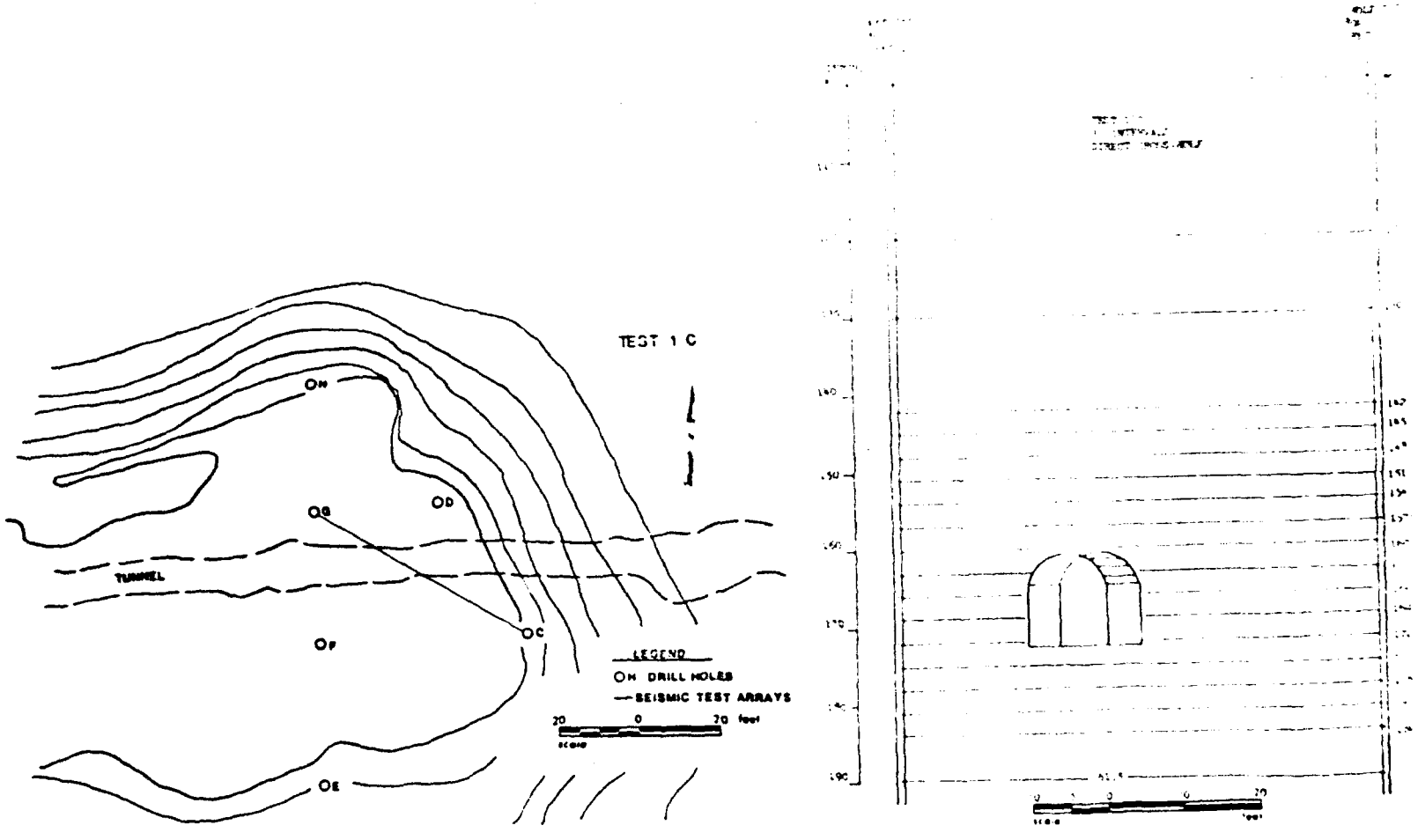

(a) Plan view

(b) Profile view

Figure 8. Test 1 C schematic

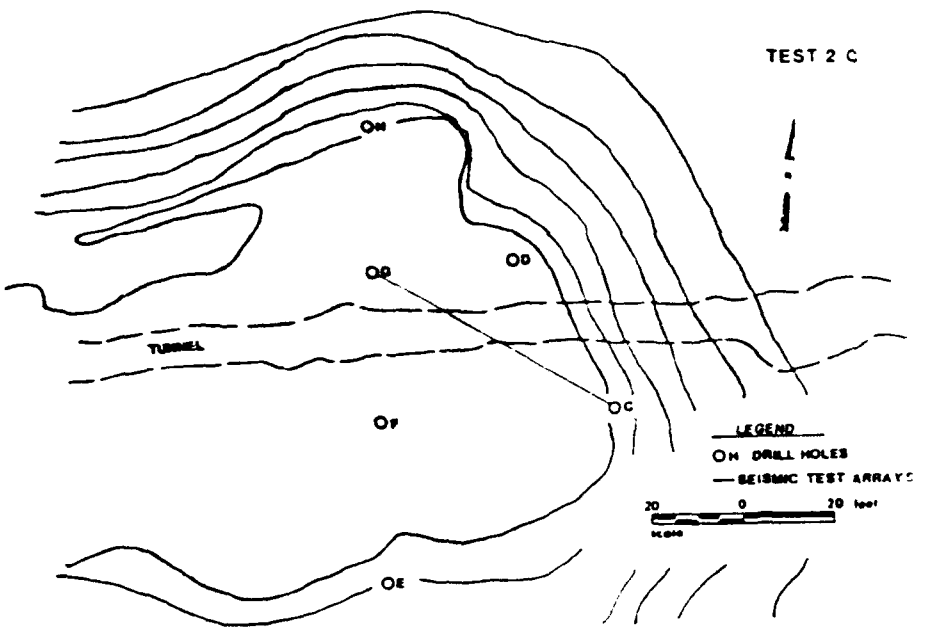

(a) Plan view

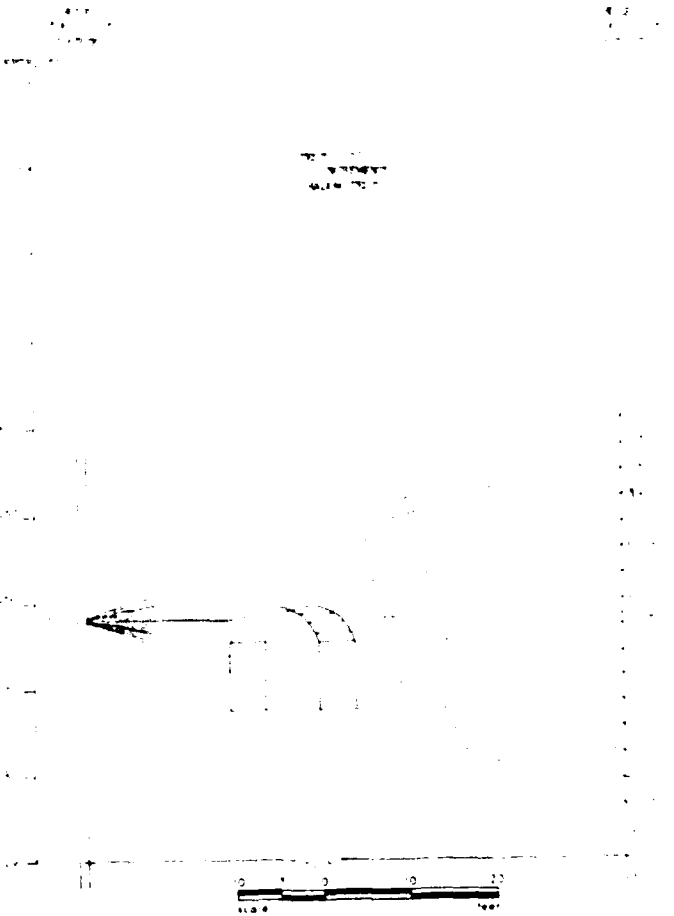

(b) Profile view

Figure 9. Test 2 C schematic

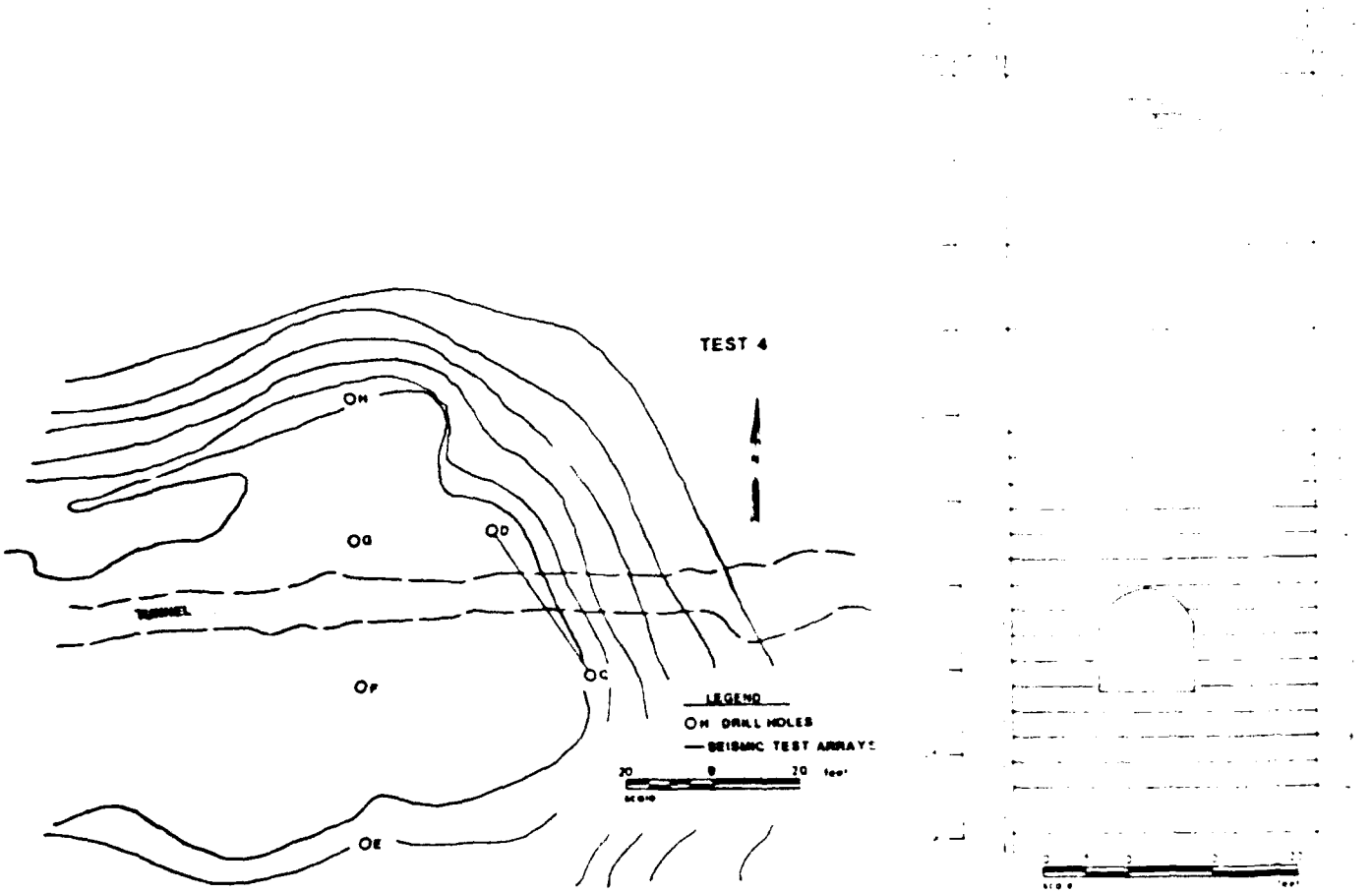

(a) Plan view

(b) Profile view

Figure 10. Test 4 C schematic

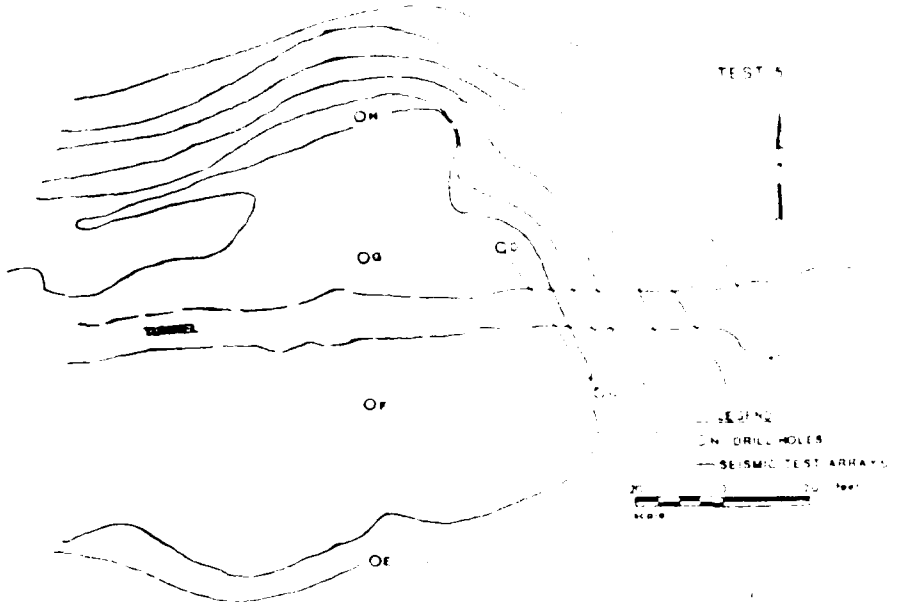
TEST A
Oh
Oa
Op
Oe
SEISMIC TEST ARRAYS

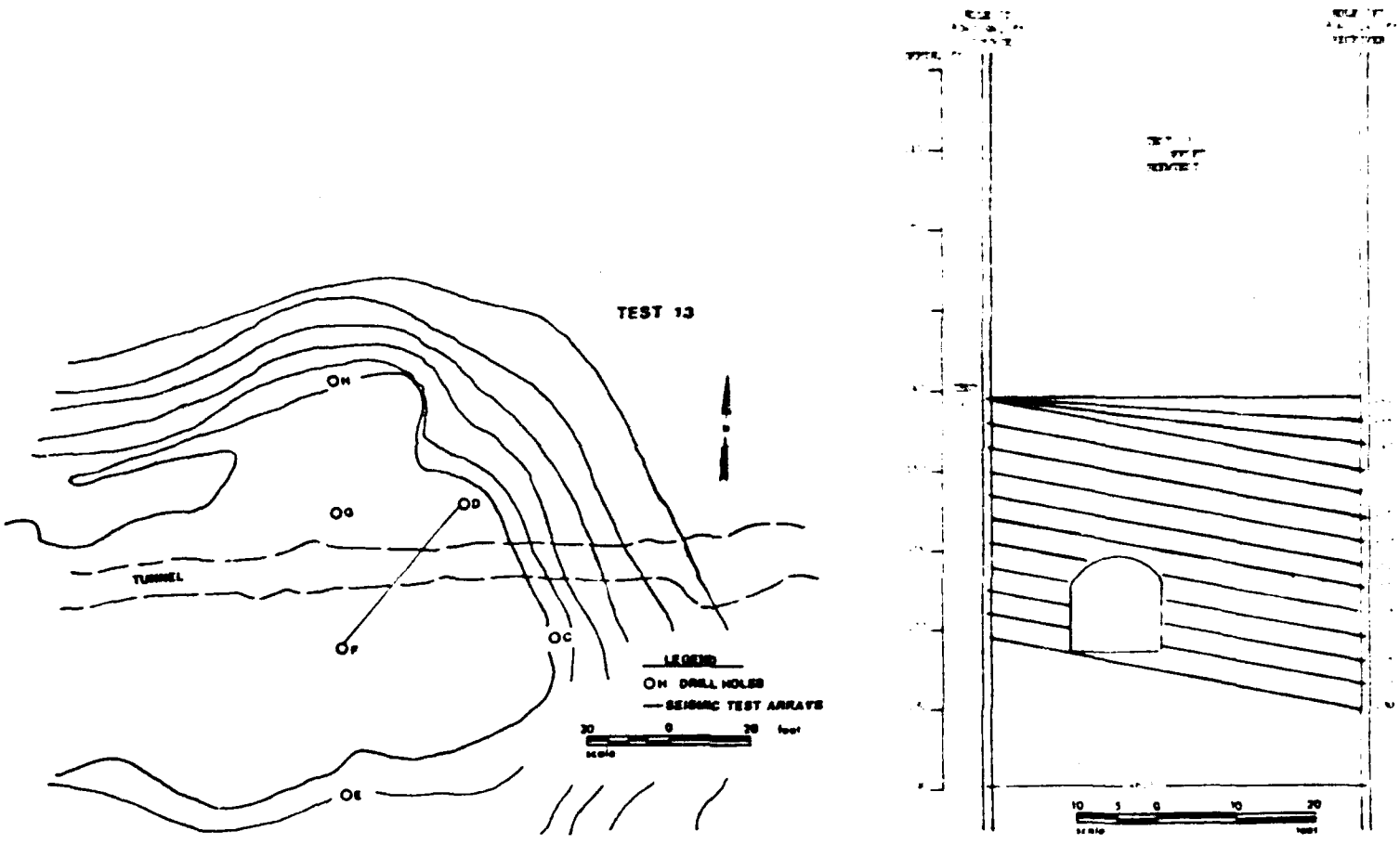

(a) Plan view

(b) Profile view

Figure 12. Test 13 F schematic

allowed for the collection of more data than would be used for analysis. In order to make this report as concise as possible, only those tests which served to illustrate the methods used were selected for presentation.

17. The test patterns fall into three basic types. The first pattern is the "Common Depth" crosshole test. This test is used to search first for changes in the velocity of materials with depth, layer variations and, in this case, the presence of an anomalous condition. In the common depth crosshole test the source and receiver are both maintained at the same depth during the test. For this set of tests, the source and receiver were raised in 3-ft increments, beginning near the bottom of the boreholes at a depth of 184 feet and progressing upward to the 142-foot depth. After this test, the two units were then raised to 130 feet, 120 feet, and 100 feet, respectively. The following are the common depth tests reported herein:

Test No.	Figure No.
1F	5
3F	7
1C	8
4C	10

18. The second test pattern used was a crosshole fan or tangent pattern where the source was held constant in each shot hole at a depth of 162 feet. (At the time of testing, this was thought to be the tunnel's center. Later information revealed the correct depth to be about 168 feet.) The geophones were advanced upward in 3-foot increments from 184 feet, in the same manner as the horizontal test. The following are the fan pattern tests reported herein:

Test No.	Figure No.
2F	6
2C	9
5C	11

19. The third test pattern, designated Test 13F, was the crosshole skew pattern. The source was first held at 141 feet, and the receiver lowered in 3-foot increments until it was 9 feet below the source. From this point, both the source and geophone were lowered together in 3-foot increments until the source was at 171 feet and the geophone was at 180 feet (Figure 12).

20. Tests conducted at Idaho Springs, Colorado, indicated that cross-hole seismic tests can provide extremely useful information which, when properly interpreted, can reveal the presence of a tunnel. The techniques of data interpretation will be addressed in the subsequent section.

PART III: TEST RESULTS

Data Reduction

21. The data which were acquired at the Idaho Springs test site were reduced in a variety of ways. The records obtained on the EG&G seismograph were not recorded on tape. Consequently, their use were limited to optical displays. A separate analysis using these records will be discussed apart from data obtained on analog tape.

22. That portion of the field data recorded on analog magnetic tape used an SIE 49-R seismograph and a RACAL 7 DS 7-channel FM tape recorder. Tape speed was 3.75 ips which provided a bandwidth of D.C. to 1,250 Hz. The data were first digitized at a rate of 20,000 samples per second. Time resolution of 0.05 msec per sample and a corresponding Nyquist frequency of 10,000 Hz were obtained. This digitizing rate far exceeded the frequency bandwidth and time resolution of both the recording equipment and recorded signal.

23. In preparation for analysis, two types of reduction were performed on the digitized data. Time domain playbacks were produced and visually inspected to determine general signal characteristics such as time of arrival and amplitude stand-out. They were also compared to digital data taken in the field by an EG&G 1210F, 12-channel seismograph. After the quality of the data was established, frequency domain techniques were employed to study the propagated seismic energy.

24. The frequency domain studies were performed using Fourier analysis techniques. Fourier analysis is the analytic decomposition of a wave form as a weighted series of sinusoidal functions. This decomposition is done via the Fast Fourier Transform (FFT) algorithm as suggested by Rabiner (1975). For the digitized record, consisting of N discrete values, the Fourier transform is defined as:

$$X(k) = \frac{1}{N} \sum_{i=1}^{N} X(i) \exp\left(\frac{-j\,2\,\pi\,i}{N}\right) \qquad (1)$$

where

$X(k)$ = the (complex) Fourier transform coefficient for the k^{th} frequency component

$X(i)$ = the i^{th} discrete value of the input time domain wave form

$-1 = \sqrt{-1}$

N = the total number of points in the record

(Division by the total number of points in the record is done to normalize the resulting series.) The wave form is, therefore, decomposed into coefficients of a sinusoidal polynomial. The original time series may now be expressed as a sum of Fourier coefficients multiplied by a complex exponential:

$$X(i) = \sum_{k=1}^{N} X(k) \exp\left(\frac{2\pi}{N} i k\right) \qquad (2)$$

Therefore, the Fourier series coefficients are the amplitudes of each frequency component in the original time series wave form. (Note that the Fourier coefficients are complex quantities. In this report the modulus - phase notation for complex numbers is used. The Fourier modulus and phase are referred to as the amplitude and phase spectra, respectively.)

25. The Fourier coefficients are also useful in determining the amount of energy a time series has in particular bands of frequencies. From Parseval's theorem one has:

$$\sum_{i=1}^{N} |X(i)|^2 = \sum_{k=1}^{N} |X(k)|^2 \qquad (3)$$

This expression states that the total squared amplitude of a time series summed over all time is equal to the total squared amplitude of its Fourier transform summed over all frequencies, as shown by Rabiner (1975). The summation of the squared time series amplitude over all time is referred to as its energy. Consequently, this theorem shows a relationship between the energy of a wave form and the square of its amplitude spectra.

26. If one requires the energy content in a band of frequencies, one simply sums the squared amplitude spectra of the frequencies in that band. A running summation of the squared amplitude spectra versus frequency will display the total cumulative energy as a function of frequency. One analysis conducted for this study utilized the running summation method of displaying the total cumulative energy (Tests 3F, 5C, and 13F). The displays were normalized by dividing by the total energy. The result is fraction of total cumulative energy versus frequency. This analysis is referred to as energy buildup versus frequency.

27. The main frequency techniques used in this report were displays of the amplitude spectra and energy buildup. These two techniques reinforce each other. That is, they convey similar information displayed in two different ways. The amplitude spectra show the distribution of energy as a function of frequency. The energy buildup displays the cumulative fraction of total energy as a function of frequency. These methods do show that frequency content and energy distribution vary as seismic energy is passed near the tunnel.

28. Along with the two major techniques discussed so far, several other procedures were employed for analysis of the data. They included cross-correlation, phase spectrum analysis, amplitude envelope studies, and energy buildup versus time. Each of these techniques had its merits and drawbacks.

29. Cross-correlation is a method of determining the degree of similarity between two time series (x and y) when a time lag is applied to one. The cross-correlation is defined by Claerbout (1976) as:

$$s(i) = \frac{1}{N} \sum_{k=1}^{N} x(k)y(k+i) \qquad (4)$$

where

s(i) = the cross-correlation at a time lag of i units.

Note that if the y() time series were a time delayed version of the x() time series, then the cross-correlation, s(), would have a maximum when the time lag was equal to the delay time between y() and x(). Hence, the cross-correlation contains, among other things, the time delay information. The Fourier transform of the cross-correlation is known as the cross-spectrum and is the amplitude of common frequency components between two signals. Both of these operations were performed on the data from the horizontal geophones; however, neither produced any usable insight into the tunnel identification problem.

30. Another scheme of tunnel identification was to explore the possibility that the tunnel produced a dispersive effect. That is, the group velocity, the velocity at which the seismic energy travels, would be different for different frequency components. This dispersive effect might be detected in two ways; first, as a phase shift in particular frequency ranges or a

change in arrival time of the main amplitude envelope. To study this effect, the phase spectra and envelope amplitudes were used. However, the phase spectrum was not considered to be particularly useful in the examined frequencies and the given signal-to-noise ratio. The characteristics of the amplitude envelope may be explored in the future when a higher energy seismic source is used. It is possible that the distances between boreholes may not have been enough for dispersion to be detected. Also, any noise present in the time series produces even more noise in the phase spectrum. Hence, the dispersive effects may have been hidden within this procedure.

31. Another method to detect deviations in group velocity near the tunnel is the energy buildup versus time analysis. Here the fraction of total energy versus time delay is plotted. Although this technique shows some information, it was not exploited. One of the problems with this method is noise. In this case, the noise adds to the energy buildup even though the seismic energy arrival does stand out over the background.

Data Analysis

EG&G records

32. The data analysis will be addressed in the following sequence: First, the time domain signals recorded on the EG&G seismograph will be discussed, followed by the digitally-processed data obtained on the SIE analog tape recorder. The digital analysis was guided by the original time domain records obtained on the EG&G unit. Even though all data were digitally processed, it was felt that only those tests which served to illustrate the analysis techniques would be used. Consequently, Tests 3F, 5C, and 13F were subjected to frequency domain analysis. Test 13F was also subjected to further time domain analysis and will also be included.

33. Analysis was performed on the EG&G data by first re-copying and arranging the records in order of increasing depth. Then, arrival times, travel distances, and wave velocities were computed and tabulated.

34. Tests 1F, 2F, and 3F were conducted at two different hole spacings. Tests 1F and 2F were between holes G and F over a distance of about 33 feet. Test 3F was conducted between holes H and F over a distance of 65 feet.

35. Test 1F. Test 1F was a common depth crosshole test illustrated in Figure 5. The time domain signals recorded at each depth are shown in Figure 13. Table 1 is a tabulation of P-wave arrival times and associated

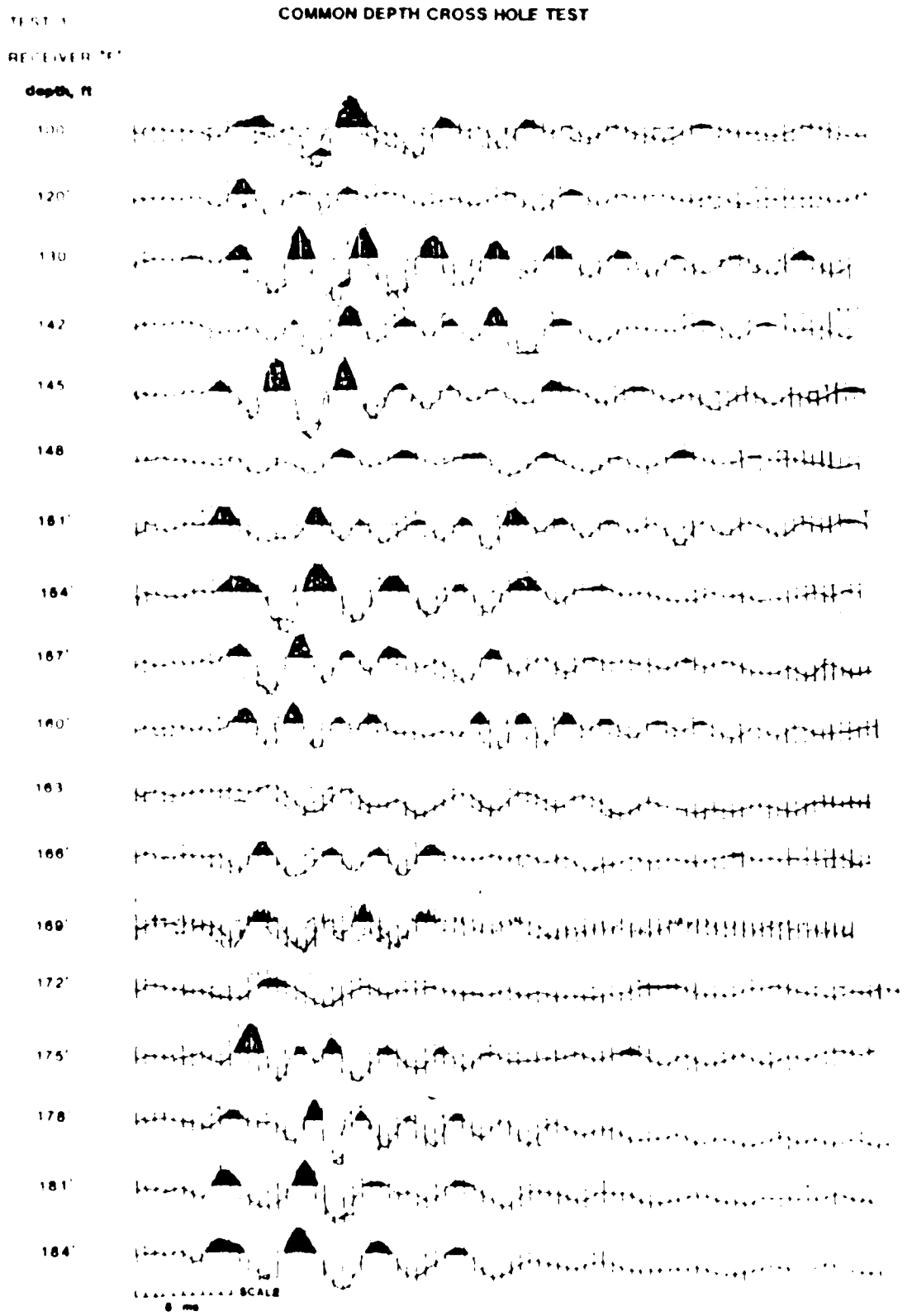

Figure 13. EGAG time domain records, test 1F

velocities. Test 1F showed consistent arrival times of 3.5 msec until a depth of 166 feet was reached. At this time, the presence of the tunnel can be seen. Within the tunnel zone, time delays of about 1 msec or a total lapsed time of 4.5 msec were prevalent. As testing progressed below the bottom of the tunnel, the P-wave arrival, once again, occurred at 3.5 msec until a more competent zone was reached at a depth of 184 feet, at which time the P-wave arrival decreased to 2.5 msec. Velocities are plotted as a function of depth in Figure 14. They averaged about 9,400 fps above the tunnel to a low of 7,300 fps when the tunnel was encountered. The competent zone, at a depth of 184 feet, exhibited a P-wave velocity of 11,000 to 13,000 fps. Observing the time domain signal, one can see an apparent phase shift and the signal is severely attenuated because of the presence of the tunnel.

36. Test 2F. The plan and profile views of Test 2F are shown in Figure 6. The test was conducted by holding the source constant in boring G at a depth of 162 feet and moving the receiver in 3-foot increments in hole F. This resulted in a fan-type pattern. Observing the time domain plot in Figure 15, the first arrivals of the P-wave were determined and tabulated in Table 2. The shortest distance between source and receiver would, of course, be at a depth of 162 feet. As the receiver moved in 3-foot increments above and below this point, the distances to the receiver increased. Using these distances divided by the appropriate arrival times, apparent velocities were computed and plotted as a function of receiver depth in Figure 16. This presentation yielded a rather explicit "picture" of the tunnel because of the radical decrease in the velocity when the wave travel path was interrupted. The test conducted at a depth of 162 and 163 feet showed marked decreases in signal amplitude. However, an increase in amplitude was noted from a depth of 167 feet to 184 feet. This apparent increase in amplitude could not be explained.

37. Test 3F. Test 3F was a common depth crosshole test with the seismic source placed in hole H and receivers simultaneously in holes F and E. Plan and profile views are shown in Figure 7. The data acquired in hole E were not of sufficient quality to warrant in-depth analysis. This was because the decision was made to keep all gain controls at the same setting so that relative comparisons between different locations could be made at any time. As a consequence, the amplitudes were too low for accurate measurement of first arrival times. Figure 17 is the EG&G time domain signal recorded in hole F. The tabulated velocities and first

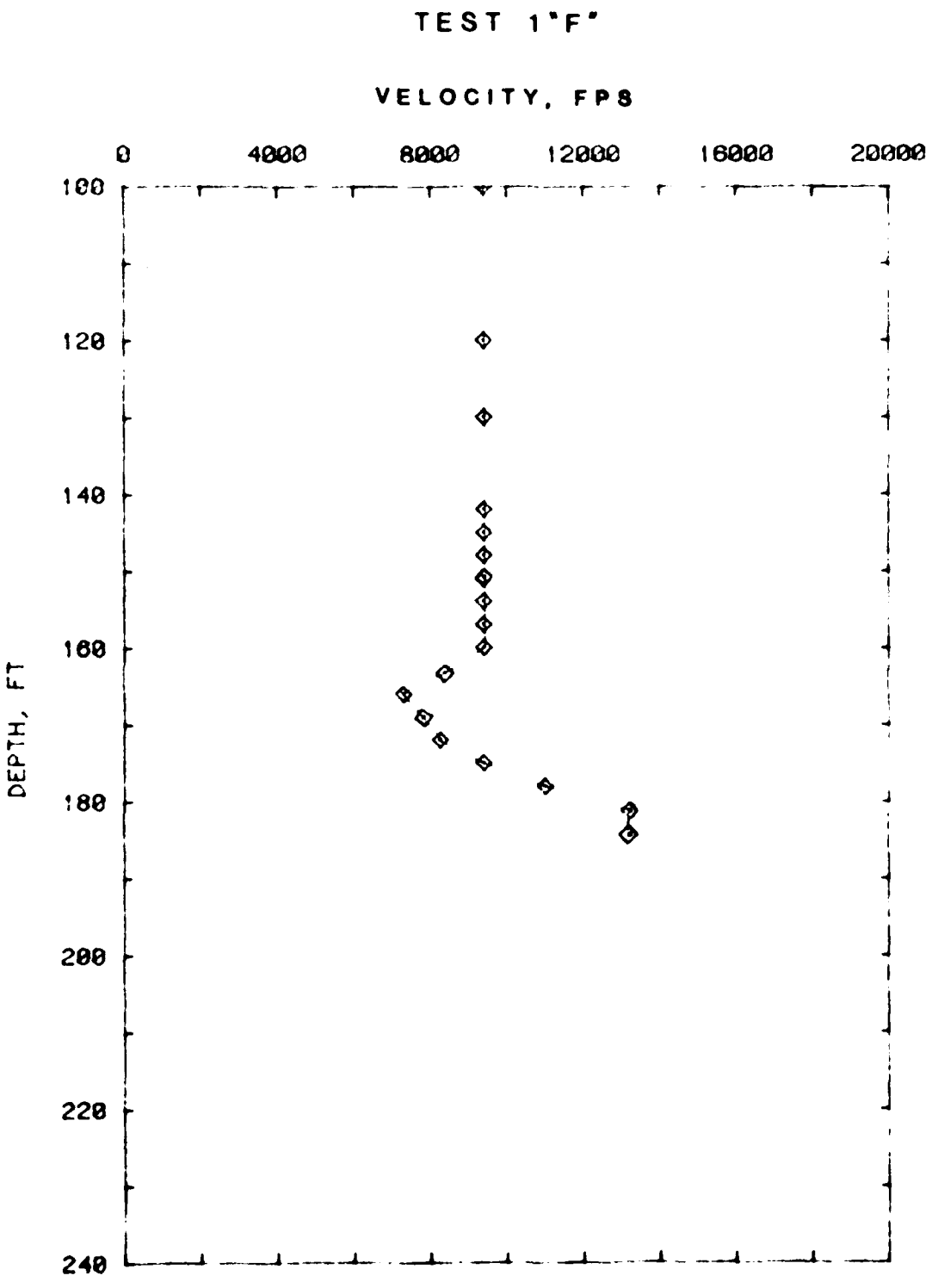

Figure 14. Velocity versus Depth, Test 1F

TANGENT TEST OR FAN OUT

TEST 2

RECEIVER "A"

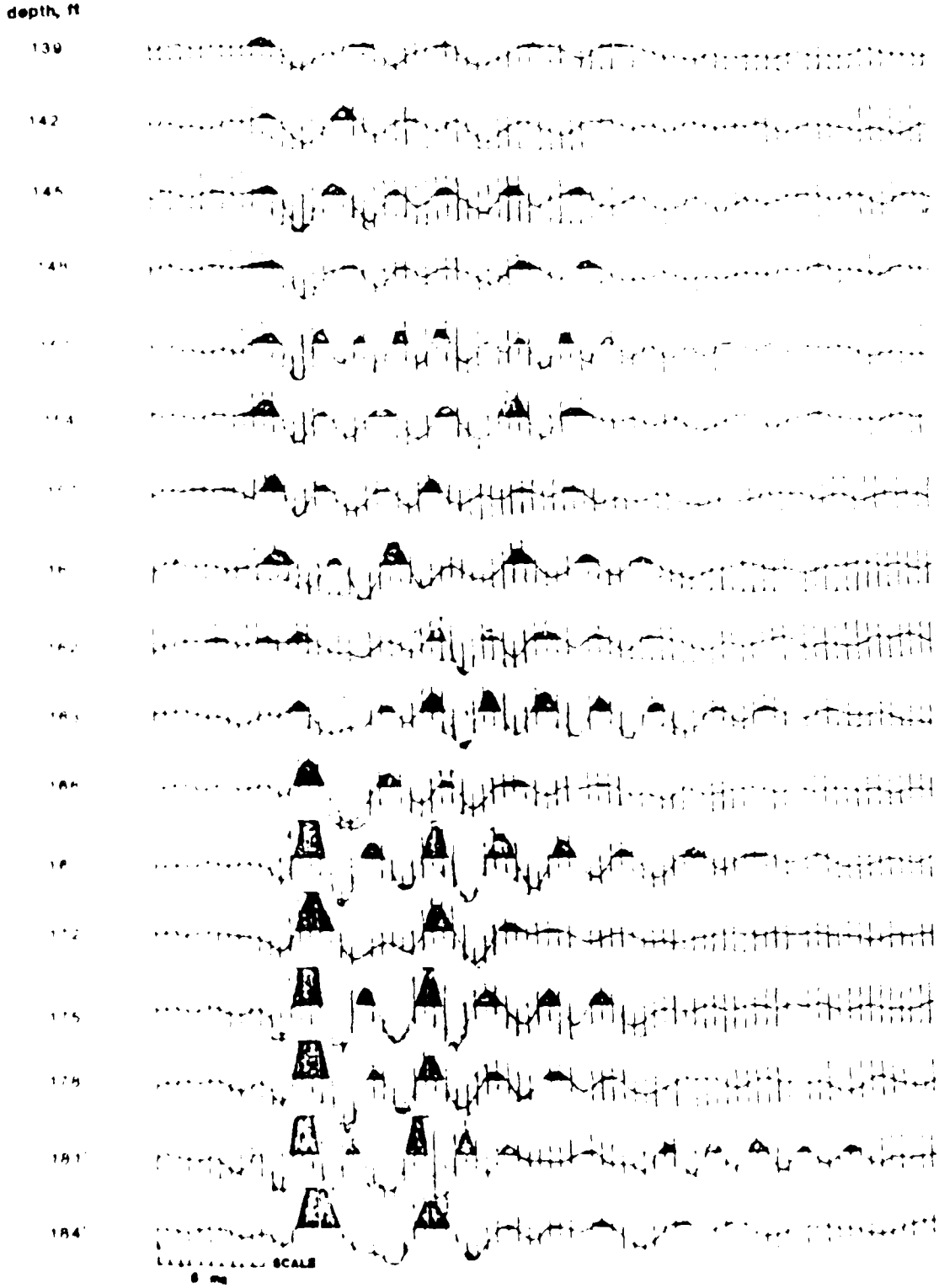

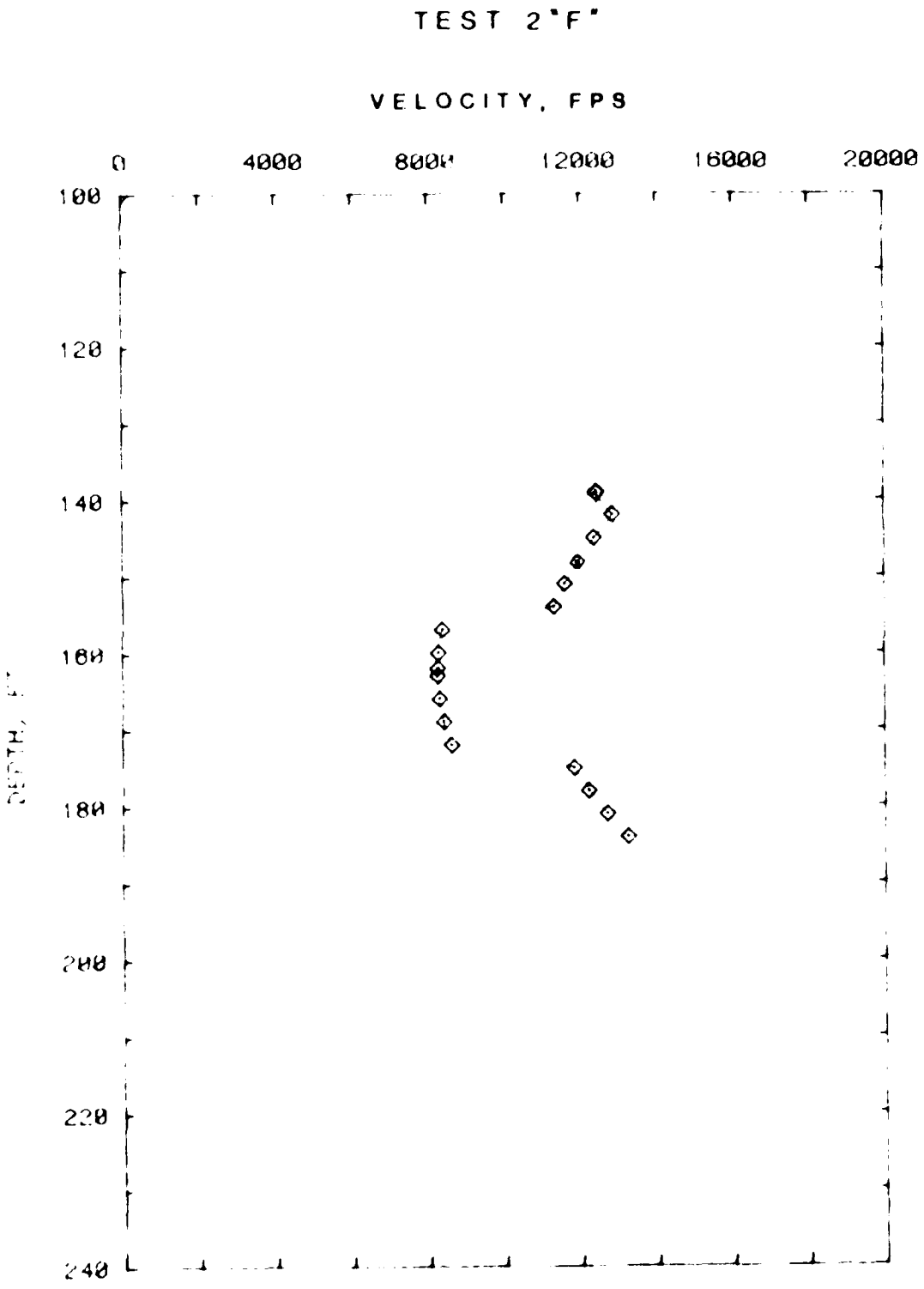

Figure [illegible]. Velocity versus Depth, Test 2F

TEST 3

RECEIVER "F"

COMMON DEPTH CROSS HOLE TEST

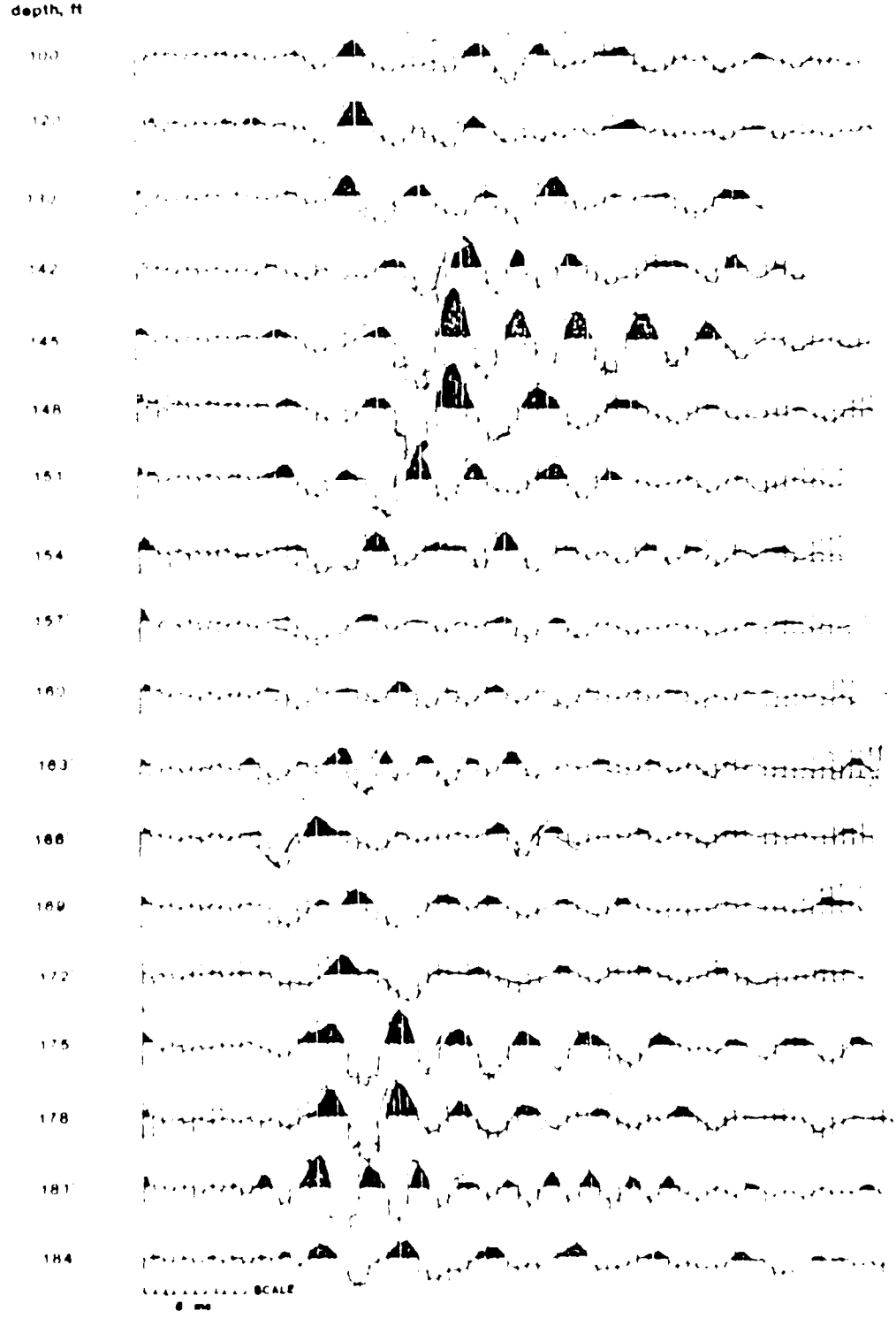

[illegible] data are shown in Table [illegible] and plotted graphically in Figure 18, [illegible] as a function of depth. Again, in this presentation the effect of the presence of the tunnel stands out. Figure 17, the time [illegible] also shows a pronounced [illegible] signal amplitude and a change [illegible] content in the area influenced by the tunnel's presence.

[illegible] Test 1b. Test 1b was conducted between borings [illegible] and [illegible], a distance [illegible] approximately [illegible] feet. The test configuration was termed common depth [illegible] the source and receiver were maintained at the same elevation for [illegible] test. Figure [illegible] shows the plan and profile views used in [illegible] test series. Figure 19 is the time domain signal recorded by the [illegible] [illegible] at each test depth. Table [illegible] is a tabulation of arrival times [illegible] computed velocities for each test point. Figure 20 is a plot of those velocities as a function of depth. Note that the velocities decrease in the zone where the tunnel is located.

[illegible] Test [illegible]. Test [illegible] was conducted between the same borings as 1b. [illegible] this case, however, the source was held constant at a depth of 162 feet [illegible] and the receiver moved in increments of 3 feet in hole [illegible]. The test configuration is shown in Figure 9. The time domain signal for all test points [illegible] shown in Figure [illegible]. It is interesting to note that the signal [illegible] at a depth of [illegible] feet corresponds directly to the test conducted at the same elevation in Test 1b. It is readily observed that the seismic signatures are virtually identical and an example of the repeatability of the [illegible] seismic system. Table [illegible] is the tabulation of arrival times, distances, and computed velocities obtained during Test [illegible]. Figure [illegible] is the graphic representation of velocity as a function of depth. It is interesting to note that the configuration of this test shows the construction trace [illegible] the tunnel. The anomalous zone created by the tunnel attenuates a great deal of the seismic energy and tends to smear the first arrival [illegible]. [illegible], the velocities calculated in the tunnel zone of [illegible] records are somewhat questionable.

[illegible] Test [illegible]. The common depth mode was used for the conduct of test [illegible]. The source was located in hole D and receiver in boring [illegible]. The approximate distance between source and receiver was [illegible] feet, as shown in the plan and profile views in Figure 10. The time domain signal as a function of depth is shown in Figure 23. The signal amplitude is noticeably greater in this test sequence than in the prior test. All gains remain the same.

TEST 3 "F"

VELOCITY, FPS

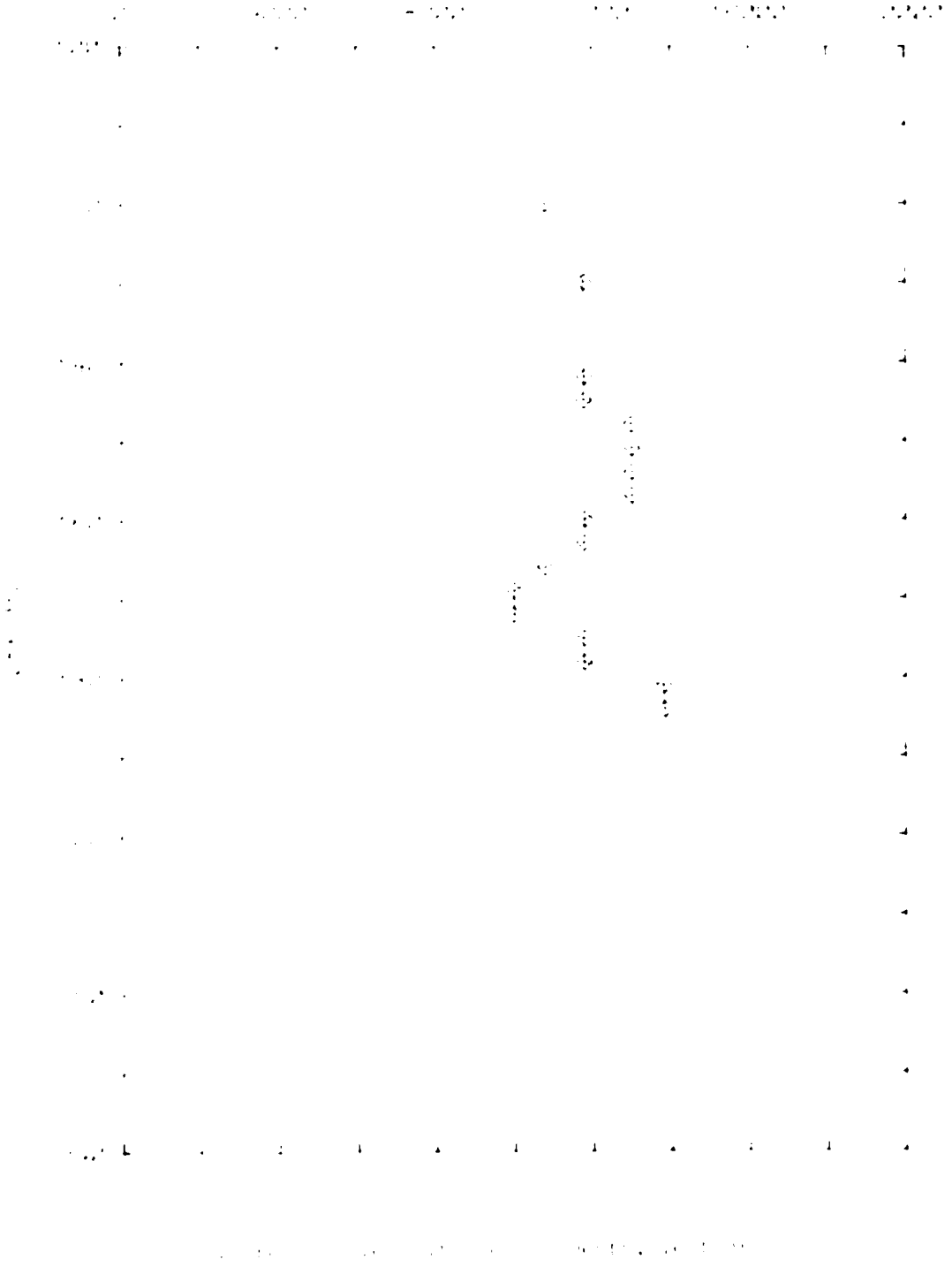

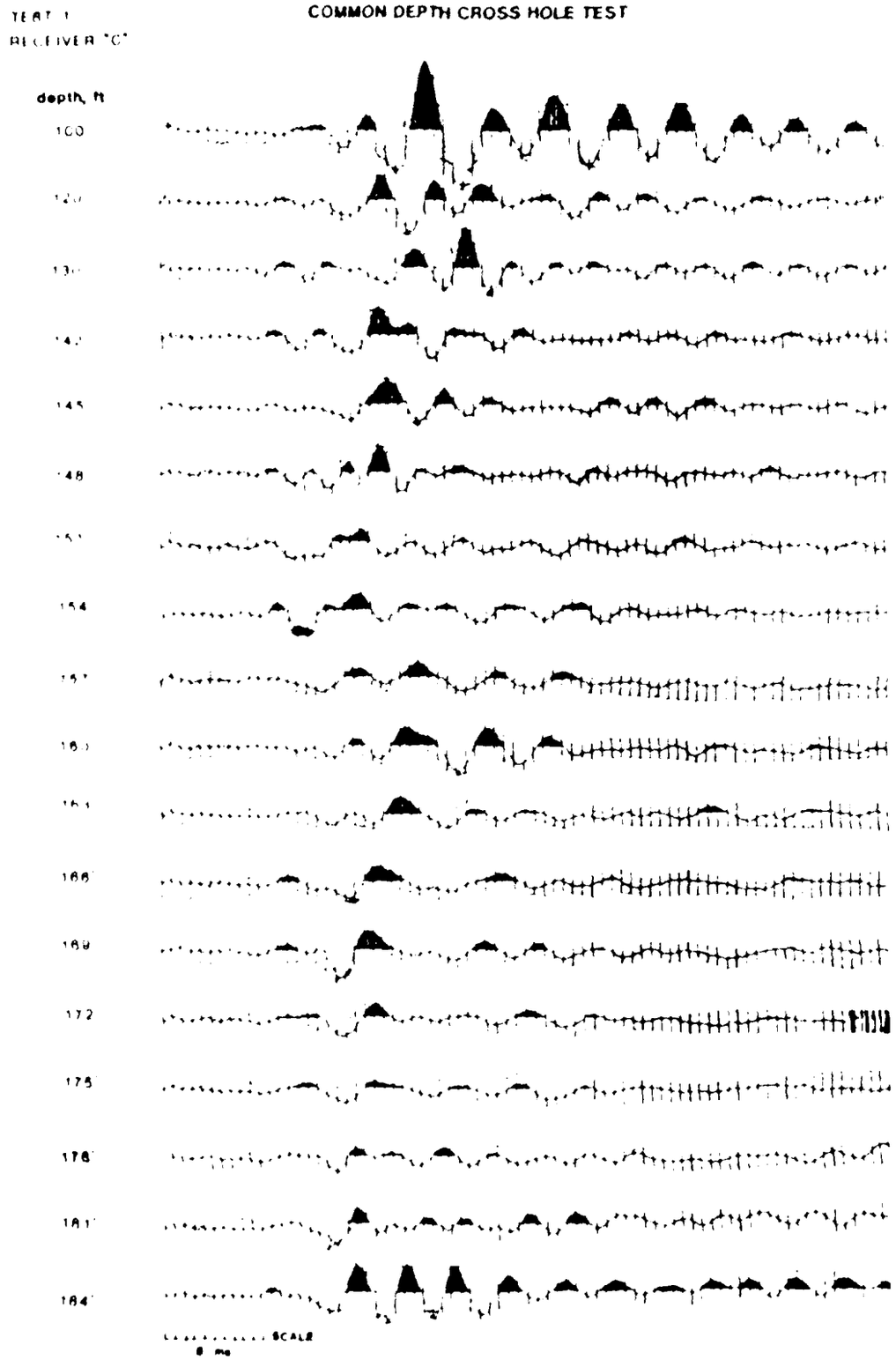

Figure 30. Field Time Domain Records, Test 10

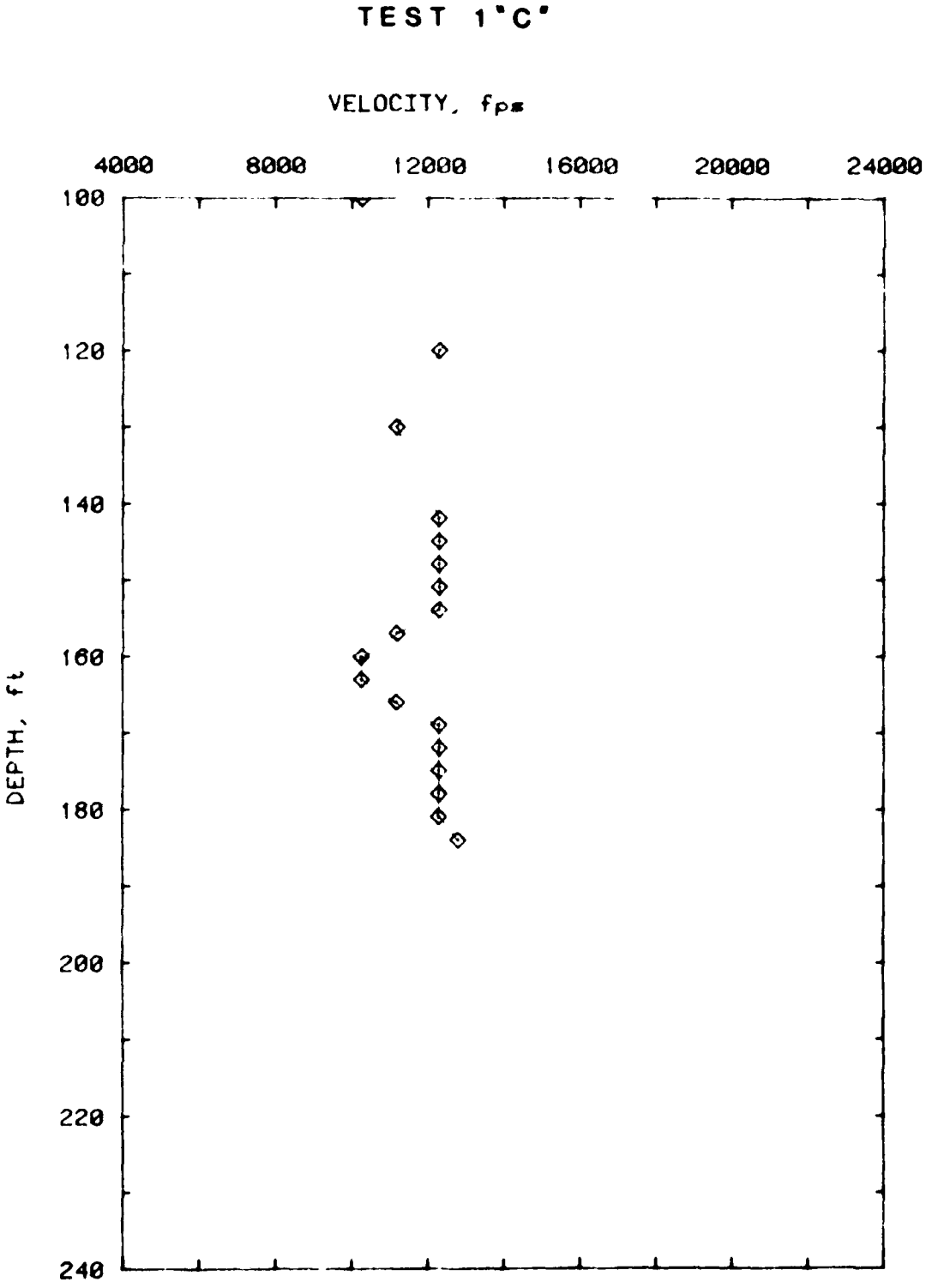

Figure 20. Velocity versus Depth, Test 1C

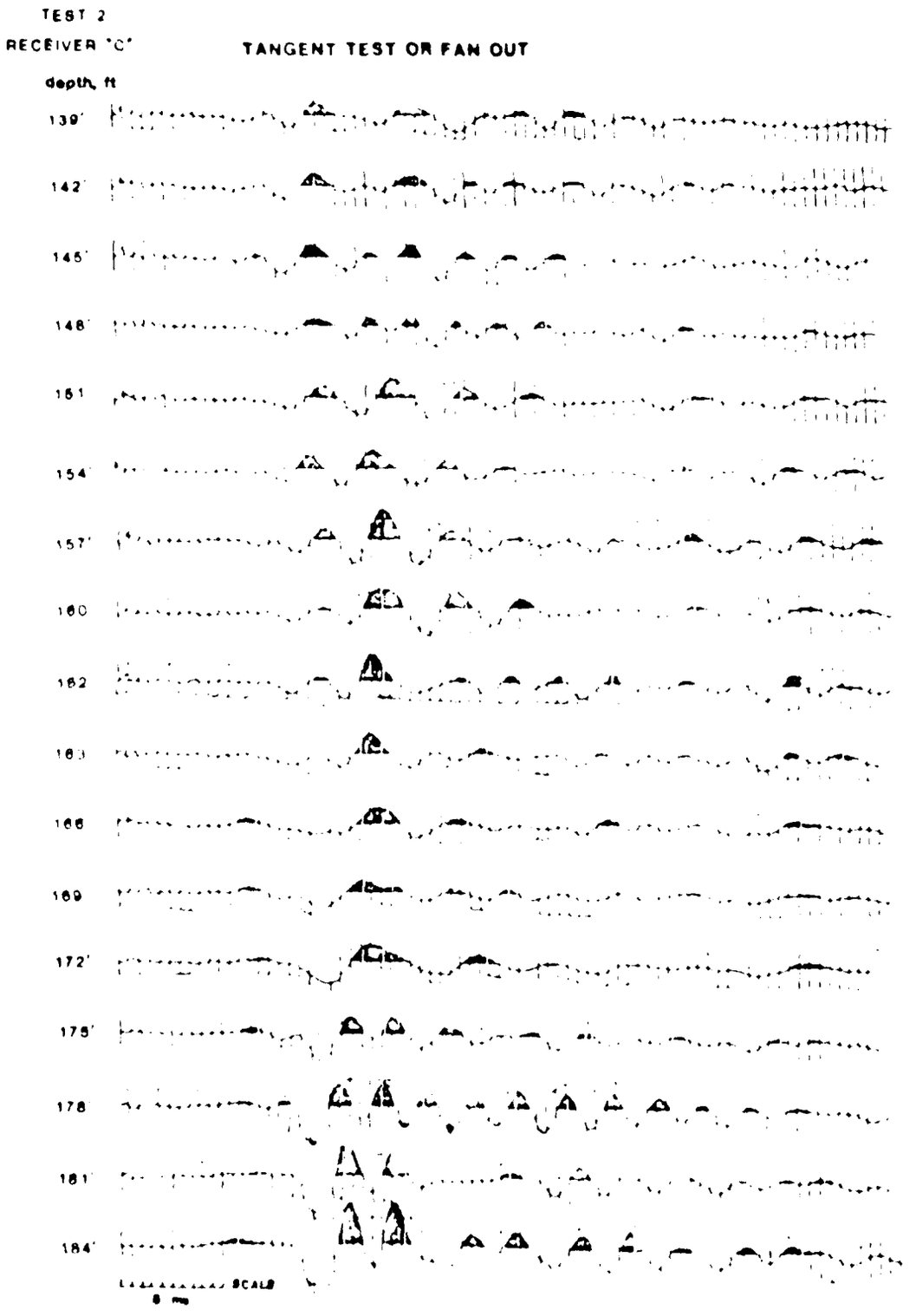

Figure 21. EGAG Time Domain Records, Test 2C

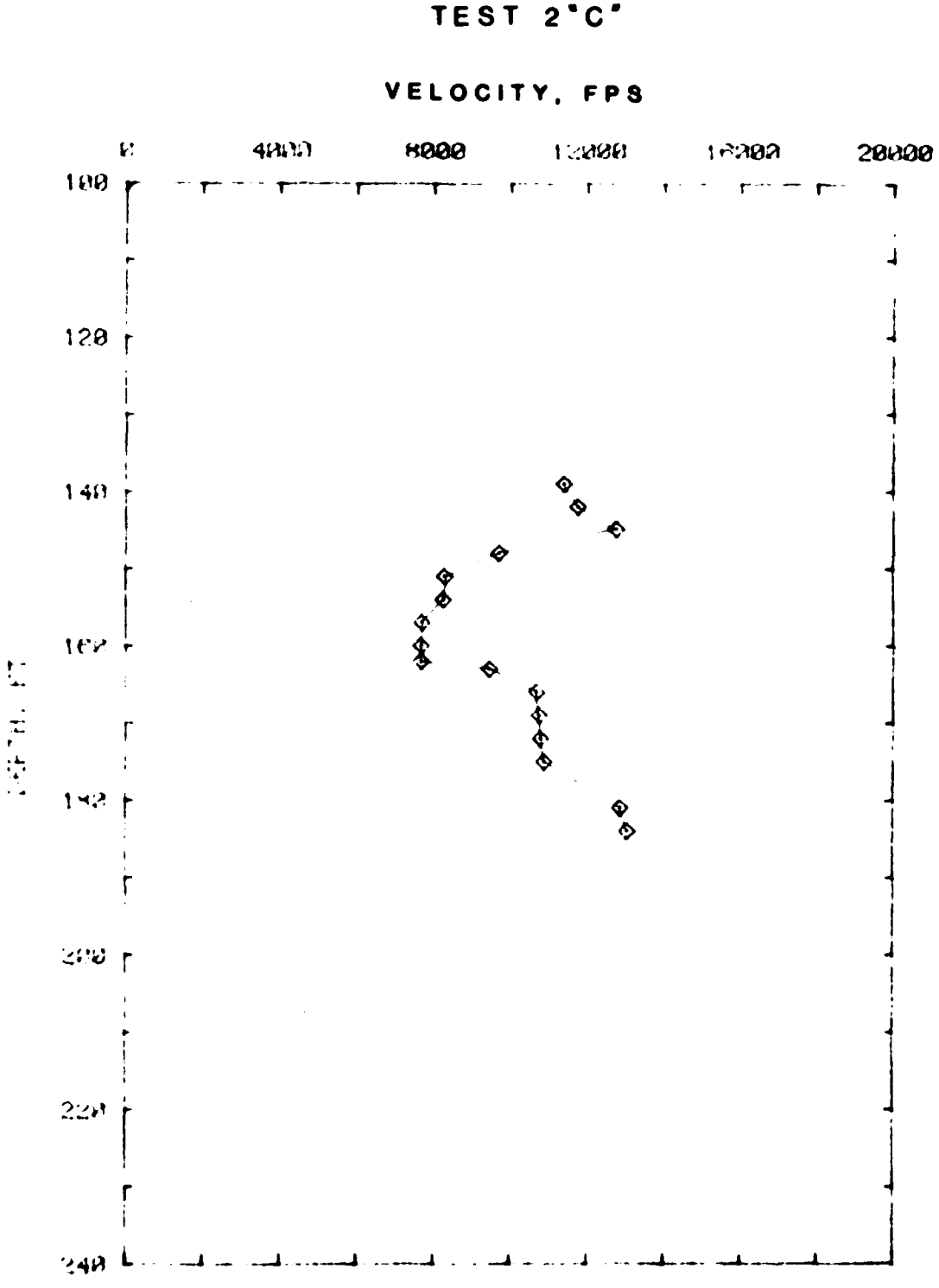

Figure 22. Velocity versus Depth, Test 2C

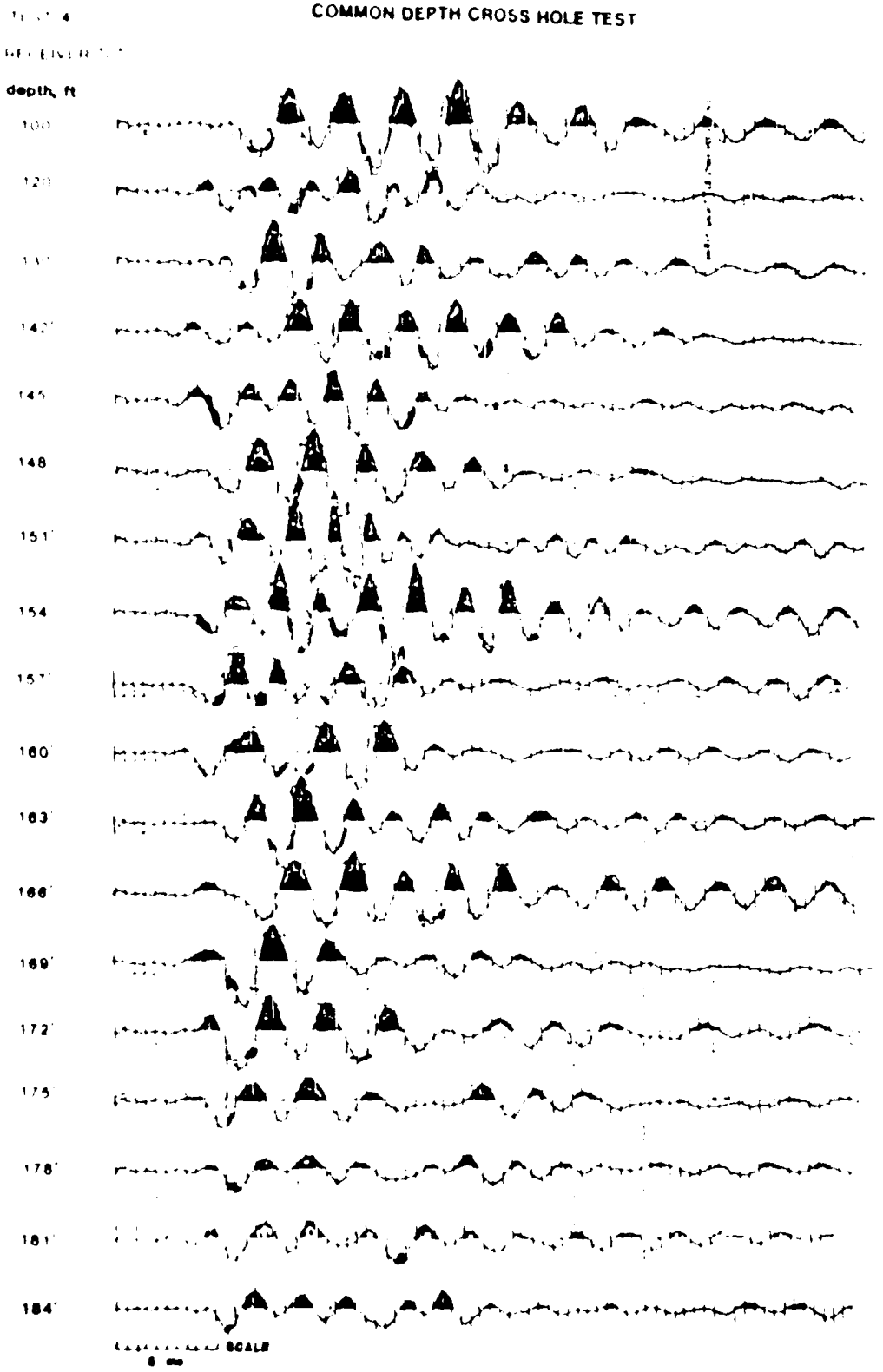

Figure [illegible] Typical Time Domain Records, Test [illegible]

but the tunnel was approximitely half way between source and receiver as opposed to the other test where the location of the tunnel is closer to either the source or the receiver. The tabulation of arrival time, distance, and associated velocities are shown in Table 6, and a plot of velocity as a function of depth is graphically displayed in Figure 24. The time domain signal shows not only time delay in the tunnel zone but a loss in amplitude and high frequency signal content.

41. Test 5C. Observing Figure 11, it will be seen that Test 5 was conducted between the same borings as Test 4. The test configuration was different, however, in that the source was maintained at a constant depth of 162 feet and the receiver moved in increments of 3 feet in borehole C to create a fan-type effect. The signal quality observed in Figure 25 (time domain as a function of depth) is quite good from a depth of 142 feet to 184 feet and the tests conducted at a depth of 163 feet, which is common with Test 4C, exhibit a comparable signature. The tabulation of arrival times and computed velocities are shown in Table 7, and the graphic display of these velocities as a function of depth is Figure 26. Although it will be observed that the general pattern of velocities shows a decrease in the area where the tunnel is located, the fan-type test does not appear to be as definitive as either the common depth or the offset depth tests for this case.

SIE records

42. Data acquired using the analog SIE seismograph and associated FM tape recorder were analyzed in greater detail than the previous data acquired with the EG&G unit. The previous section on data reduction discussed in some detail the procedures used to present the data in a manner favorable for in-depth analysis. This discussion of in-depth analysis contains only that data which was considered representative of the entire test series at the Idaho Springs site. Only those methods which were thought to have given a positive indication of the tunnel's presence are presented herein.

43. Fourier (FFT) analysis of the seismic wave train provided a great deal of additional information concerning the identification and delineation of tunnels located between boreholes. It was demonstrated that the FFT analysis provides data which allow the determination of the tunnel location from the frequency and amplitude effects of the wave train due to a tunnel-seismic signal interaction. Different portions of the tunnel cause different

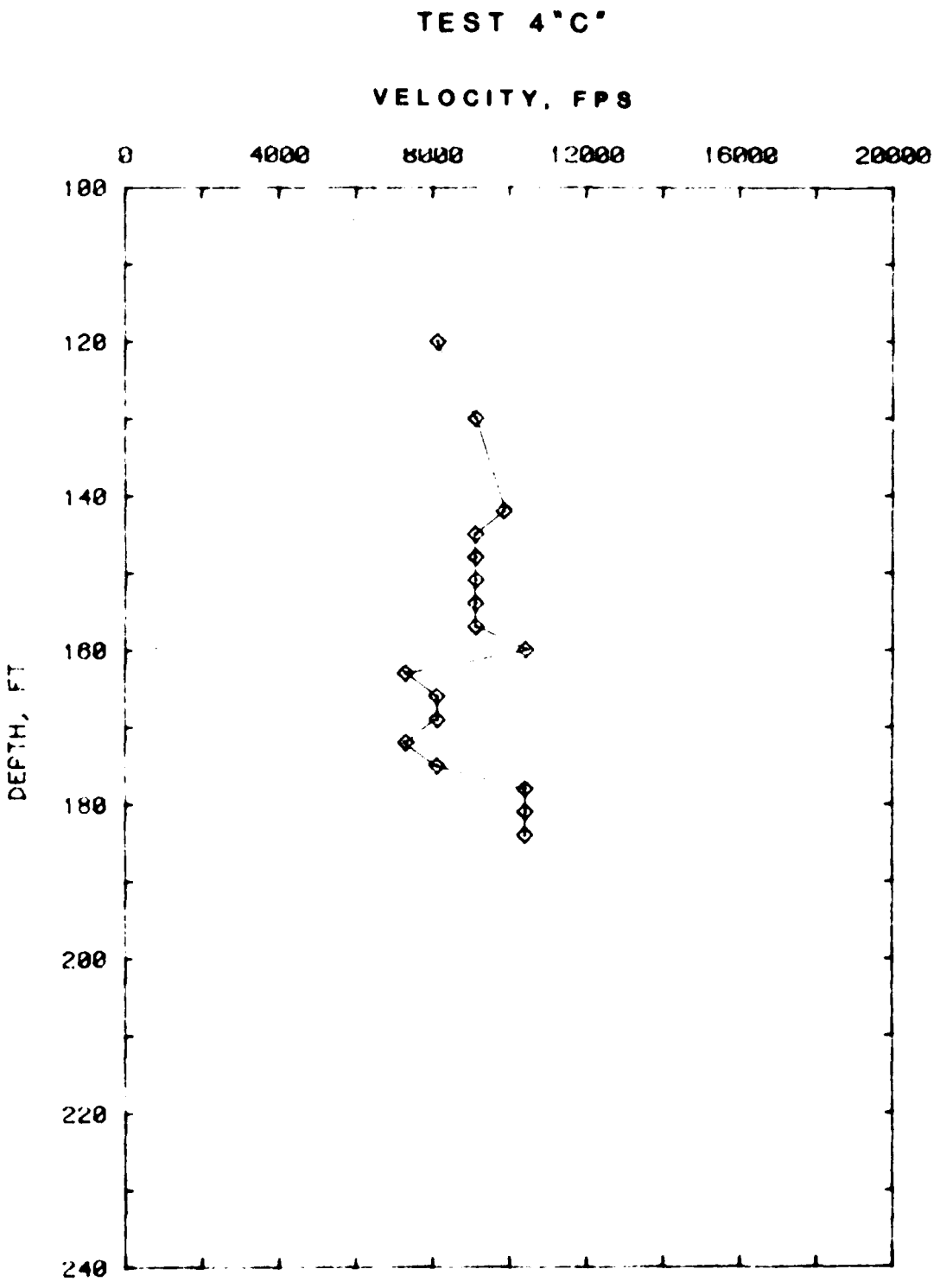

Figure 24. Velocity versus Depth, Test 4C

TANGENT TEST OR FAN OUT

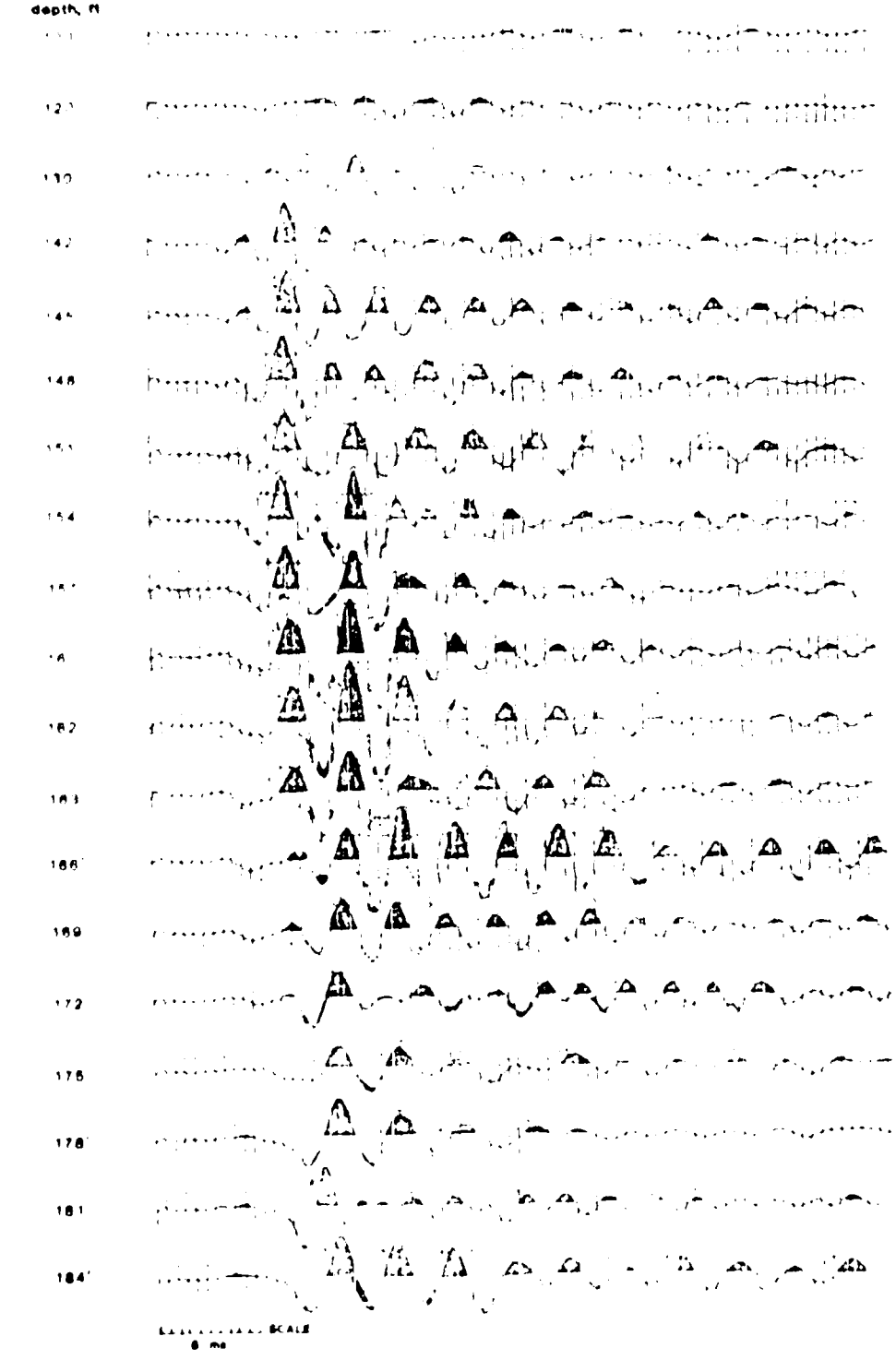

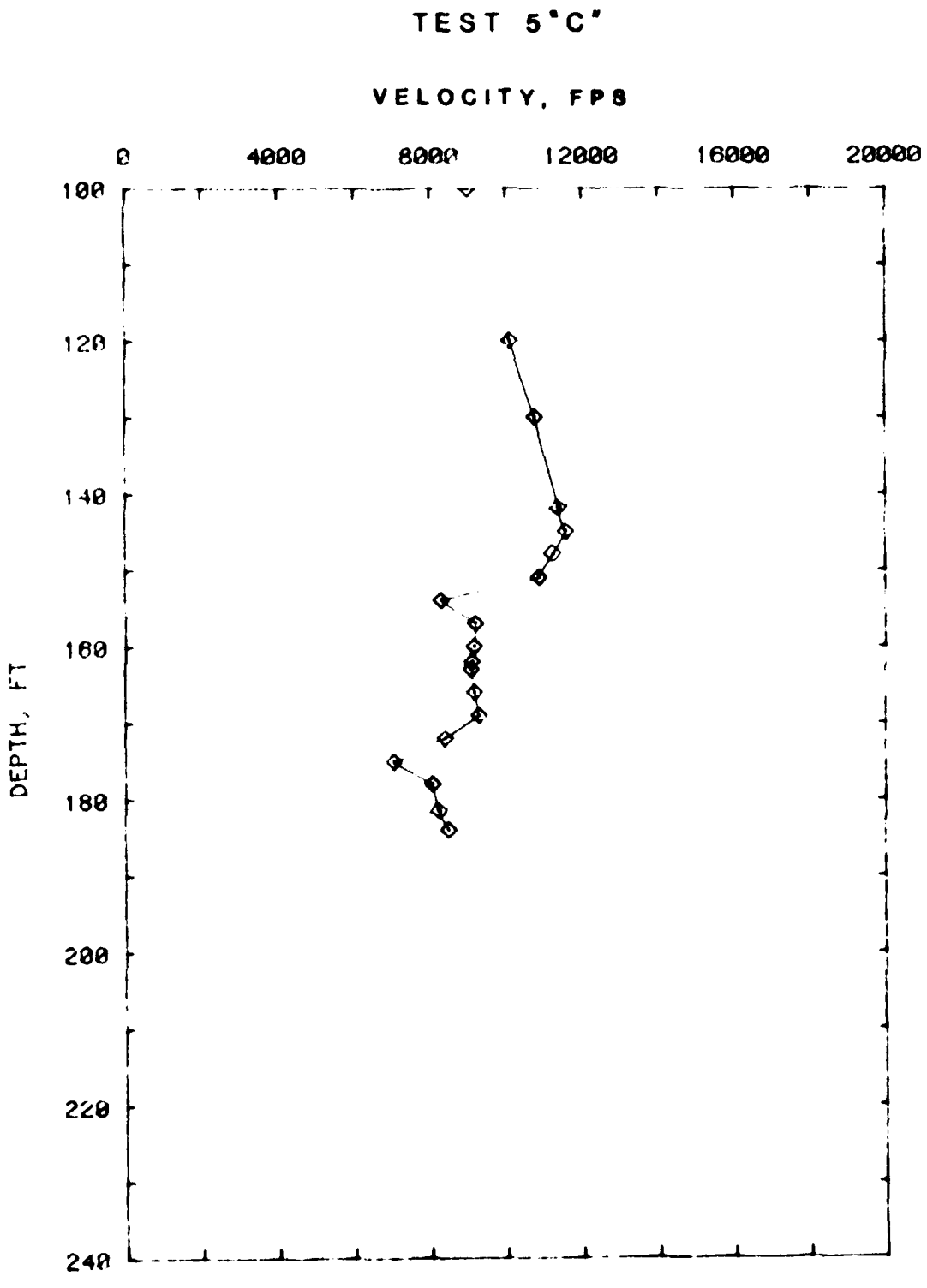

Figure 26. Velocity versus Depth, Test 5C

effects. These include [illegible] an energy shift to lower frequencies in the [illegible], and [illegible] amplitude attenuation. For each [illegible] seismic [illegible], the above effects can be displayed as [illegible] amplitude versus frequency of the Fourier analysis, and [illegible] cumulative energy of increasing frequencies in the wave train. The latter is a cumulative summation of the energy [illegible] the wave train starting at low frequencies [illegible] to higher frequencies [illegible]. The [illegible] and [illegible] above can then be arranged from top to bottom [illegible] in order to visually inspect the [illegible] changes which [illegible] place [illegible] from a cavity interaction.

[illegible] Test [illegible] (Frequency Domain). In this crosshole test of [illegible] feet, [illegible] (Figure 27), a normal frequency and amplitude [illegible] [illegible] 145, 151, [illegible], 178, and 181 feet, as shown in Figure 28. [illegible] have retained half of the energy [illegible] between [illegible] locations 100 and 12[illegible] feet have lower amplitudes as a result [illegible] rock joints which occur closer to the ground surface. This [illegible] typical for granitic rock and amplitudes will generally continue [illegible] as the surface is approached. Amplitude effects from signal-tunnel interaction [illegible] starting at shot 1[illegible] and continuing to 166 feet [illegible] over all frequencies [illegible] recorded. [illegible] the fractured area in tension above the tunnel (154, 157, [illegible] feet) and the fractured area in tension around the top half of the [illegible] 16[illegible] feet) cause a large decrease in signal amplitudes in [illegible] Hz range. These portions of the tunnel are behaving as a [illegible] filter, passing low frequency energy but absorbing that at higher [illegible]. The [illegible] half of the tunnel (160 and 172 feet) is behaving [illegible] absorbing a large percentage of the energy above [illegible] and transferring some of the signal to the 1.0 to 220 Hz range, thus [illegible] portion of the spectrum. This area of the tunnel [illegible] a filter with portions of the filter function being greater than [illegible]. In other words, this is derived from a non-linear filter process.

[illegible] Test [illegible] (Frequency Domain). This test demonstrates different characteristics than those documented in Tests 3F and 13F. These changes may be accounted by the different source/receiver geometry (Figure 29). In this test a normal seismic signal was received at all geophones except

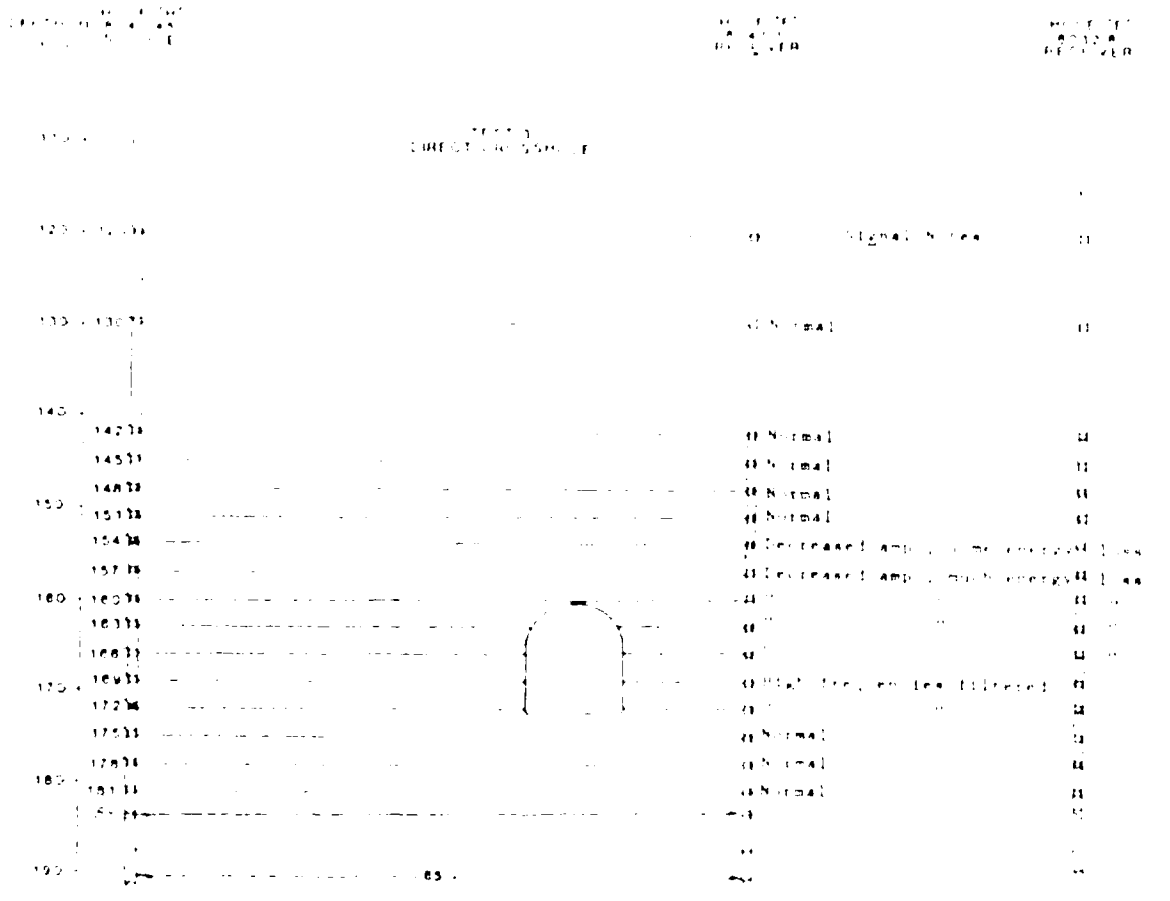

Figure [illegible] — [illegible] Receiver Geometries, Test [illegible]

Fourier Analysis and Signal Energy Summation Plots for Test 3 F

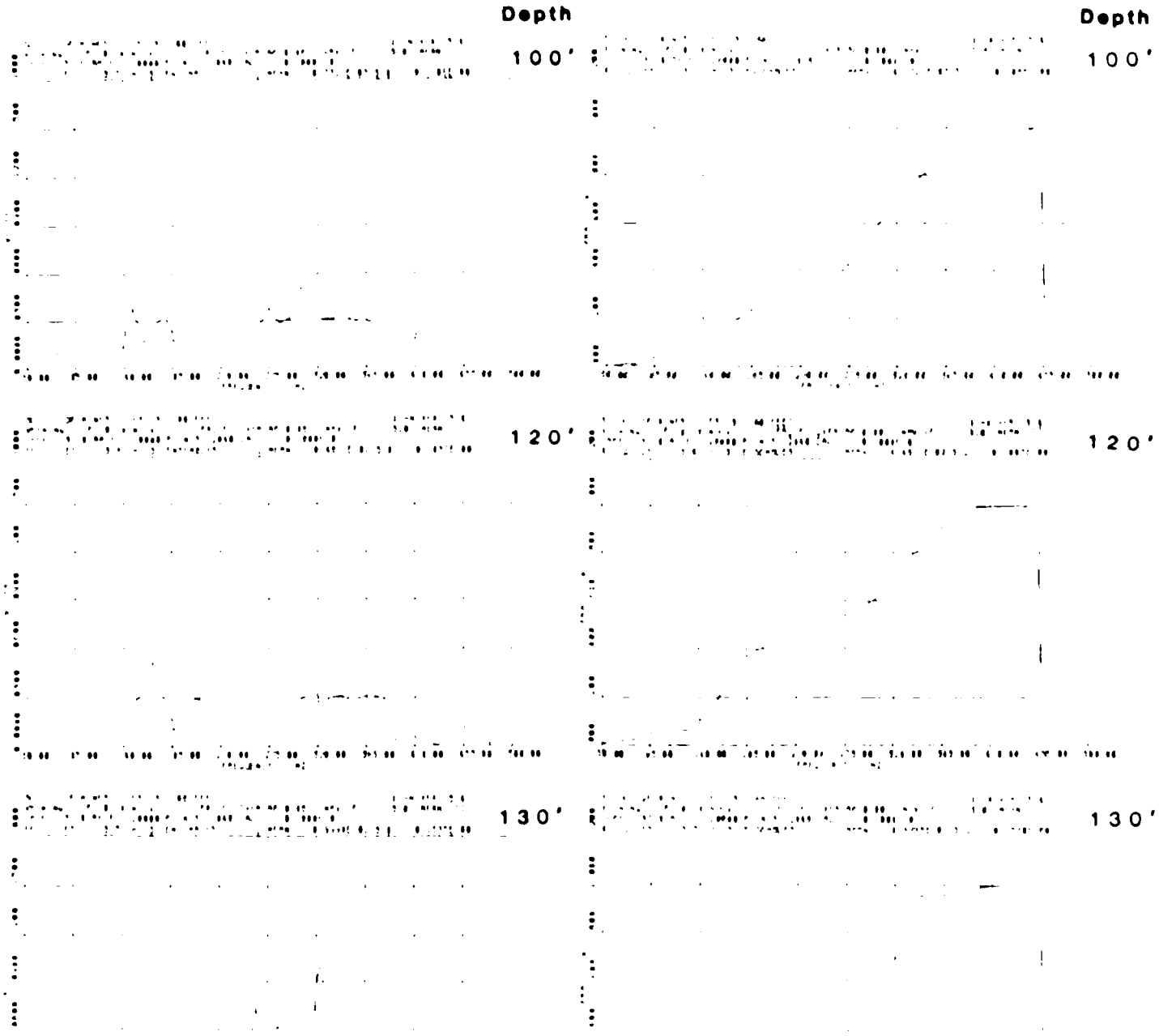

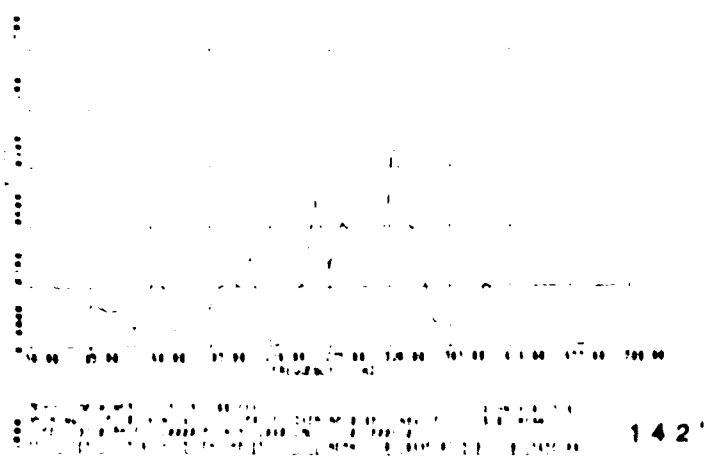
142'


142'

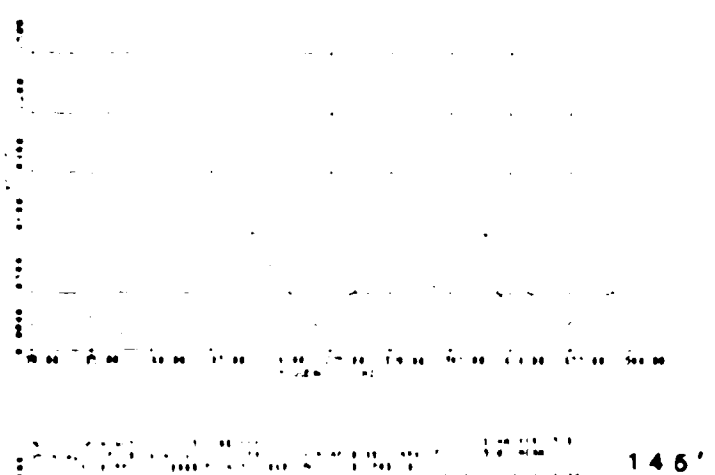
146'

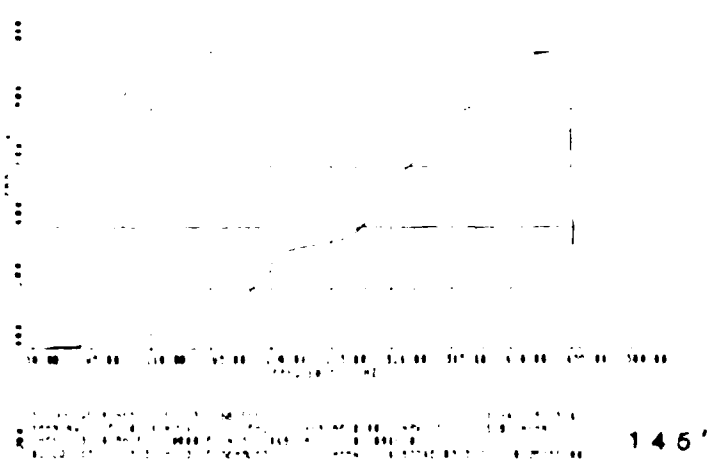
146'

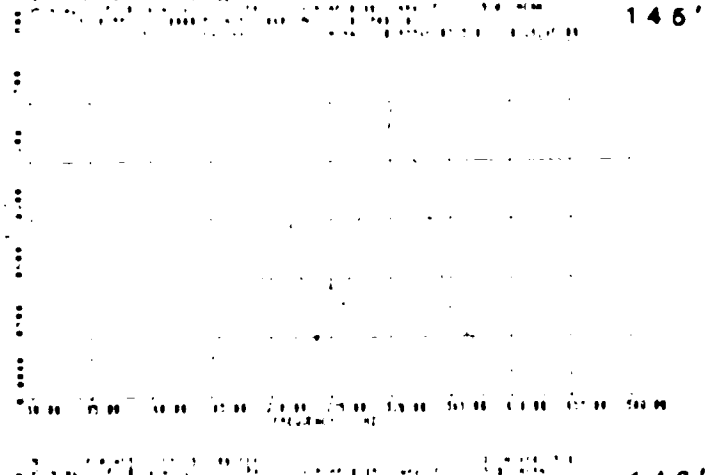
148'

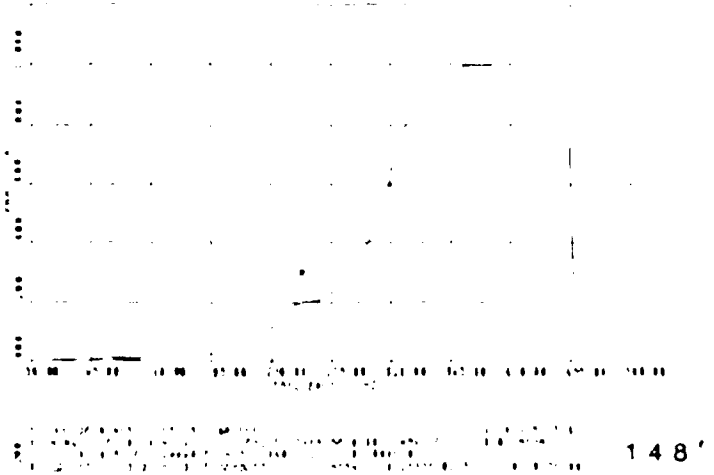
148'

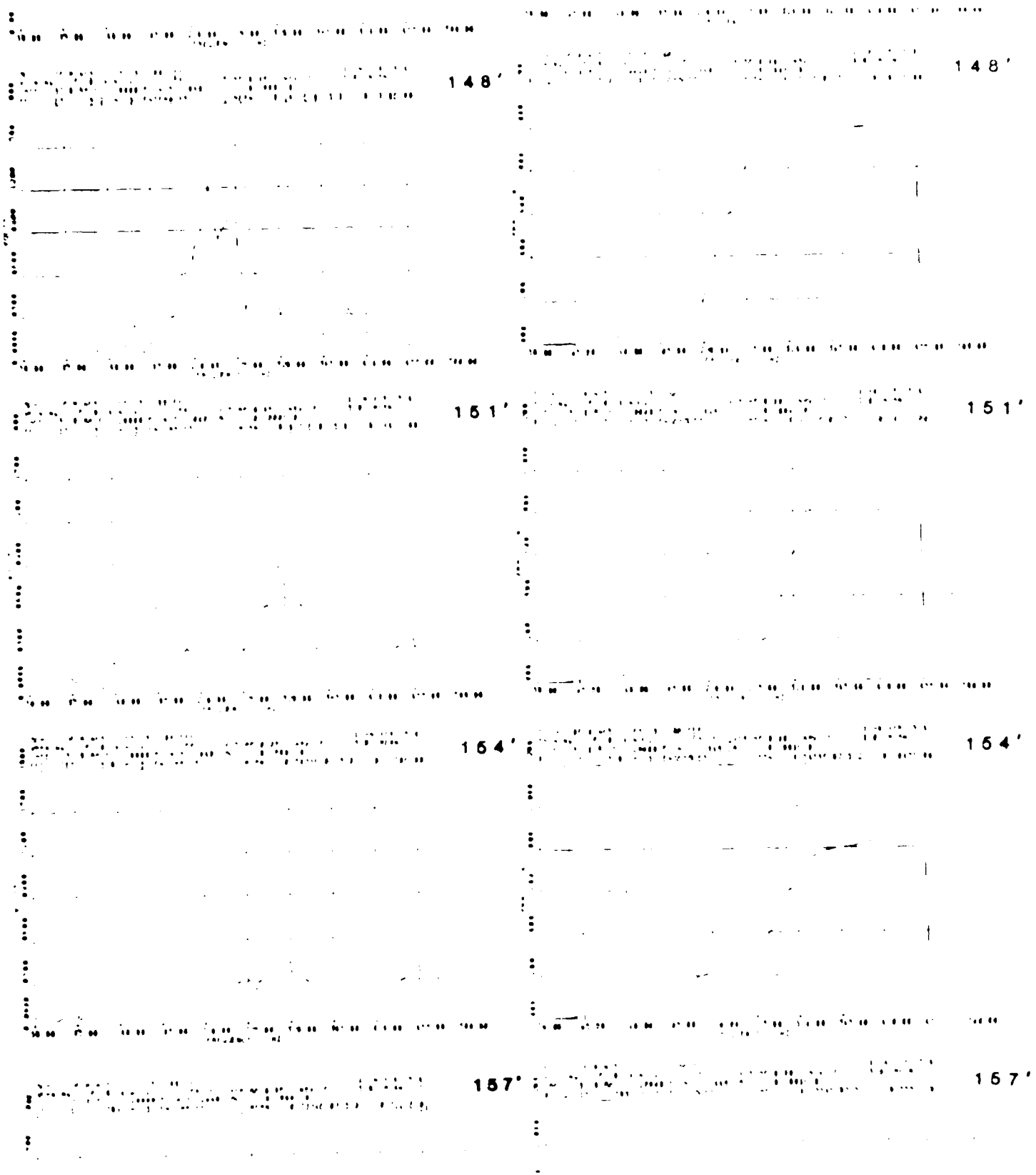
148'
148'
151'
151'
154'
154'
157'
157'

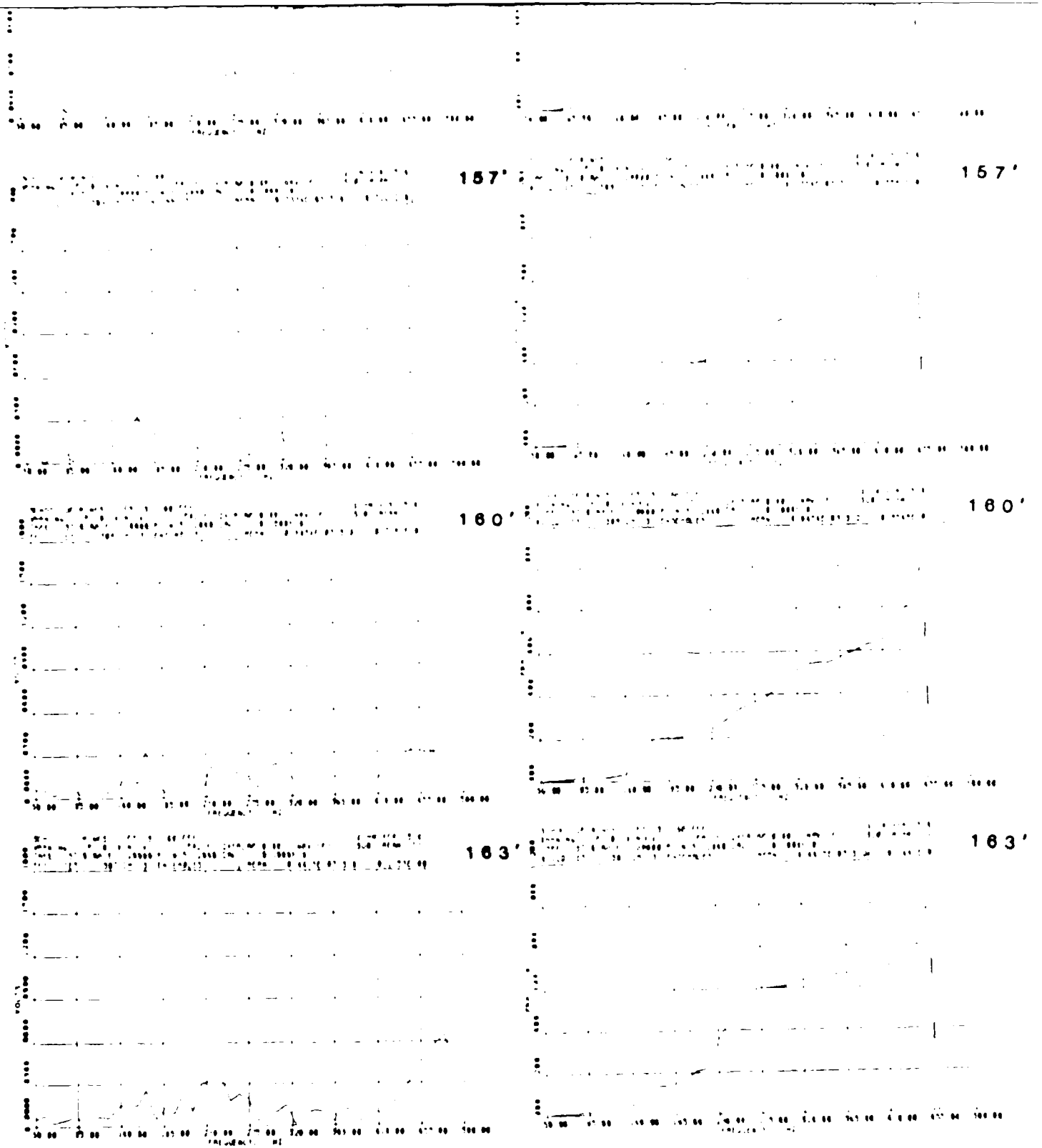
157'
157'
160'
160'
163'
163'

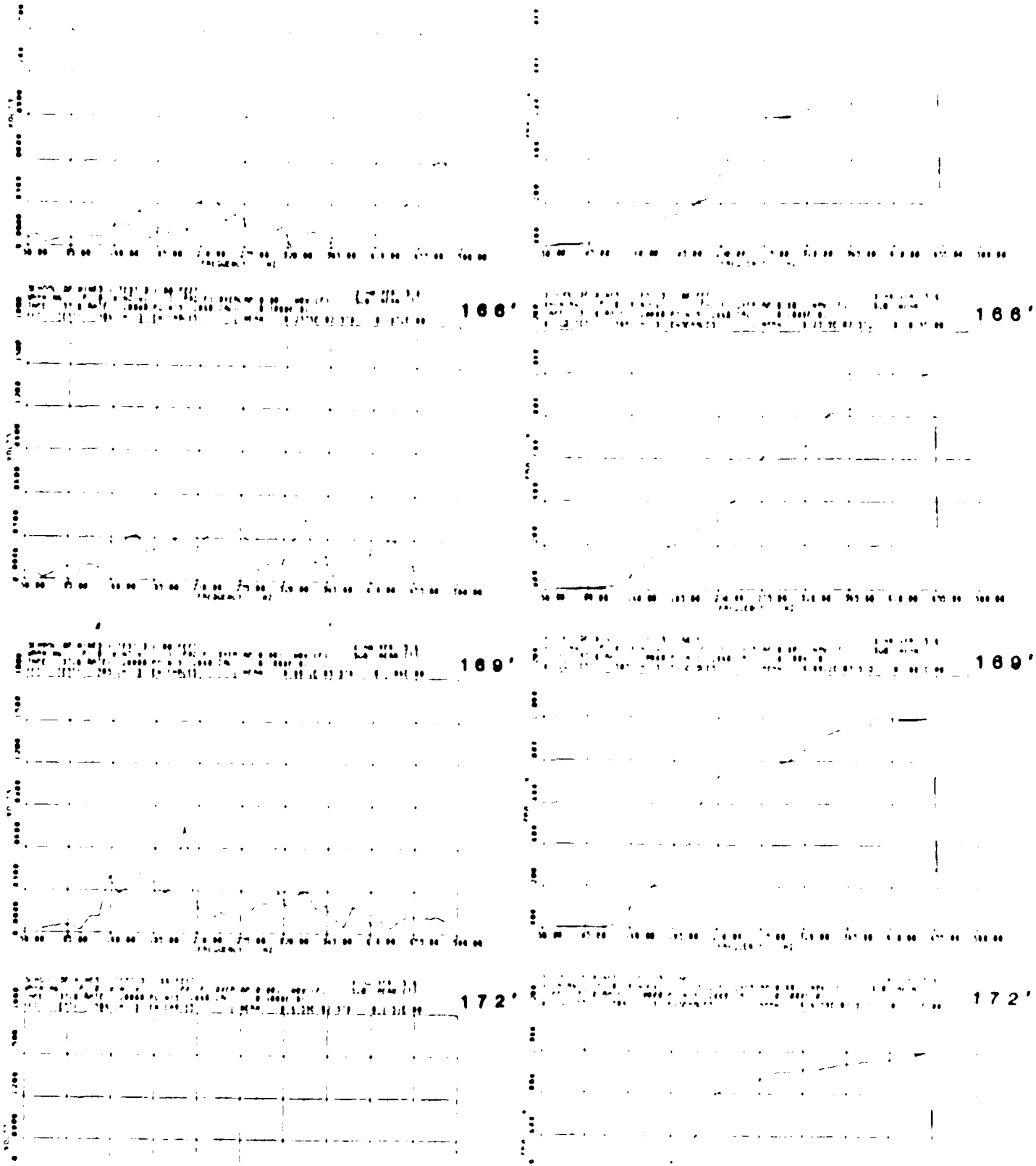
166'
166'
169'
169'
172'
172'

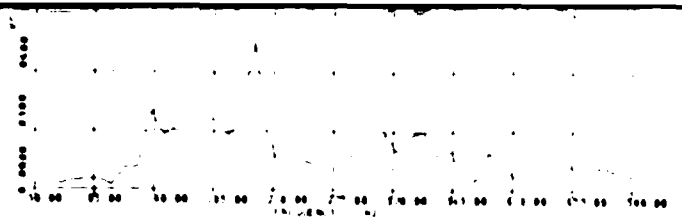

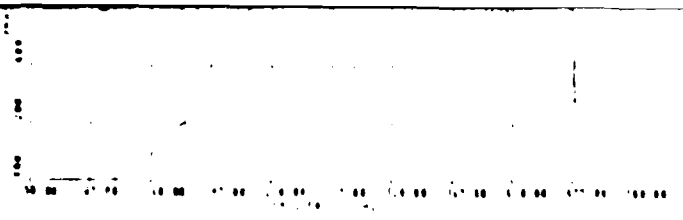

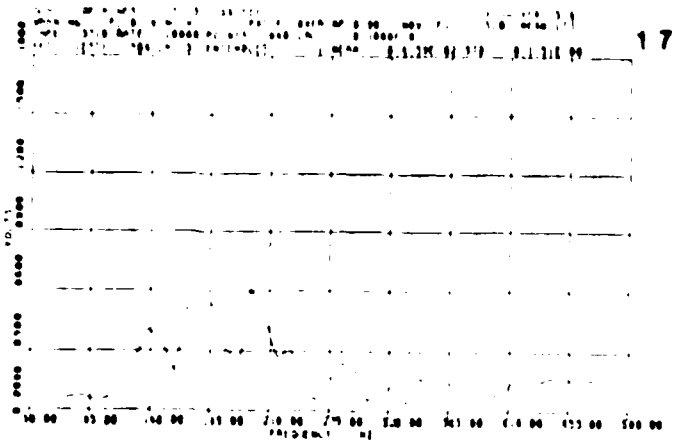
172'

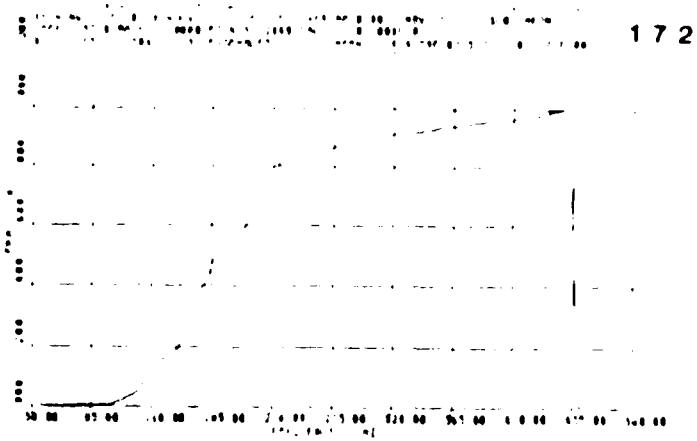
172'

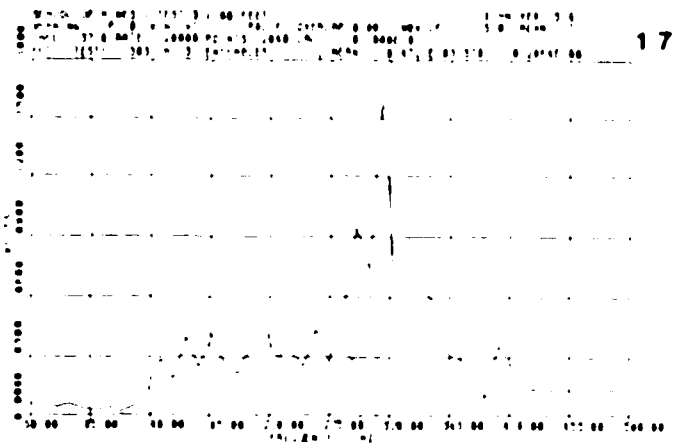
176'

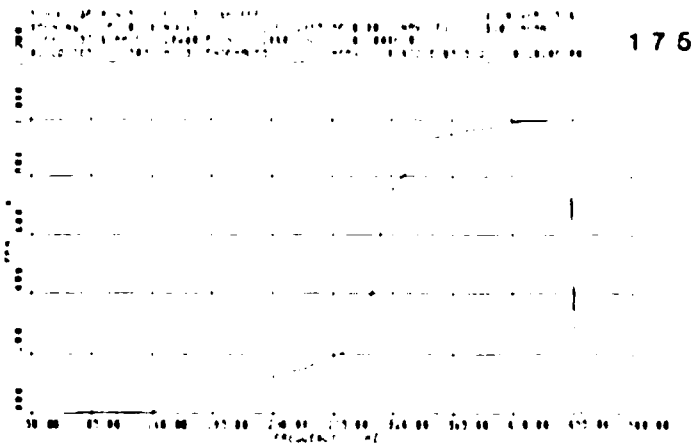
176'

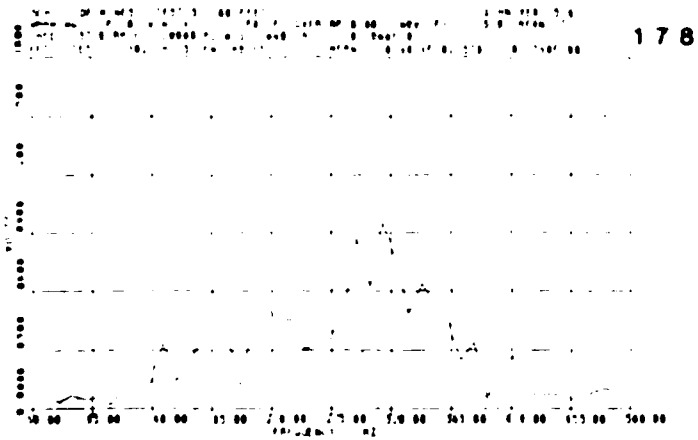
178'

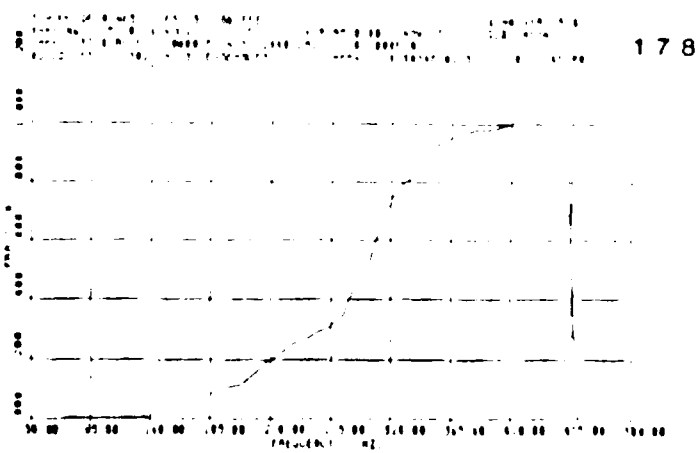
178'

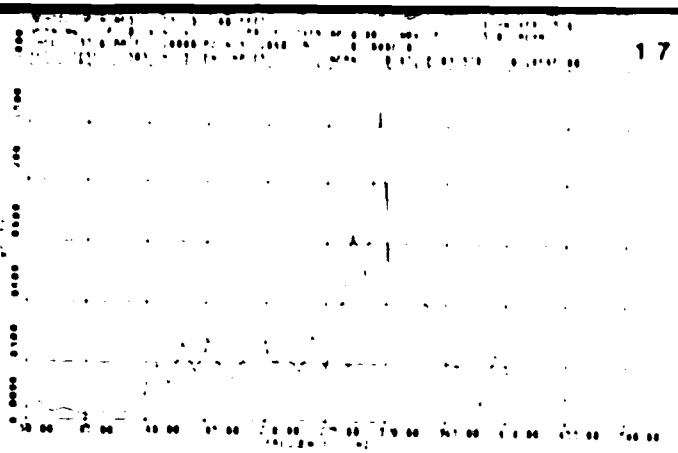
176'

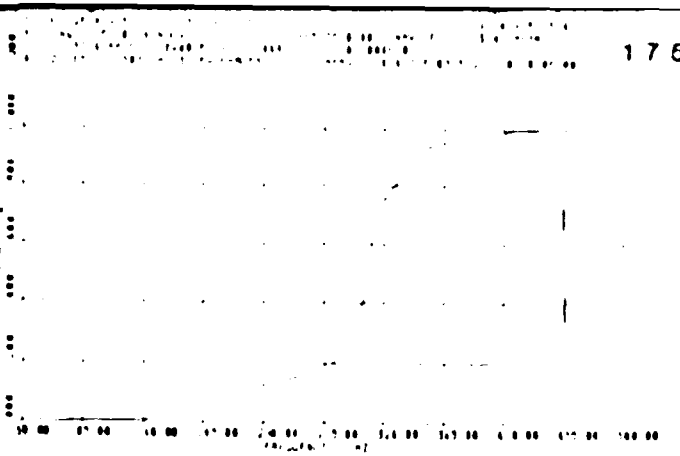
176'

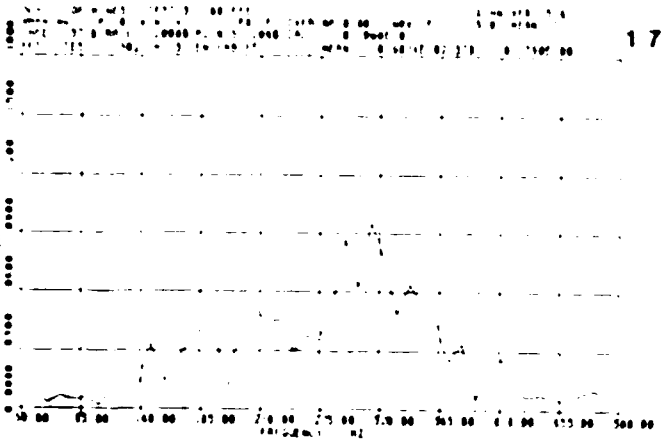
178'

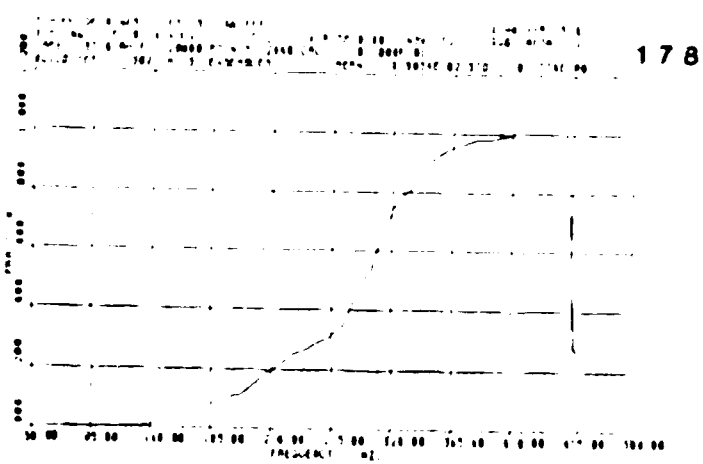
178'

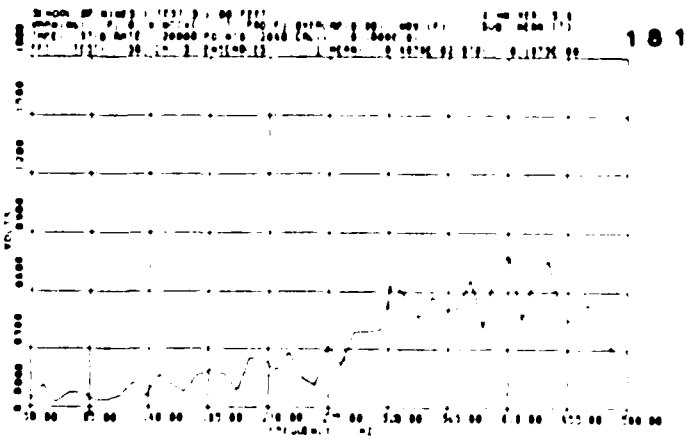
181'

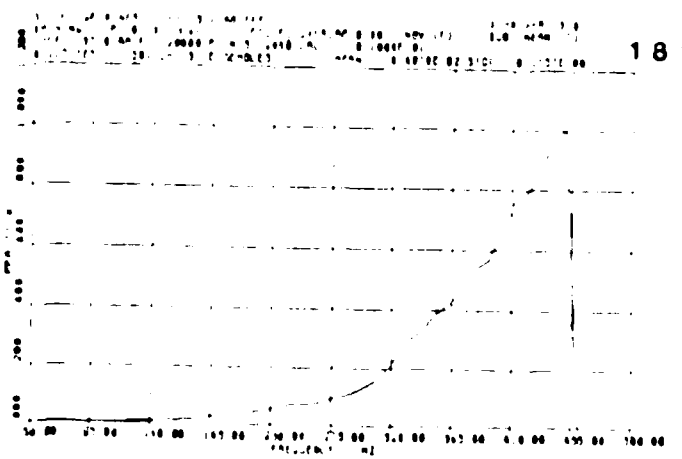
181'

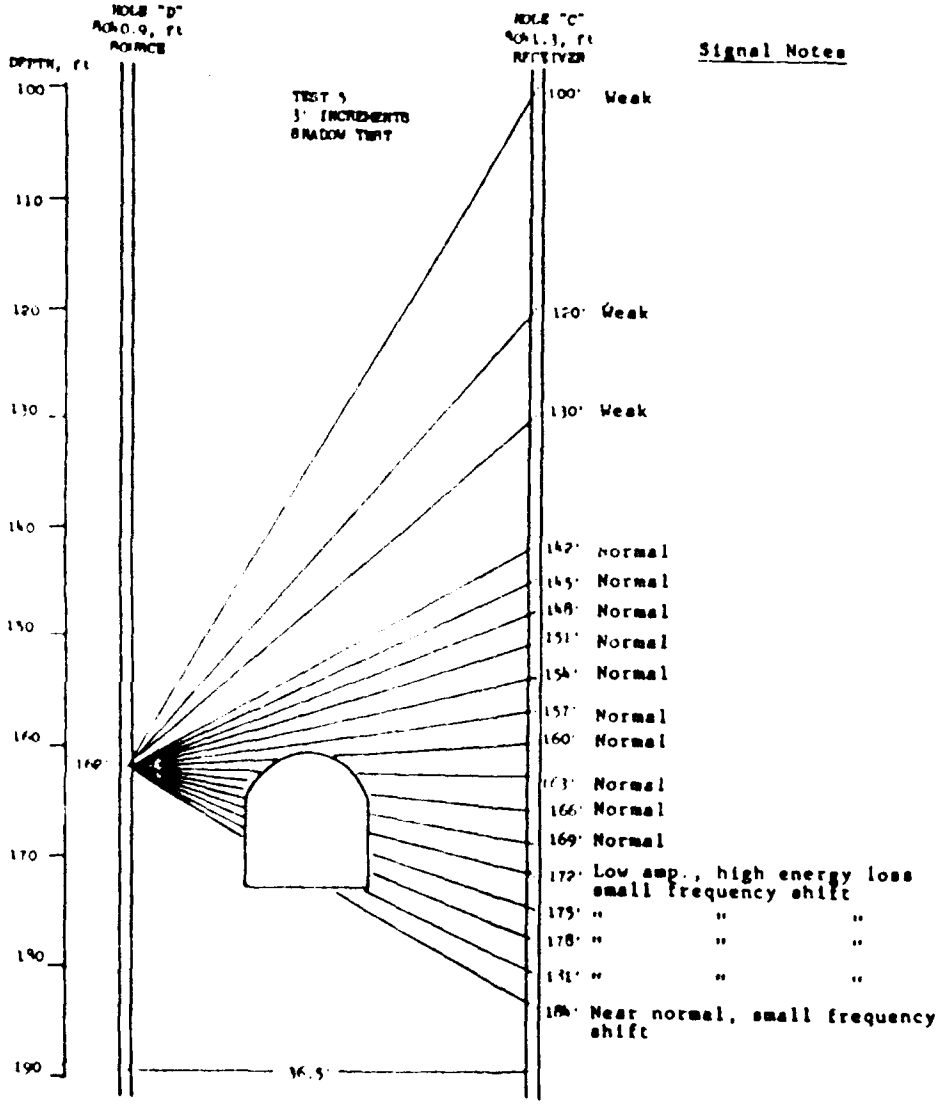

Figure 29. Transmitter and Receiver Geometries, Test 5C

172, 175, 178, and 181 feet. These four travel paths have the longest apparent travel time through the tunnel and should demonstrate the greatest seismic wave tunnel interaction effects. As can be seen in Figure 30, in all four cases the predominant signal strength from 250 to 500 Hz is greatly attenuated. A slight signal strength buildup can be seen between 100 and 220 Hz in shots 175, 178, 181, and 184 feet. All of these last four travel paths are through the lower half of the tunnel where an energy buildup was documented in this frequency range for Tests 3F and 13F. The lack of a larger buildup of these lower frequencies may be due to the inclination of seismic wave travel path in relationship to the tunnel. In Test 5C the seismic wave train of shots 175, 178, 181, and 184 feet actually have an apparent travel path for a significant distance in areas above and below the tunnel which were shown in 3F and 13F to highly attenuate the seismic signal. Due to this situation, a large frequency shift may not be achieved.

46. Test 13F (Frequency Domain). The results of Test 13F are similar to Test 3F (Figure 31) except for the shorter travel path and the tunnel location which is closer to the transmitter than the receiver. In shots 144, 147, 150, 153, 159, and 180 feet, an unaffected signal is recorded with half of the energy buildup at frequencies from 330 to 450 Hz (Figure 32). These frequencies in Test 13F are higher than Test 3F due to the shorter travel distance in 3F. Although this is only a small dispersive effect over a short distance, it will greatly increase with longer travel times. Such phenomena need to be carefully studied before an undocumented tunnel is investigated in the frequency domain at larger drill hole spacings. In shots at 140 and 156 feet, weak coupling between the drill hole wall and the seismic source or the geophone results in a poor signal strength. Shots at 162, 165, and 168 feet demonstrate the same signal attenuation above the tunnel, as documented in 3F. As before, most of the energy above 220 Hz has been filtered out. At 171 and 174 feet (ray paths which transect the lower half of the tunnel) a large energy shift from higher to lower frequencies is evident. This is similar to case 3F, but in this instance a much larger portion of the energy is transformed from higher to lower frequencies. This frequency shift appears to be more than 100 Hz with almost all of the energy in the signal now being under 270 Hz. Test 13F also has one travel path (177 feet) which passes near the tunnel floor where the signal

Fourier Analysis and Signal Energy Summation Plots for Test 5 C

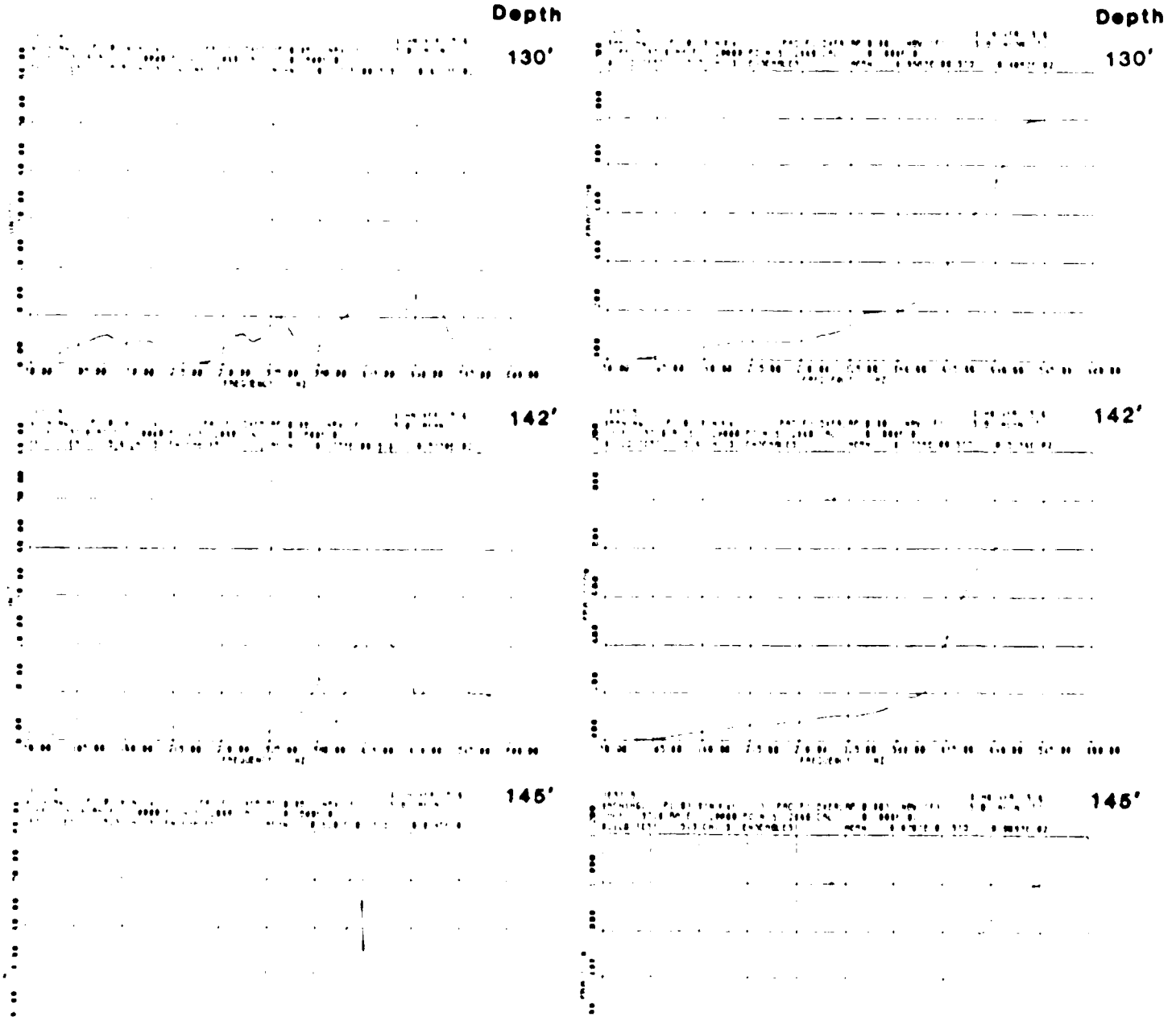

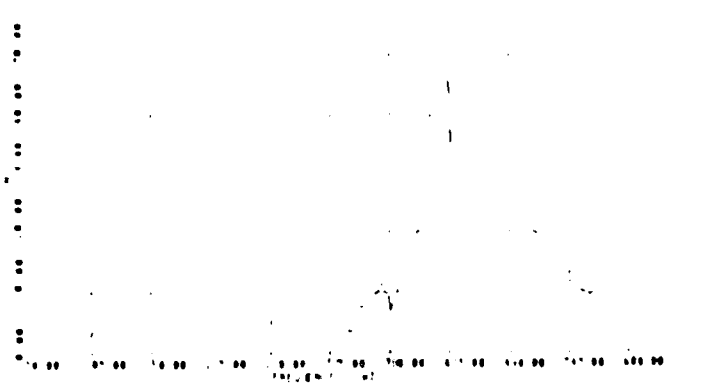

148'

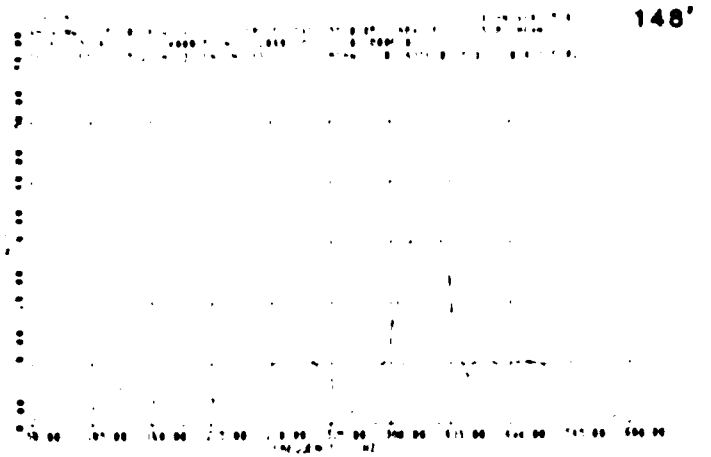

151'

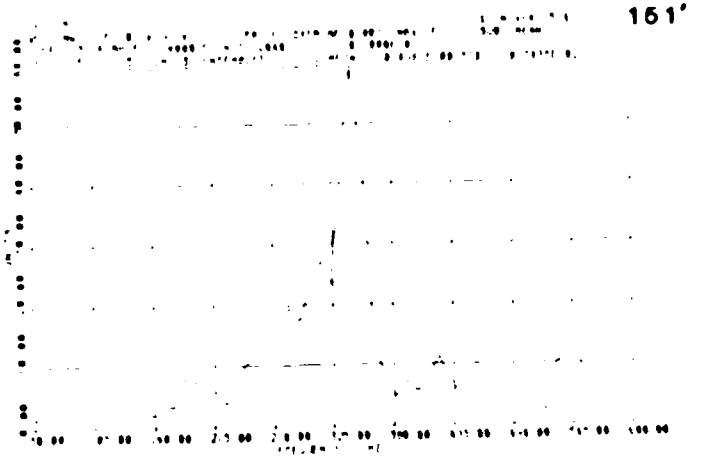

154'

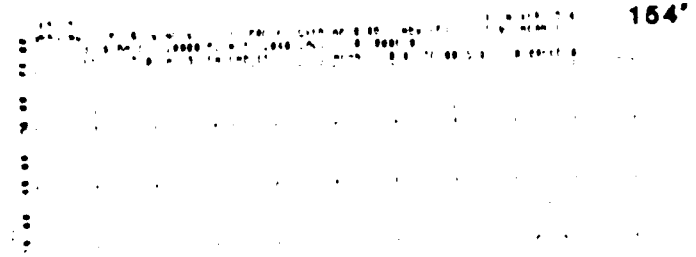

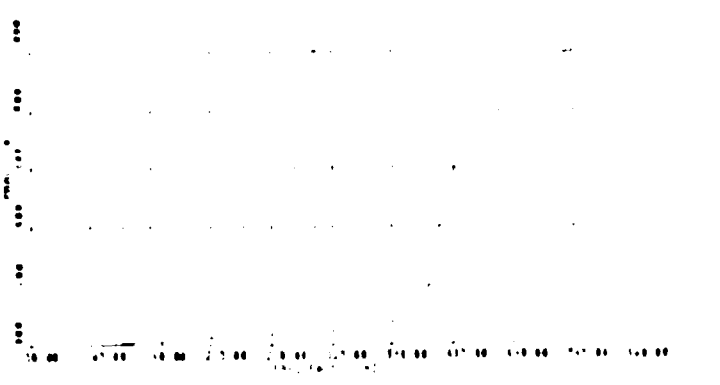

148'

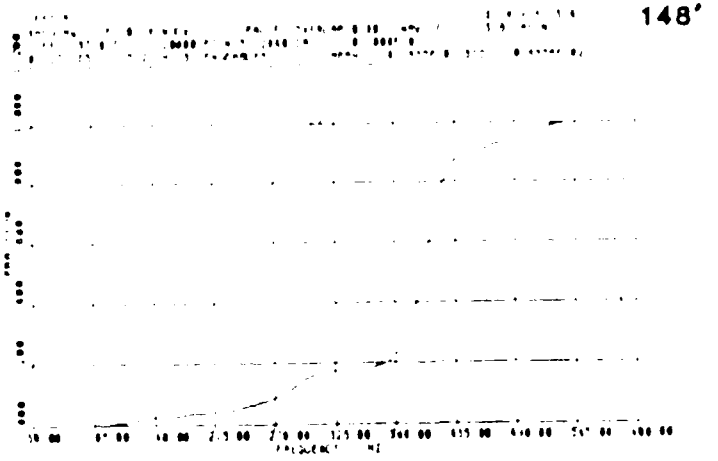

151'

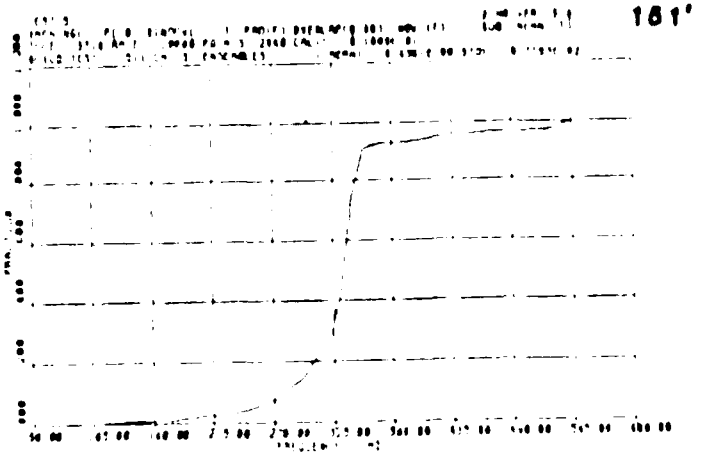

154'

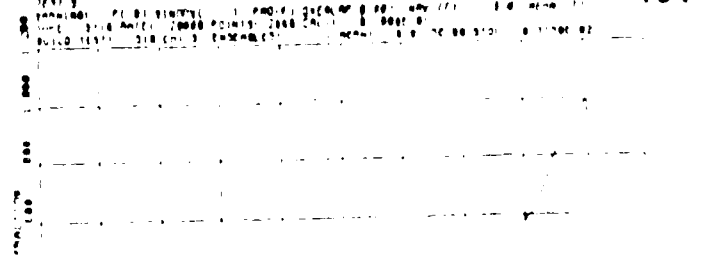

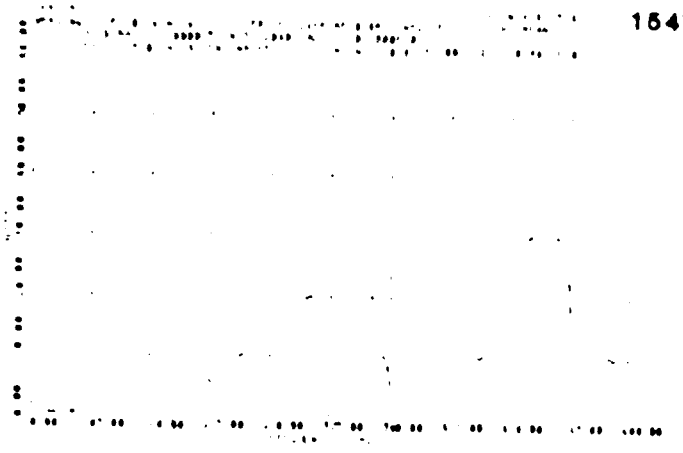
154'

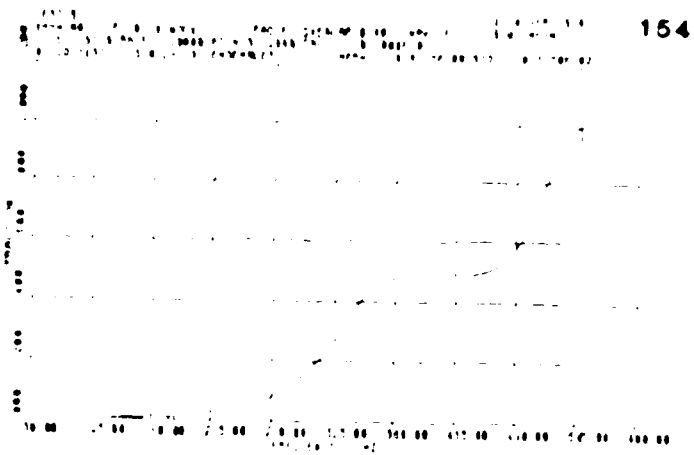
154'

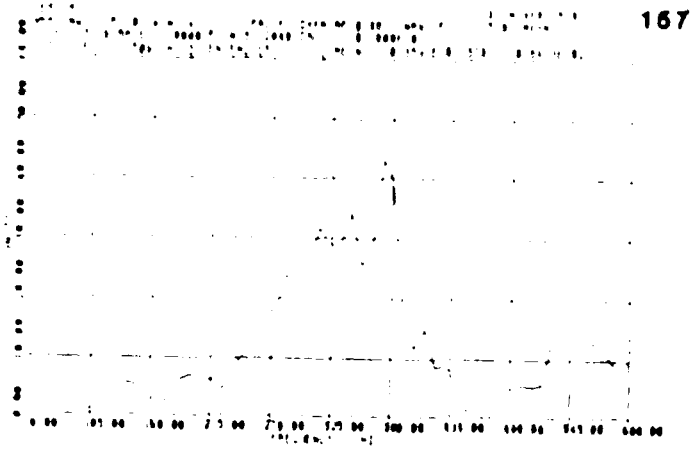
157'

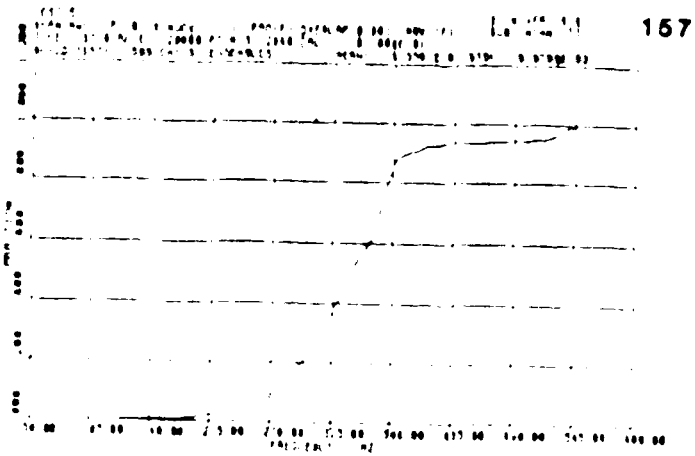
157'

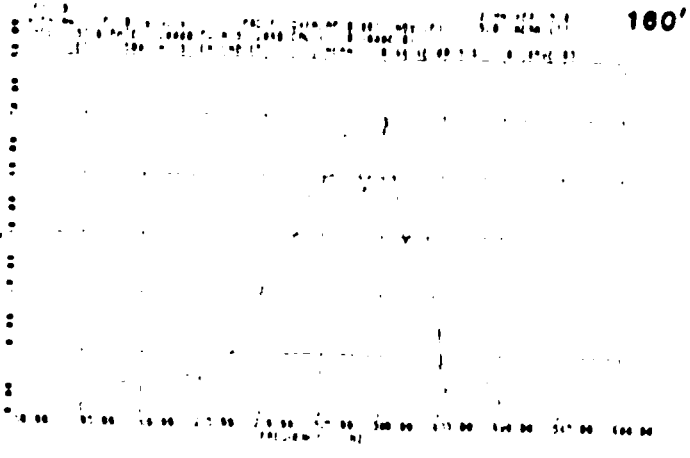
160'

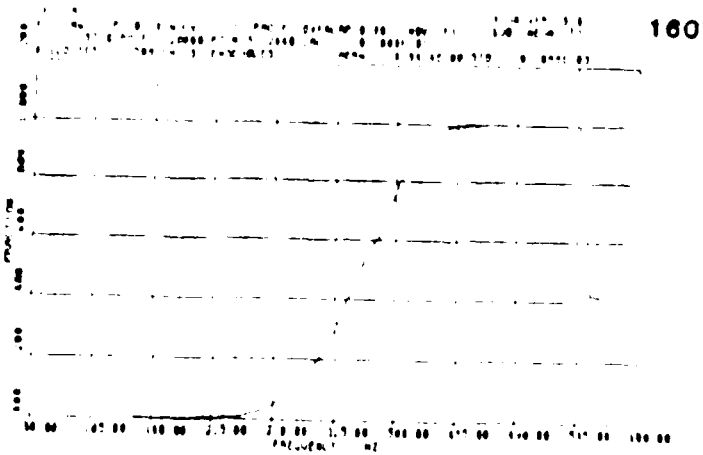
160'

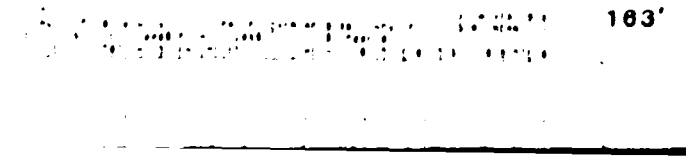
163'

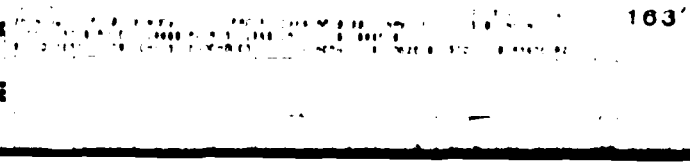
163'

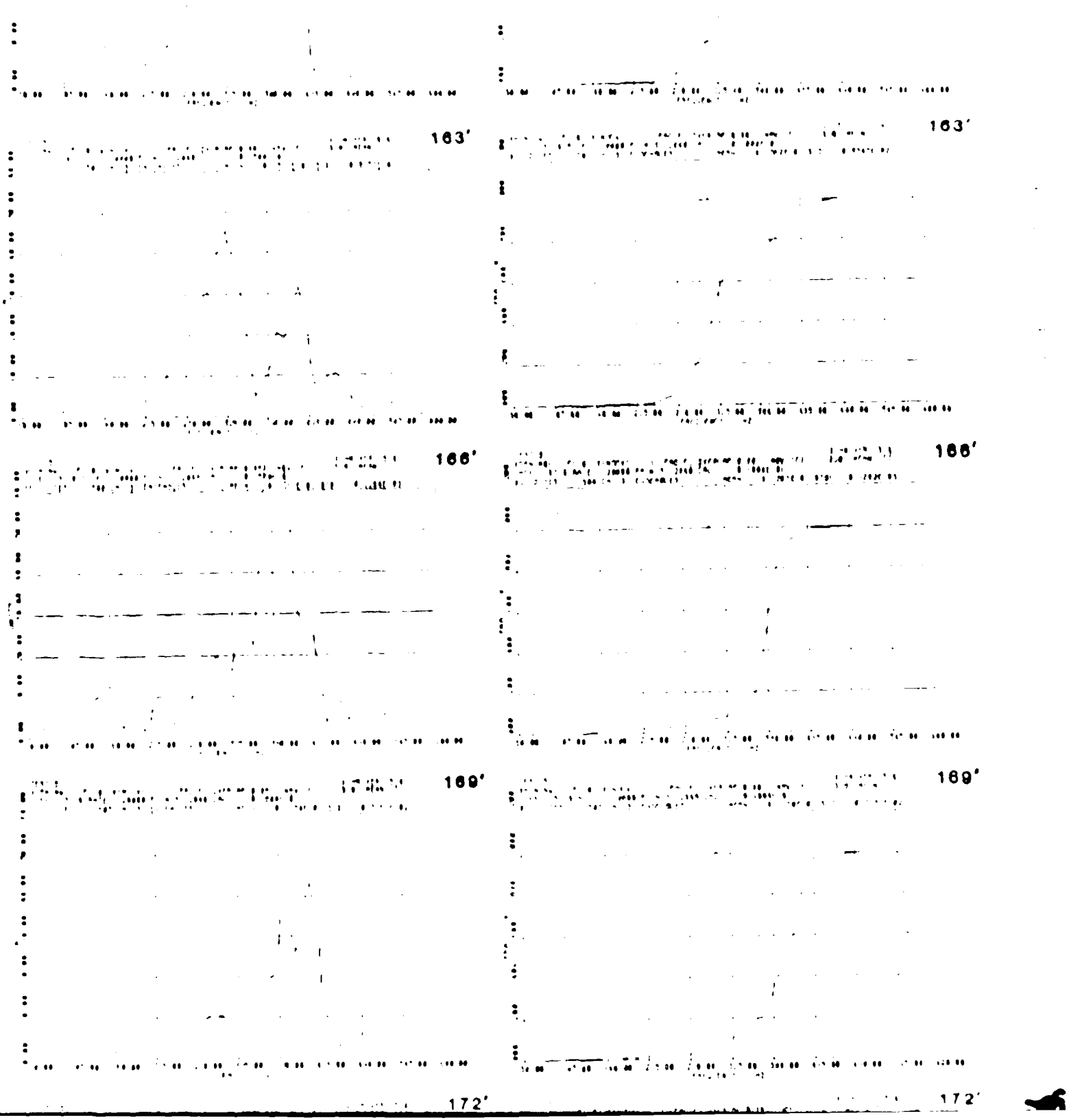
163'
163'
166'
166'
169'
169'
172'
172'

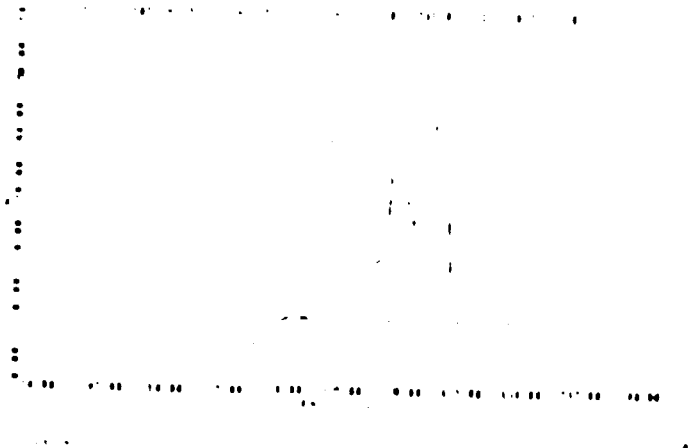

172'

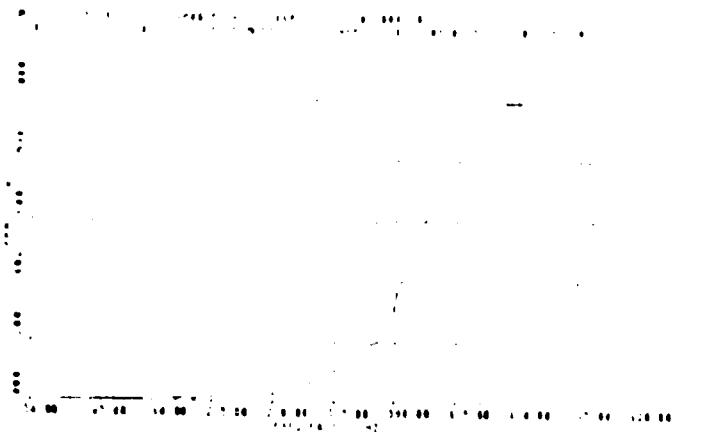

172'

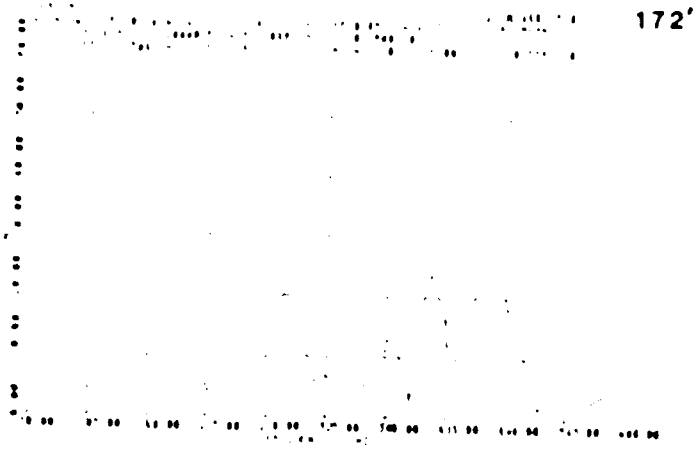

176'

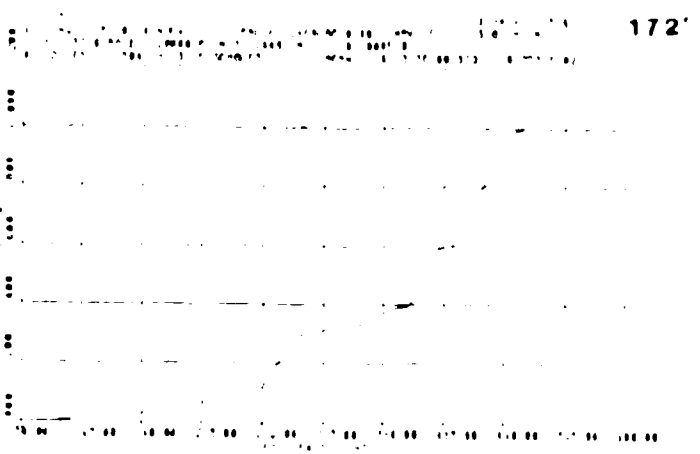

176'

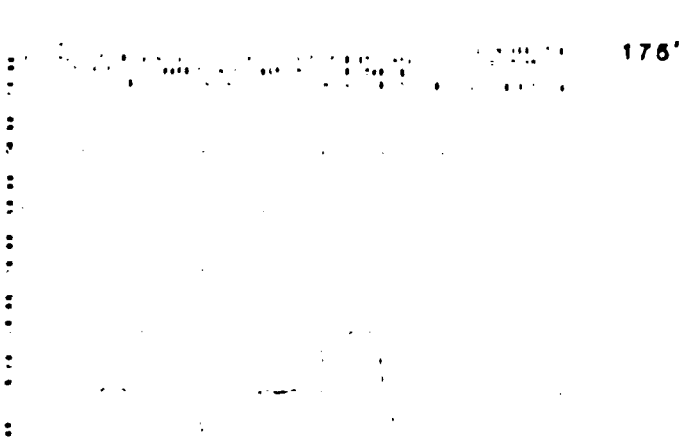

178'

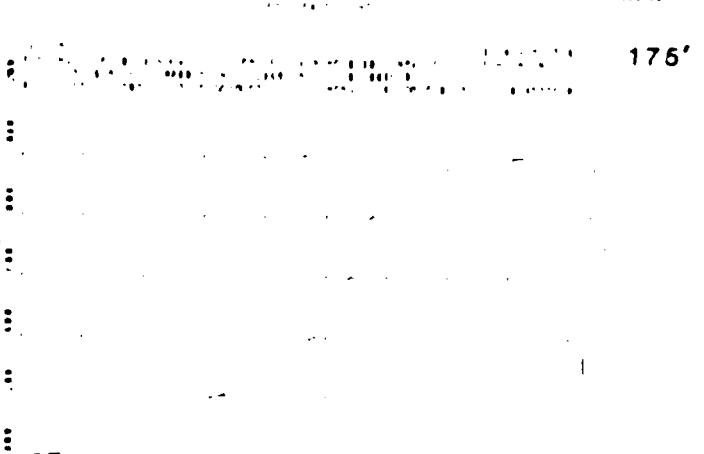

178'

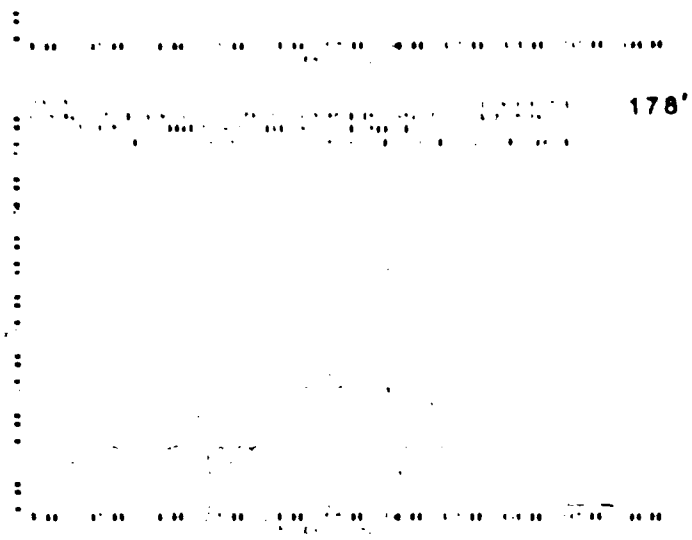
178'

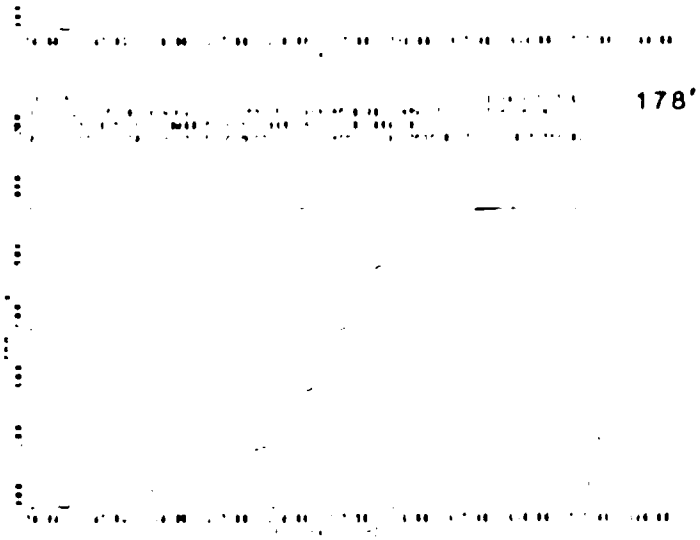
178'

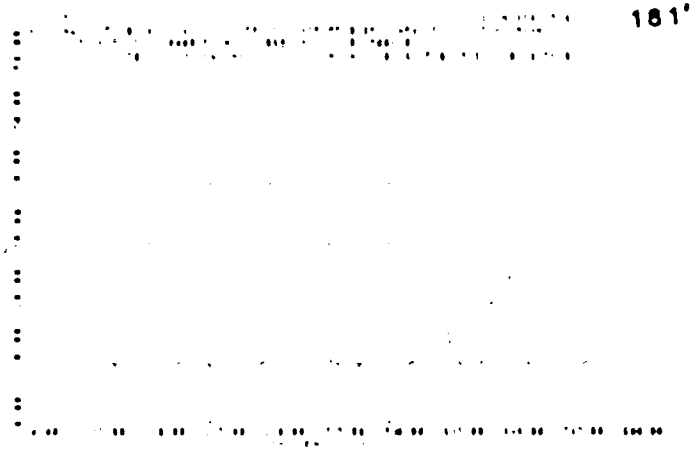
181'

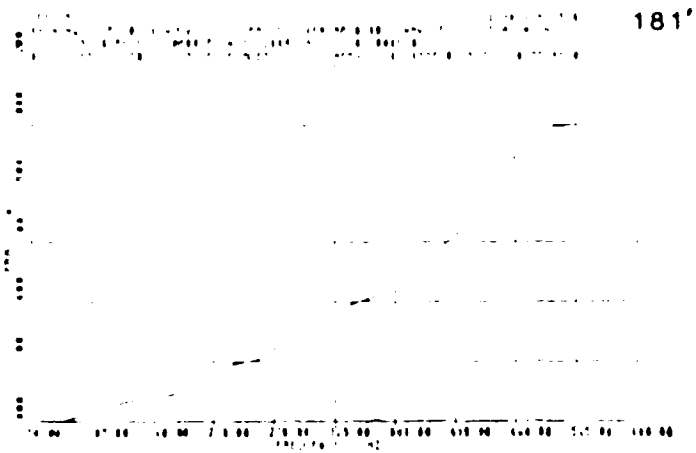
181'

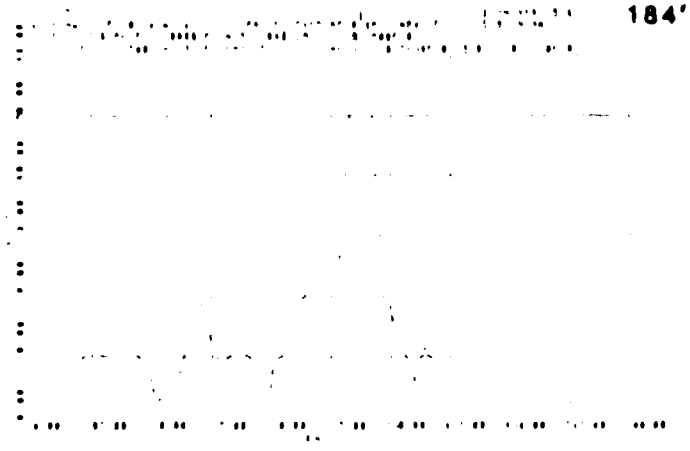
184'

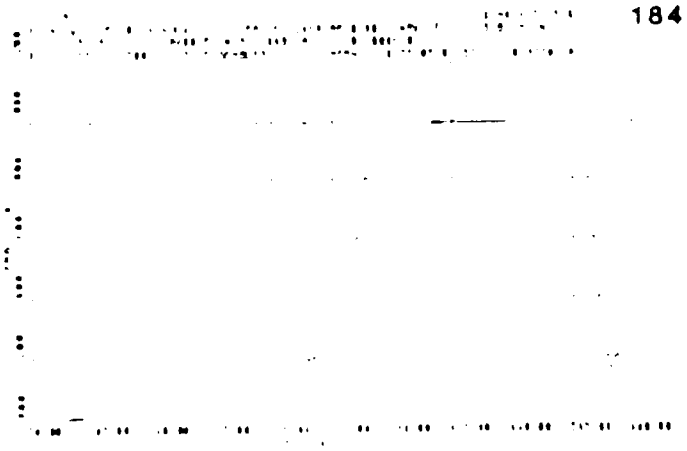
184'

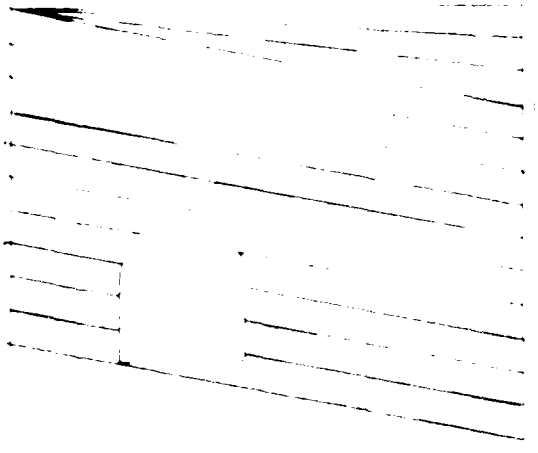

Fourier Analysis and Signal Energy Summation Plots for Test 13 C

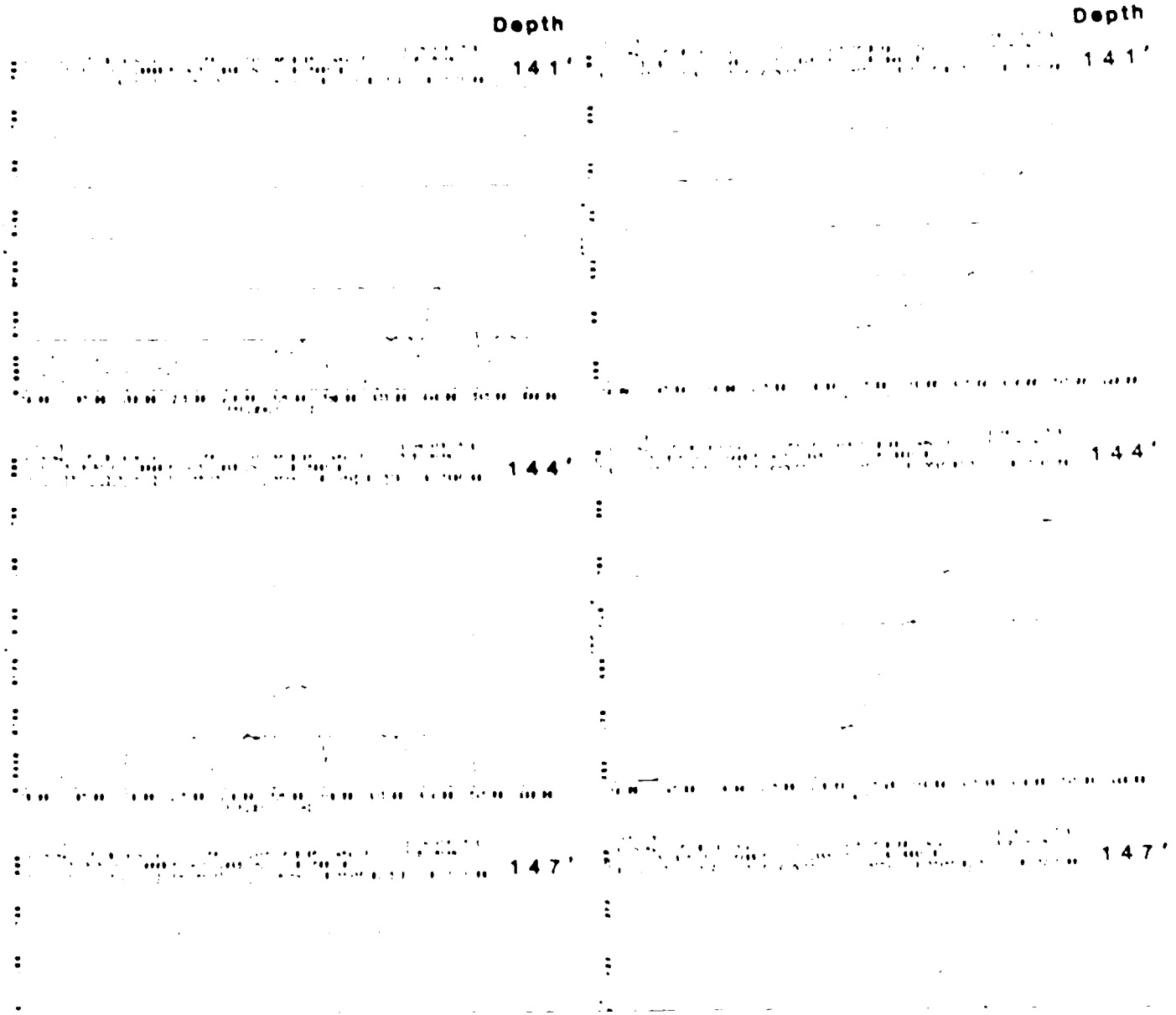

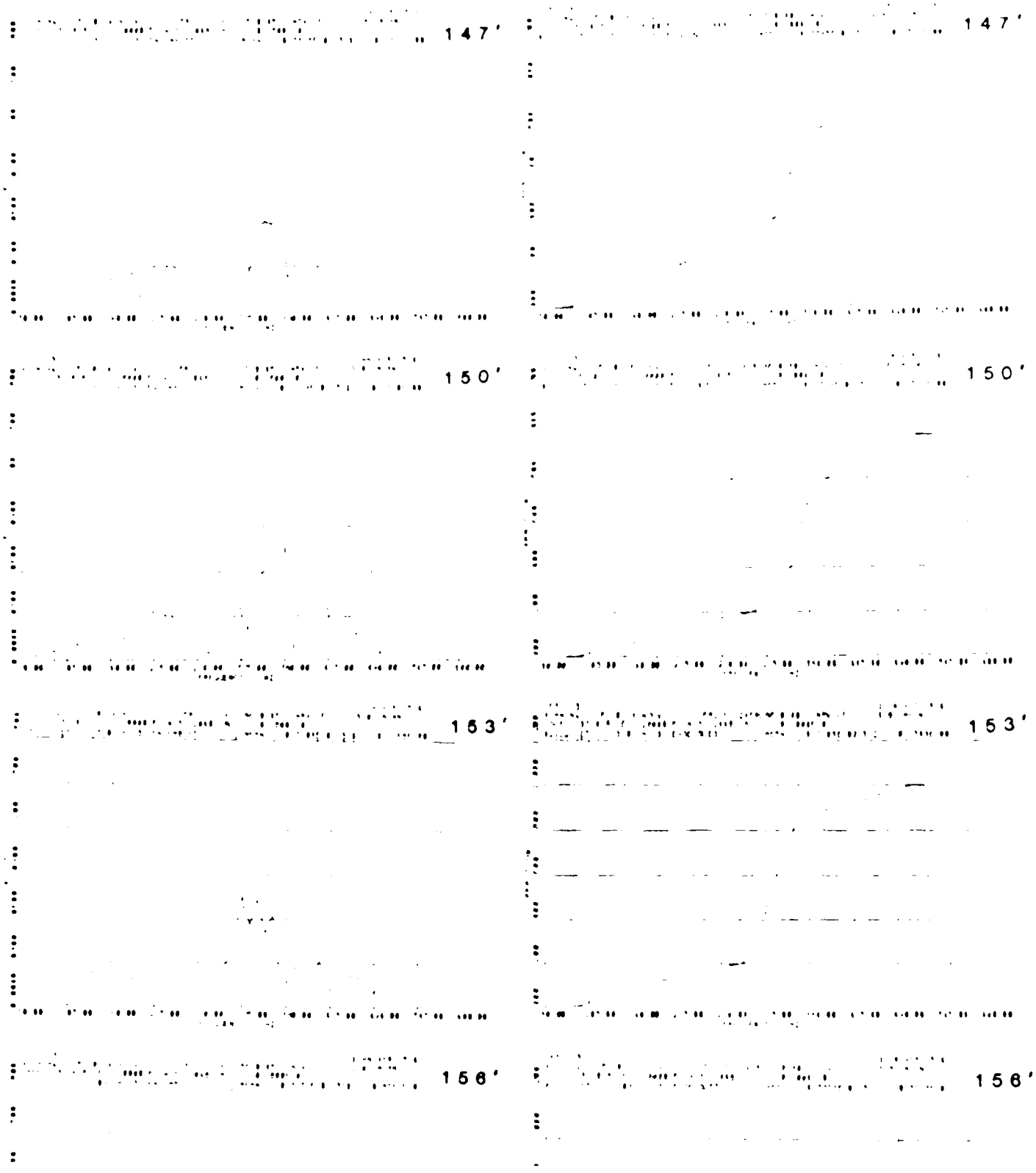
147'
147'
150'
150'
153'
153'
156'
156'

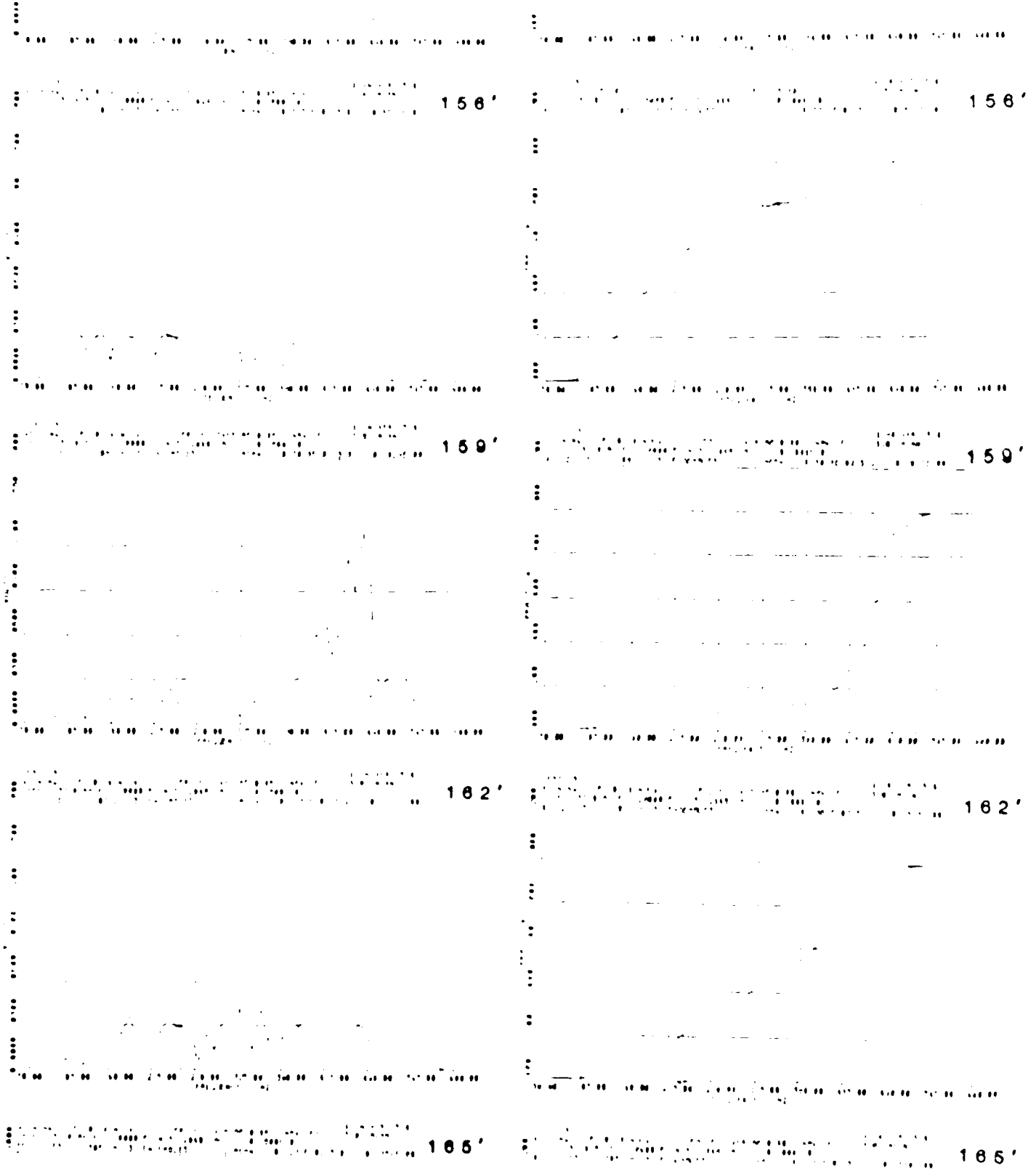
156'
156'
159'
159'
162'
162'
165'
165'

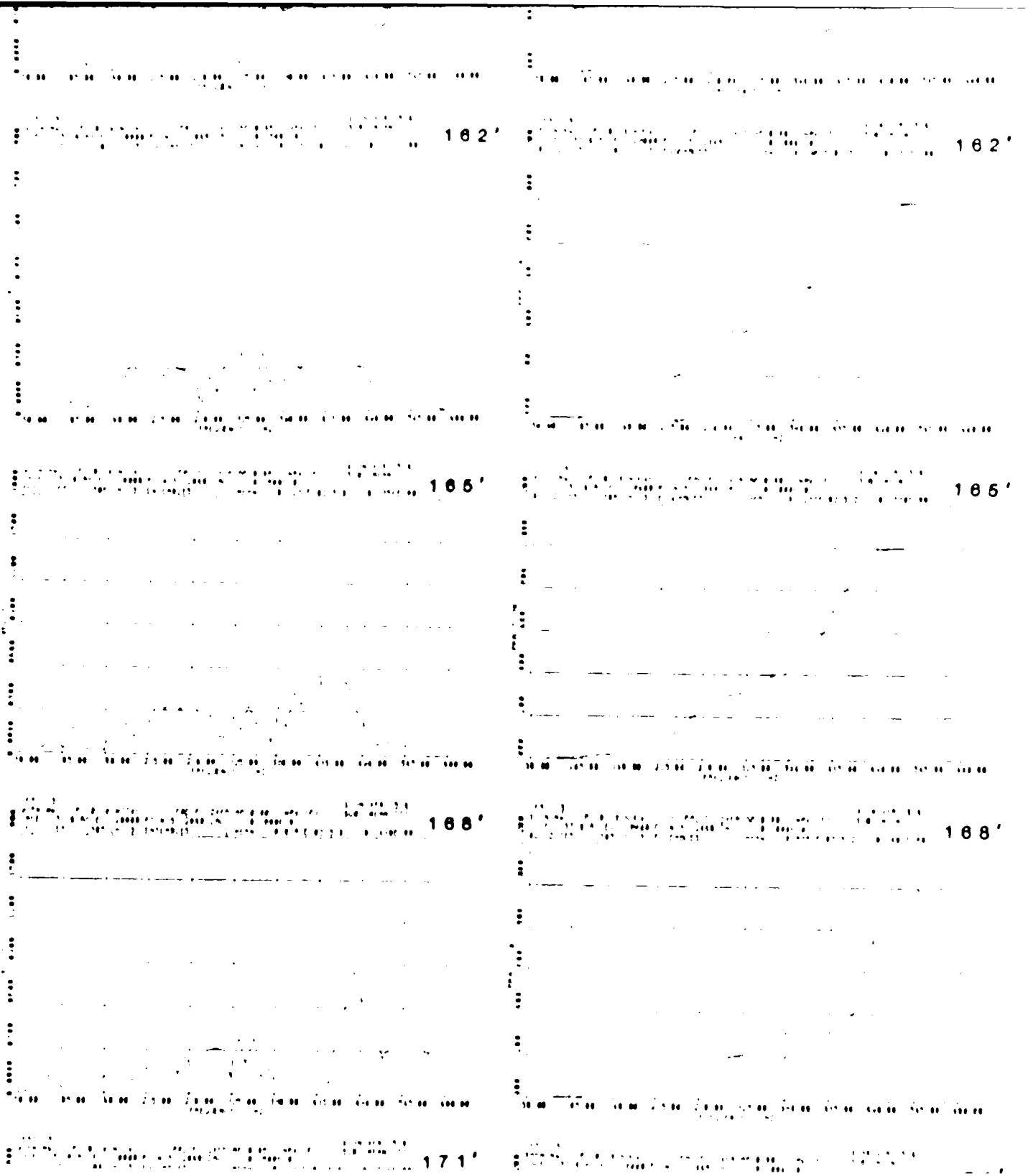
162'
162'
165'
165'
168'
168'
171'

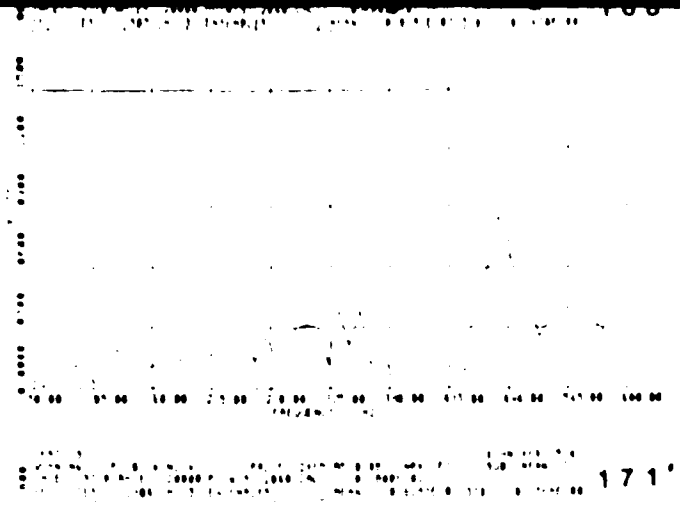
171'

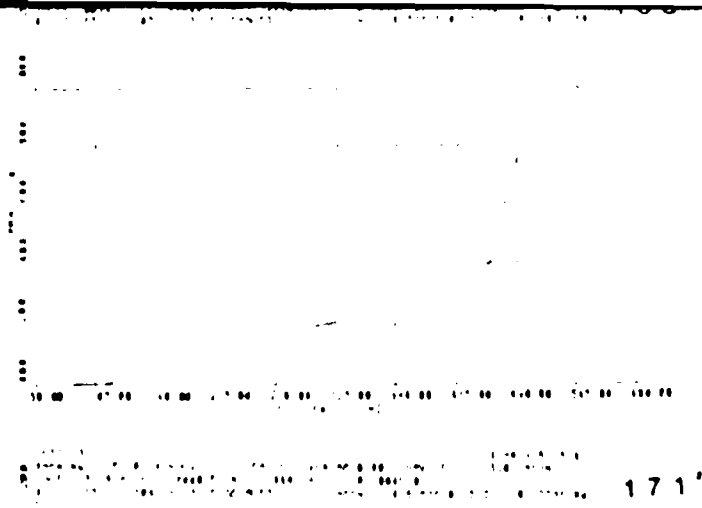
171'

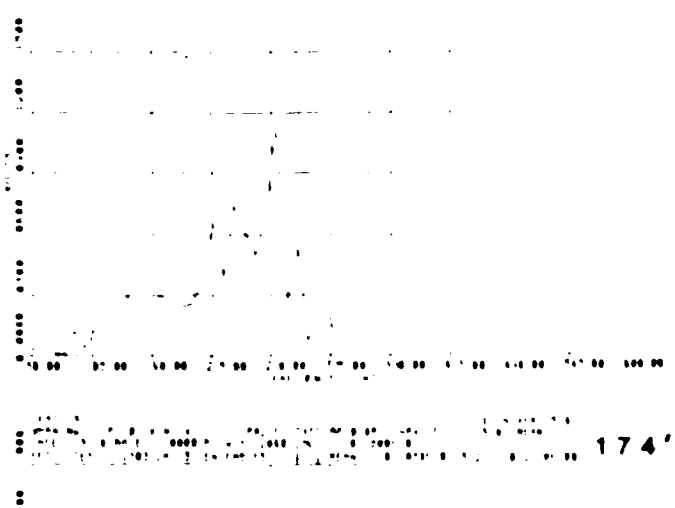
174'

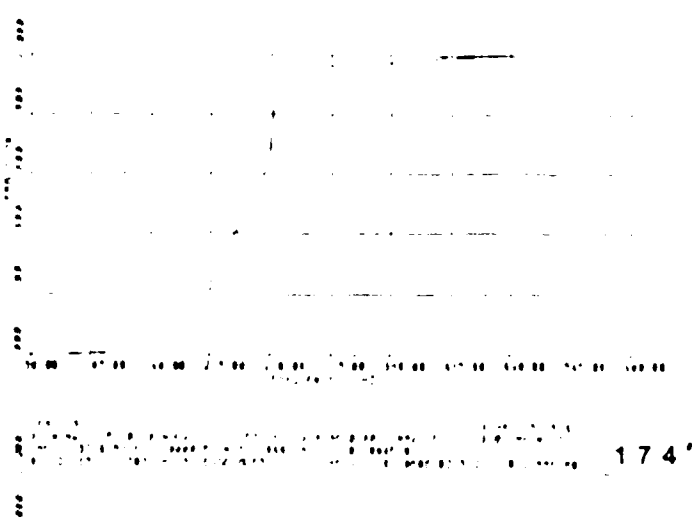
174'

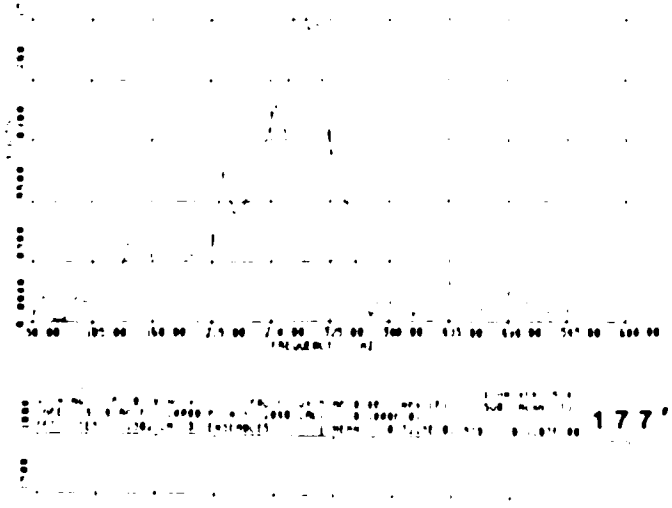
177'

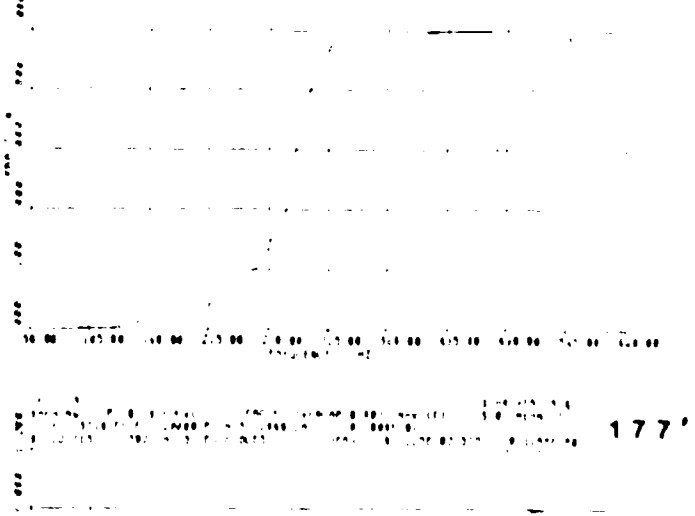
177'

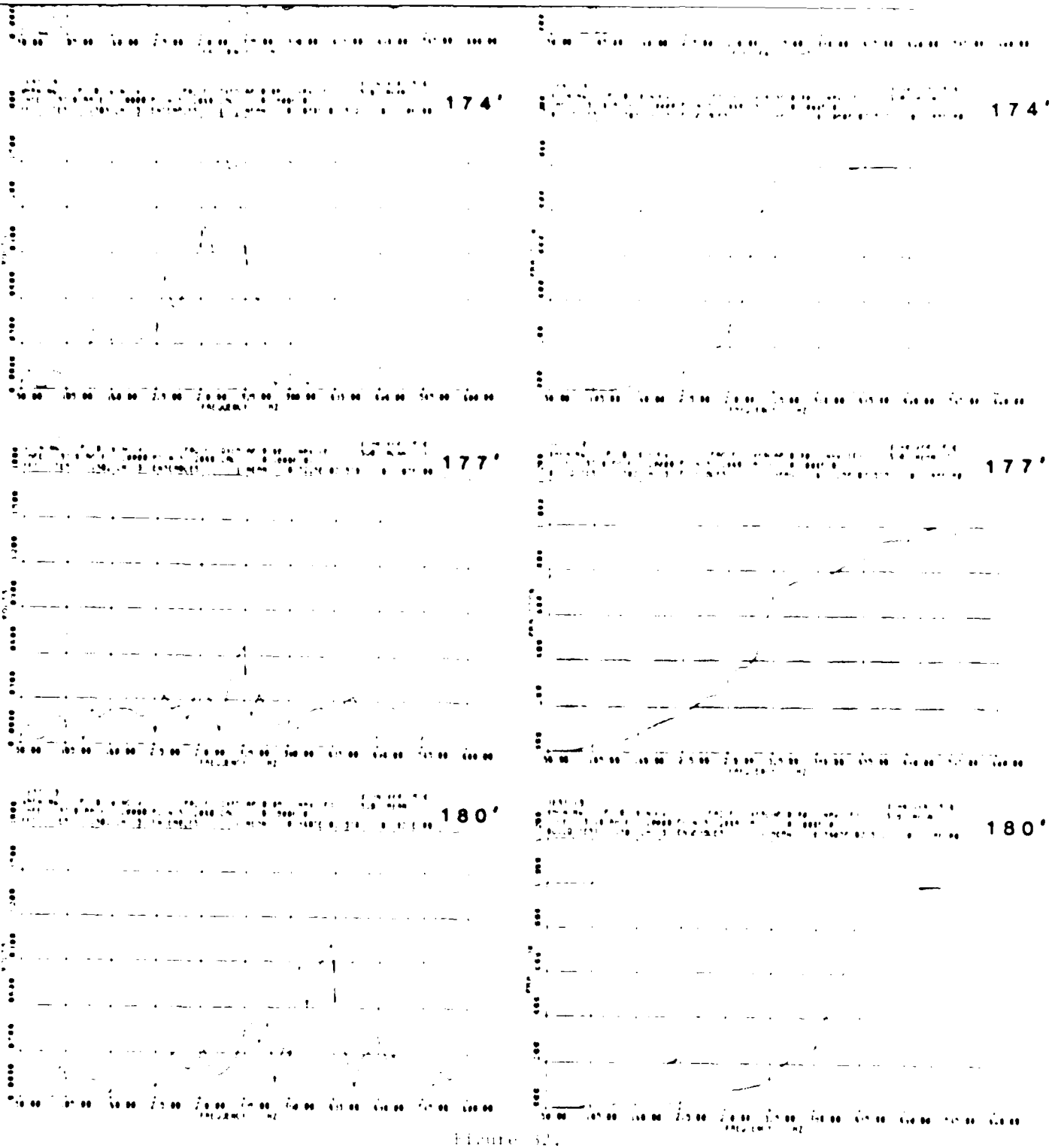
174'
174'
177'
177'
180'
180'

is attenuated or filtered in the same way as above the roof. This indicates a similar, but not as extensive, stress/fracturing regime in the tunnel floor.

47. Test 13F (Time Domain). The primary purpose of this discussion is to illustrate the significance of identifiable events which influence the entire wave signature at the receiver over a time domain of approximately 50 milliseconds after initiation of the seismic pulse. In addition to the first arrival of the P-wave, which under ordinary circumstances will be the shortest travel path, other travel paths will be discussed. The presence of an air-filled anomaly (tunnel) between the two boreholes creates the possibility for multiple reflection, refraction, and diffraction, and some of these possibilities will be addressed.

48. One secondary source thought to be a primary influencing factor on the overall wave train is the reflection that occurs when the initial wave encounters the air-filled tunnel. The length of its travel path will obviously be related to the position of the source and receiver relative to the fixed position of the tunnel. In the conduct of Test 13F, the sequence began with the source and receiver at a common depth well above the top of the tunnel. As the source and receiver were lowered in the boreholes, the travel path of the reflected wave became progressively shorter until it was almost equal to the length of the direct wave path. This occurred with the source at a depth of 156 feet and the receiver at a depth of 165 feet (the top and bottom of the tunnel are at depths of approximately 161 feet and 172 feet, respectively).

49. A schematic of the test concept is shown in Figure 33. Note that in addition to the straight-line travel paths between source and receiver the possible paths of the reflected signal from the top of the tunnel are also shown when the source and receiver were positioned above the tunnel. A third event, the arrival of the reflected signal from the ground surface, will also be considered. Although numerous other possibilities for reflections probably exist, the discussion will be concluded with the diffracted signal which occurs when the tunnel lies between the source and receiver.

50. A tabulation summarizing depth of source and receiver, distance to the receiver by way of the direct travel path, a reflected and diffracted signal from the tunnel, and a reflected signal from the ground surface is compiled in Table 8. The corresponding P-wave travel times related to each

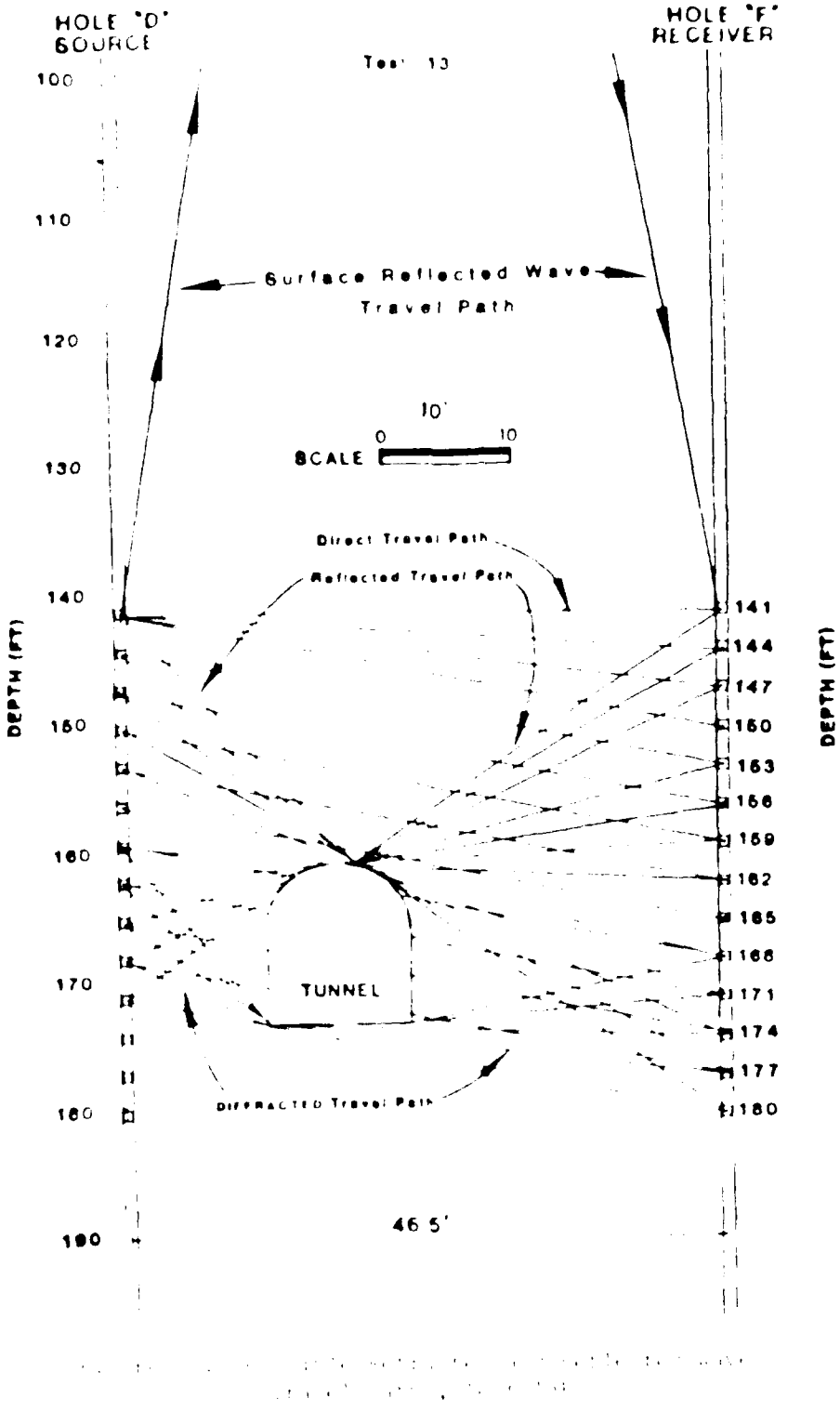
HOLE "D"
SOURCE
HOLE "F"
RECEIVER
Test 13
100
110
120
130
140
150
160
170
180
190
DEPTH (FT)
Surface Reflected Wave
Travel Path
10'
0
10
SCALE
Direct Travel Path
Reflected Travel Path
141
144
147
150
153
156
159
162
165
168
171
174
177
180
DEPTH (FT)
TUNNEL
DIFFRACTED Travel Path
46.5'

of these events are also shown in the tabulation. This tabulation will be used in conjunction with the time domain signal to discuss various events which can be observed on the seismic signature.

51. Figure 34 shows the digitized time domain signal recorded by the vertical receiver over a period of approximately 50 milliseconds in each of the 14 shots. The first event which can be readily observed is the arrival of the first signal which is the P-wave train journeying along the shortest direct travel path between the seismic source and the receiver. A tabulation of these travel times appears in column 7 of Table 8. When the tunnel begins to affect the length of the travel path (Records 10-13), it can be observed that the signal is diffracted and delayed when compared to the uninterrupted direct travel path. A maximum time of 8.5 msec, a delay of about 4 msec, will be observed on Record 12. In this case, the locations of source and receiver are almost on an imaginary centerline through the central part of the tunnel. The presence of the tunnel also affects the signature of Records 1-6 which are located well above the top of the tunnel. A high degree of distortion in the elapsed time frame of 5 to 12 msec is caused by the signal reflected from the top of the tunnel arriving about 1 to 2 msec later than the direct wave. Compare columns 7 and 8 of Table 8. This distortion can be used as a possible tunnel identifier.

52. A possible diffracted path was also computed using an average velocity determined from the direct path measurements. As an example, shot no. 14 was recorded with the source at a depth of 171 feet and the receiver at a depth of 180 feet. The direct travel path was 47.5 feet and a possible secondary path would have been around the top of the tunnel resulting in an overall distance of about 56.0 feet. Its travel time would have been about 1 millisecond longer than that of the direct path. However, no noticeable effect from this theoretical possibility is observed on Record 14. This diffracted arrival either did not exist or its signal amplitude was too small to cause a visible distortion.

53. Observing Records 1 and 14, it can be seen that a primary reflection (circled) occurs at a time of 27.5 msec on Record 1 and at a time of 34.2 msec on Record 14. Using these times in conjunction with appropriate source-surface-receiver distances, an average vertical P-wave velocity of 10,250 fps can be computed. Consequently, these reflections could very well be the product of the P-wave signal traveling to the ground surface, reflecting

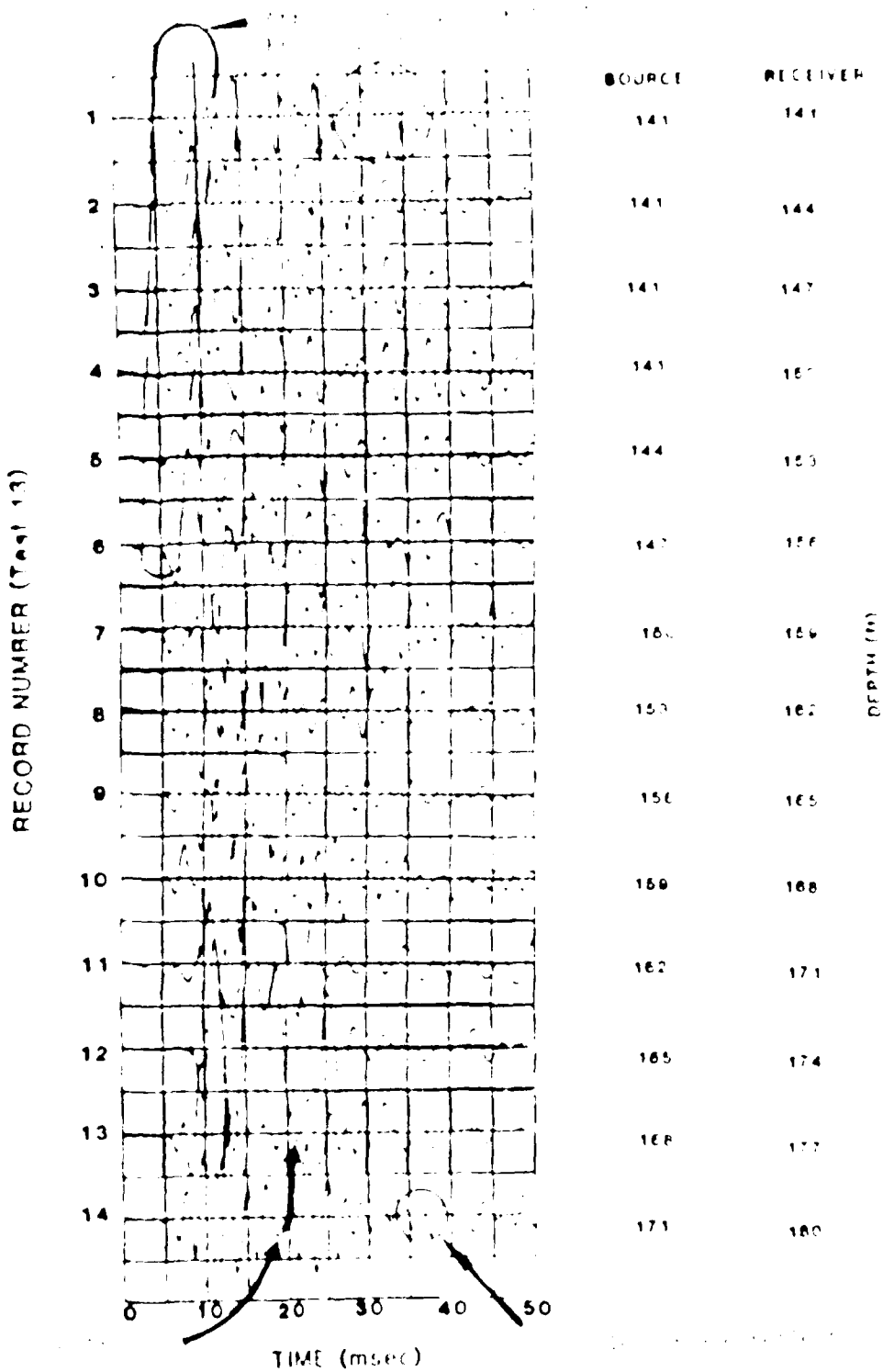
RECORD NUMBER (Test 13)
SOURCE
RECEIVER
DEPTH (m)
1
2
3
4
5
6
7
8
9
10
11
12
13
14
141
141
141
141
144
141
144
147
150
156
162
165
168
171
174
177
180
0
10
20
30
40
50
TIME (msec)

from that interface and back down to the receiver. Using this velocity, which was determined from two high-quality reflections, and the known total distance for Records 2-13, the predicted arrival time for each was computed and tabulated in column 9. In most instances, the surface-reflected signal can be recognized on the records; however, in some instances, the arrival of other events tends to mask the reflection.

54. Another interesting observation can be made concerning the presence of the tunnel. During the construction process, in which drilling and blasting were used, a great deal of fracturing occurred in the rock around the tunnel (possibly as much as one tunnel radius) (5 feet). This observation was confirmed by the lower velocities measured in this region and supports the observation made by King, et. al., (1984). King stated that the construction effect extended more than 6 feet from a tunnel driven through basaltic rock. The existence of these fractures will also cause severe attenuation of short-wavelength, high-frequency signals. Consequently, low frequency signals would be expected to dominate the seismic signature, as discussed in more detail in the previous frequency domain analysis. This effect can be readily observed on Records 11 and 12. Additionally, Record 12 shows near-perfect in-phase merging of the diffracted signals which traveled around the top and bottom of the tunnel re-uniting on the far side. This can be explained by the fact that the travel paths are virtually equal around the top and bottom of the tunnel. Record 11, however, shows distortion caused by slightly out-of-phase signals which traveled around the top and bottom of the tunnel. In this case, the travel path is appreciably longer around the bottom of the tunnel than around the top of the tunnel. Consequently, the time domain signal readily shows the distortion caused by the slightly later wave train lagging and combining with the first signal.

55. In most cases, the S-wave arrival was very difficult to determine. Observing Records 1-4, a distinct wave train arrival can be seen occurring in the 12 to 13 msec range. This wave train, even though somewhat distorted by the first primary P-wave reflection from the tunnel, is most likely the S-wave. Its velocity is about 3,800 fps. As testing neared the tunnel, the S-wave arrival became incoherent. Record 14, however, displays a prominent wave train arrival at an elapsed time of 18 msec. This signature can be traced and overlain on Record 1 to establish a correlation. Since the

[illegible]	[illegible]	[illegible]	[illegible]
[illegible]	[illegible]	[illegible]	[illegible]
[illegible]	[illegible]	[illegible]	[illegible]
[illegible]	[illegible]	[illegible]	11180
[illegible]	[illegible]	[illegible]	[illegible]
[illegible]	[illegible]	[illegible]	[illegible]
[illegible]	[illegible]	[illegible]	[illegible]
[illegible]	[illegible]	61.5	12300
[illegible]	[illegible]	61.5	12300
[illegible]	[illegible]	61.5	11180
[illegible]	[illegible]	61.5	10250
[illegible]	[illegible]	61.5	10250
[illegible]	[illegible]	61.5	[illegible]
[illegible]	[illegible]	61.5	[illegible]
[illegible]	[illegible]	61.	12300
[illegible]	[illegible]	61.5	12300
[illegible]	[illegible]	[illegible]	12300
[illegible]	[illegible]	[illegible]	12300
[illegible]	[illegible]	[illegible]	12800

Table 6

Common Depth - Possible, Best = "0"

[illegible]	ARRIVAL TIME	TRAVEL DIST.	VELOCITY
[illegible]	Msec	Ft	Fps
[illegible]	[illegible]	36.5	[illegible]
[illegible]	[illegible]	36.5	8111
[illegible]	[illegible]	36.5	9125
[illegible]	[illegible]	36.5	9864
[illegible]	[illegible]	36.5	9125
[illegible]	[illegible]	36.5	9125
[illegible]	[illegible]	36.5	9125
[illegible]	[illegible]	36.5	9125
[illegible]	[illegible]	36.5	9125
[illegible]	3.5	36.5	10428
[illegible]	5.0	36.5	7300
[illegible]	[illegible]	36.5	8111
[illegible]	[illegible]	36.5	8111
[illegible]	[illegible]	36.5	7300
[illegible]	[illegible]	36.5	8111
[illegible]	[illegible]	36.5	[illegible]
[illegible]	[illegible]	36.5	10428
[illegible]	[illegible]	36.5	10428

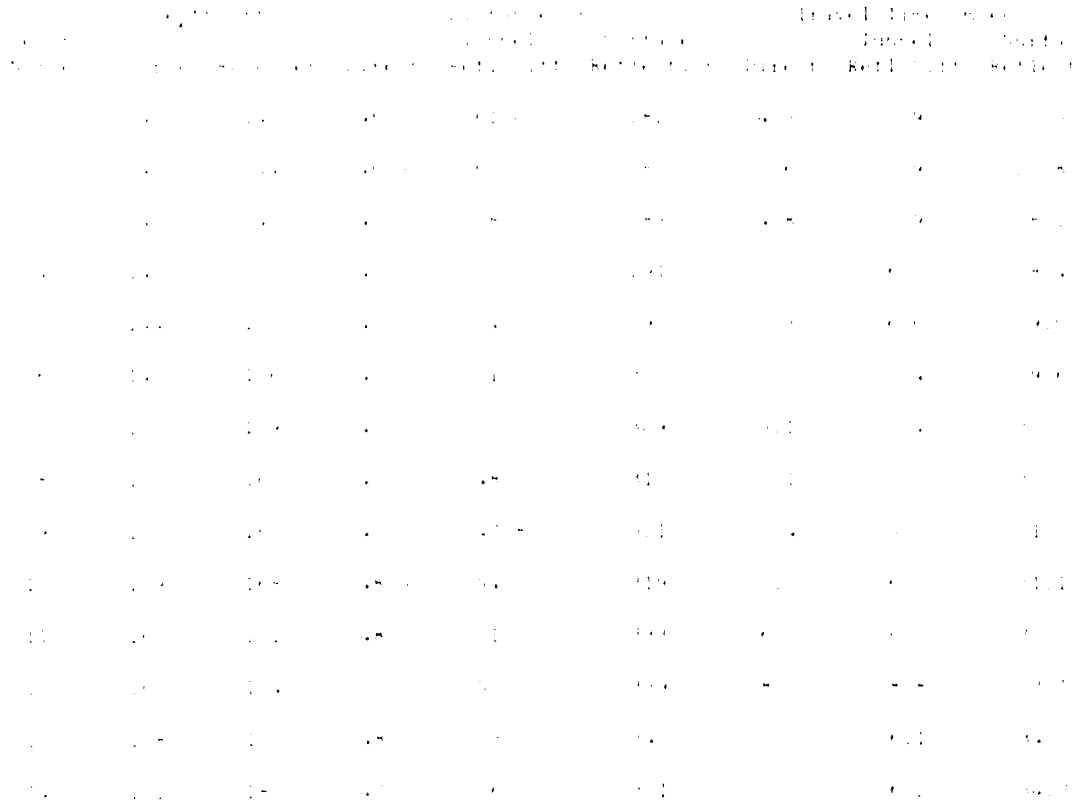

END

DATE
FILMED
3-85

DTIC


ED
85